



NeuroPercept: Towards a Motor Related Epileptic Seizure Paradigm to Study Novel Closed-loop Neurostimulation Approaches

Ana Rita de Melo Ferreira Sampaio

WORKING VERSION

MESTRADO INTEGRADO EM BIOENGENHARIA

Supervisor: João Paulo Trigueiros da Silva Cunha, PhD

October 3, 2021

NeuroPercept: Towards a Motor Related Epileptic Seizure Paradigm to Study Novel Closed-loop Neurostimulation Approaches

Ana Rita de Melo Ferreira Sampaio

MESTRADO INTEGRADO EM BIOENGENHARIA

Resumo

A epilepsia é uma doença neurológica que se manifesta através de convulsões recorrentes e inesperadas. Parte dos doentes epiléticos apresentam crises motoras que envolvem mecanismos característicos. Embora a maioria dos pacientes responda bem à medicação anti-epiléptica, uma percentagem dos pacientes continua a relatar a ocorrência de convulsões após o devido tratamento medicamentoso. A estimulação cerebral profunda dos núcleos anteriores do tálamo (NAT) é um tratamento seguro e eficaz capaz de ultrapassar esta limitação.

O Percept™ PC é o novo neuroestimulador da Medtronic e permite registar sinais de potenciais locais de campo em simultâneo com a estimulação de um alvo profundo.

Esta dissertação apresenta um protocolo experimental baseado num paradigma motor que visa verificar a existência de biomarcadores associados à crise epilética, nomeadamente aos movimentos característicos à mesma, no NAT e os efeitos da estimulação profunda na sua execução. O protocolo experimental foi reproduzido em dois estudos utilizando sinais EEG não invasivo e invasivo. No primeiro participaram voluntários saudáveis, enquanto que no segundo participou um único doente epilético. Para além disso, utilizou-se dados de uma experiência baseada no uso de sinais LFP provenientes do NAT durante a execução de um paradigma motor simples. Nesta experiência participou um doente epilético com o Percept™ PC implantado que efetuou a aquisição dos sinais.

Nos estudos com EEG, os resultados foram coerentes com os encontrados na literatura. Ao usar-se sinais de EEG observou-se o aparecimento de dessincronização na zona contralateral à do movimento, dois segundos antes do seu início para atividades realizadas com os membros superiores. Isto observou-se quer para o ritmo alfa como para o ritmo beta. Após o término do movimento, verificou-se que o ritmo beta sincronizou quase imediatamente, enquanto que na gama de frequências alfa se verificou um maior período de recuperação. No estudo baseado em EEG invasivo não foi possível detetar padrões de dessincronização e sincronização durante a atividade motora no hipocampo. O estudo efetuado com os sinais eletrofisiológicos adquiridos com o Percept™ PC revelou a possibilidade do NAT estar envolvido no processamento motor uma vez que foram observados padrões de sincronização aquando da execução do paradigma. Os resultados deste estudo são totalmente inovadores e poderão abrir portas para uma nova linha de investigação.

Contudo, os resultados obtidos nestes estudos não são estatisticamente significativos devido ao reduzido número de participantes.

O protocolo experimental desenvolvido está pronto para ser implementado num estudo de sinais de potenciais locais de campo adquiridos com o novo Percept™ PC.

Abstract

Epilepsy is a neurological disease that manifests itself through recurrent and unexpected seizures. Part of epileptic patients has motor seizures characterized by the presence of automatisms. Although most patients respond well to anti-epileptic medication, a percentage of patients continue to report the occurrence of seizures after proper drug treatment. Deep brain stimulation of the anterior nuclei of the thalamus (ANT) is a safe and effective treatment that can overcome this limitation.

The Percept™ PC is Medtronic's new neurostimulator that allows the recording of local field potential (LFP) signals simultaneously with stimulation of a deep target.

This dissertation presents an experimental protocol based on a motor paradigm that aims to verify the existence of biomarkers associated with the movements of an epileptic seizure, in the ANT and the effects of deep stimulation on its execution. The experimental protocol was reproduced in two studies using non-invasive and invasive EEG signals. In the first healthy volunteers participated, while in the second, a single epileptic patient was enrolled. In addition, data from an experiment based on the use of LFP signals from the ANT during the execution of a simple motor paradigm was used. The first ever epileptic patient to be implanted with a Percept™ PC neurostimulator that under went a 5 day video-EEG monitoring, participated in this study.

In the EEG studies, the results were consistent with those found in the literature. When using noninvasive EEG signals, the appearance of desynchronization was observed in the zone contralateral to that of the movement, two seconds before its onset for activities performed with the upper limbs. This was observed for both alpha and beta rhythms. After the end of the movement, it was found that the beta rhythm synchronized almost immediately while in the alpha frequency range, there was a long recovery period. In the study based on invasive EEG, it was impossible to detect patterns of desynchronization and synchronization during motor activity in the hippocampus. The study performed with the electrophysiological signals acquired with the Percept™ PC revealed the possibility of the ANT being involved in motor processing since synchronization patterns were observed during the execution of the paradigm.

However, the results obtained in these studies are not statistically significant due to the small number of participants.

The developed experimental protocol is ready to be implemented in a study of local field potential signals acquired with the new Percept™ PC.

Agradecimentos

Em primeiro lugar, quero agradecer do fundo do meu coração aos meus pais que com mais ou menos dificuldade tornaram possível o meu desejo e ambição de ingressar num curso superior. Foram quem me abriu as asas para poder voar, quem me incentivou nos momentos de maior insegurança, quem me amparou e segurou nos braços nos momentos em que desabei e, principalmente, quem me apoiou incondicionalmente em todas as minhas decisões. Obrigada aos melhores pais do mundo por tudo o que fizeram durante este percurso e continuam a fazer por mim!

Ao meu irmão que é o melhor amigo e ser humano que alguma vez conheci e que é o melhor exemplo de coragem, superação e crescimento que eu poderia ter. Foi um dos meus portos de abrigo nos maus momentos e o um confidente nos bons, ao longo destes 5 anos.

De seguida, um grande agradecimento ao professor João Paulo Cunha que sempre me apoiou e aconselhou para realizar o melhor trabalho possível e que sempre me incentivou a seguir as minhas ideias e ajudou a concretizá-las. À Elodie e ao Duarte que estiveram sempre disponíveis para me esclarecer acerca de qualquer dúvida e a ajudar sempre que necessário.

Ao Dr. António Campos e ao Dr. Ricardo Rego por me facilitarem a entrada na Unidade de Monitorização de Epilepsia do Hospital de S.João e se disponibilizarem a ajudar e a fornecer todo o material e equipamento necessário para a realização das minhas experiências.

Aos meus amigos que são os ouvientes pacientes dos meus desabafos, os psicólogos nas horas das indecisões, os que alinham em todas as aventuras e, sobretudo, os que arranjam sempre um motivo para me fazer sorrir e sentir-me amada.

À Maria que se cruzou no meu caminho no meu primeiro dia de aulas na FEUP e que nunca mais saiu da minha vida. É a luz que ilumina a vida de qualquer um e que me faz sempre ver a vida com mais cor.

Ao Henrique que é uma caixinha cheia de surpresas e cada vez que se descobre mais uma, mais forte se torna a nossa amizade. É, sem dúvida, aquele amigo que não foi de sempre mas que ficará para todo o sempre.

À Xana que nasceu no mesmo dia que eu e ainda tenho as minhas dúvidas de que não nos tenham separado à nascença, porque a ligação que nos une é inabalável e ninguém adivinha aquilo que eu penso e sinto melhor do que ela.

Às Catarina, à Inês, ao Miguel e à Mariana que apareceram na minha vida de forma inesperada, que lhe vieram dar todo um novo sentido e que me orientaram e orientam sempre na direção do caminho certo: o da alegria! Um especial obrigada à Catarina Dias por ser a minha parceira de todas as horas neste lindo percurso que foi fazer parte da direção do NEB.

Às manas Fernanda, Tânia, Tania, Mariana, Rita, Maria, Carla, Vera e Filipa por serem a prova de que as amigas de infância podem durar uma vida! Mas principalmente à Mariana e à Tânia por, mais do que serem amigas, me deixarem ser genuinamente eu em todos os momentos, por me ajudarem e me acompanharem no processo de descoberta e autoconhecimento necessário ao fim de longos 5 anos na faculdades e por me darem sempre tanta força e amor.

Por fim, ao NEB que foi casa, alento, dedicação, trabalho árduo, superação e, sobretudo, muita mas muita força e união. Obrigada a todos os elementos do NEB que foram impecáveis e incansáveis. Levo-os a todos com um grande carinho no meu coração.

A todos, um gigante obrigada por aceitarem que vos lesse o mapa astral todos os dias, por alinharem os astros comigo e por me deixarem falar do meu Yang a toda a hora.

*“Life’s challenges are not supposed to paralyze you,
they’re supposed to help you discover who you are.”*

Bernice Johnson Reagon

Contents

1	Introduction	1
1.1	Context	1
1.2	Motivation	2
1.3	Contributions	3
1.4	Dissertation Outline	3
2	ANT-DBS for Epilepsy Treatment	5
2.1	Anterior Nucleus of the Thalamus	5
2.1.1	Basic Concepts of the ANT	5
2.1.2	The Role of the ANT in Seizures Propagation	7
2.2	Deep Brain Stimulation for Drug-Resistant Epilepsy	7
2.2.1	The Fundamentals of Deep Brain Stimulation	8
2.2.2	Deep Brain Stimulation Targets in Epilepsy	9
2.2.3	Adaptive and Closed-Loop DBS	12
2.2.4	Percept™ PC	14
2.3	ANT-DBS Studies for Drug Resistant Epilepsy Treatment	16
2.3.1	SANTE trial	16
2.3.2	Noncontrolled Studies	16
3	Studying the Motor Factors in Epilepsy	19
3.1	Understanding the Brain Mechanisms in Motor Processes	19
3.1.1	The Role of Motor Cortex in Movement	19
3.1.2	Neuronal Activity During Motor Functions	20
3.1.3	Recording Neurophysiological Signals	24
3.2	The Role of ANT on Motor Functions	26
3.2.1	Motor Experimental Paradigms	26
3.2.2	Motor-Cognitive Factors Processed in the ANT	26
3.3	Event-Related Desynchronization/Synchronization Analysis	27
3.3.1	Preprocessing	27
3.3.2	Quantification of ERD/ERS in Time and Space	29
3.3.3	Determination of Subject-Specific Frequency Bands	31
3.3.4	Time-frequency Domain Analysis	31
3.4	Epileptic Seizure Semiology	33
3.4.1	Motor Seizures	34
4	Understanding the Role of the ANT in Motor Function: A Study Protocol Design	37
4.1	Setup	37
4.1.1	Outline	37
4.1.2	Auditory and Visual Cue	38
4.1.3	Electrophysiological Signal Recording	38
4.2	Experimental Protocol	41
4.3	Methods	42
4.3.1	Non-invasive EEG Movement Study	42

4.3.2	iEEG Movement Study	45
4.3.3	LFP Movement Study	47
5	Results and Discussion	51
5.1	EEG Movement Study	51
5.1.1	ERD/ERS Quantification and TFA	51
5.1.2	Alpha and Beta Rhythms	55
5.2	iEEG Movement Study	58
5.2.1	Results	58
5.2.2	Discussion	60
5.3	LFP Movement Study	61
6	Conclusions and Future Work	69
A	Bi-ANT DBS in Epilepsy	71
	References	73

List of Figures

1.1	Schematic representation of seizure classification	1
2.1	Schematic representation of the Thalamic Nuclei.	6
2.2	Targets of deep brain stimulation.	9
2.3	RNS neurostimulator and NeuroPace cortical strip and depth leads. Copyright © 2020 NeuroPace, Inc.	13
3.1	Relationship between amplitude and frequency of brain oscillations in lower alpha and upper alpha bands	20
3.2	Grand average ERD curves in alpha and beta bands and the grand average maps during and after movement in alpha band.	21
3.3	ERD curves and ERD and ERS maps.	21
3.4	Individual ERD/ERS curve in the alpha frequency band and their respective grand average ERD/ERS curves for finger, thumb and wrist movements.	22
3.5	Individual ERS curve in the alpha frequency band and their respective grand average ERS curves for finger, thumb and wrist movement end.	23
3.6	Example of ERD/ERS time course for movement with right hand and both feet.	23
3.7	10-20 system of electrode placement.	24
3.8	Cortical homunculus representation	25
3.9	General schematic of a experimental motor paradigm.	26
3.10	Examples of ICs correspondent to artifacts.	28
3.11	Schematic for processing ERD and ERS.	29
3.12	ERD/ERS curves and ERD/ERS spatial maps of left arm movement.	30
3.13	A representative example of time-frequency maps for ME of two movements.	32
3.14	Epileptic seizure semiology.	33
4.1	Photograph of the experimental setup used to study movement with EEG signals in healthy subjects.	38
4.2	Photograph of the Micromed SD LTM 64 PLUS headbox.	39
4.3	Photograph of the Sony Hi8 360x Zoom digital video camera.	39
4.4	Micromed SD LTM 64 EXPRESS headbox and SD LTM Cortical Stimulator	40
4.5	Percept TM PC neurostimulator.	40
4.6	Motor paradigm tasks.	41
4.7	Developed motor paradigm.	42
4.8	Developed setup for non-invasive EEG movement study.	43
4.9	Electrode array used in EEG movement study	44
4.10	Developed setup for iEEG movement study.	45
4.11	Target positions for iEEG movement study.	46
4.12	Developed setup for LFP movement study.	48
5.1	ERD/ERS time course for finger to nose movement.	52
5.2	Time-frequency maps for finger to nose movement executed by subject 3.	52
5.3	ERD/ERS time course for hand tap movement with the right hand.	53
5.4	ERD/ERS time course for hand tap movement with the left hand.	53

5.5	ERD/ERS time course for rubbing hands movement.	54
5.6	ERD/ERS time course for circles with the hands movement.	55
5.7	ERD/ERS time course for non repetitive movements.	56
5.8	ERD/ERS time course for chewing.	57
5.9	ERD/ERS time course for finger to nose movement for alpha and beta rhythms.	57
5.10	1-second power spectra relative to the activity period 1-2 seconds after movement offset.	58
5.11	ERD/ERS time course for finger to nose movement in subject 3 specific frequency.	58
5.12	Time-frequency maps obtained for finger to nose movement in hippocampus targets.	59
5.13	ERD/ERS time course for finger to nose movement executed before and after the stimulation.	60
5.14	Time-frequency maps obtained for movement paradigm.	63
5.15	Time-frequency map for movement paradigm obtained in frequency range of 7-17 Hz.	64
5.16	ERD/ERS time course for movement paradigm in 7-17 Hz frequency range.	64
5.17	Representation of the selected target and its trajectory.	65
5.18	Y coordinates of the thumb of the patient's right hand over time.	65
5.19	Overlay of the time-frequency map in the frequency range 7-17 Hz and the representative movement signal.	66
5.20	Detected peaks in ERD/ERS time course for movement paradigm, executed without stimulation, and exemplified frames.	67
5.21	Cross-Correlation between the ERD/ERS curve and the movement signal represented by Y coordinates.	68
5.22	Overlay of the ERD/ERS curve and the representative motion signal.	68

List of Tables

2.1	Patterns and function of the subnucleus of the anterior nucleus of the thalamus.	6
2.2	Parameters most frequently used in DBS for epilepsy	12
2.3	Type of LFP data collected for each BrainSense™ feature. Adapted from (UC202013068EE© MEDTRONIC2020).	15
2.4	SANTE trial stimulation parameters.	16
3.1	EEG rhythms and its features.	24
4.1	Targets' details for iEEG movement study.	46
A.1	Clinical studies of Bi-ANT DBS for the treatment of DRE.	71
A.2	Continued -Clinical studies of Bi-ANT DBS for the treatment of DRE.	72

Abbreviations and Symbols

AED	Antiepileptic Drug
AM	Anteromedial
ANT	Anterior Nucleus of the Thalamus
AV	Anteroventral
BP	Bereitschaftspotential
BSS	BrainSenseStreaming
CHUSJ	Centro Hospitalar Universitário de São João
CMNT	Centromedian Nucleus of Thalamus
CN	Caudate Nucleus
CWT	continuous Wavelet Transform
DBS	Deep Brain Stimulation
DRE	Drug-Resistant Epilepsy
DWT	Discret Wavelet Transform
EEG	Electroencephalography
EMU	Epilepsy Monitoring Unit
ERD	Event-Related Desynchronization
ERP	Event-Related Potential
ERS	Event-Related Synchronization
ERSP	Event-Related Spectral Perturbation
ET	Essential Tremor
FMS	Focal Motor Seizures
GUI	Graphical User Interface
IC	Independent Component
ICA	Independent Component Analysis
iEEG	Invasive Electroencephalography
ILAE	International League Against Epilepsy
IPG	Implantable Pulse Generator
LFP	Local Field Potentials
MB	Mamillary Bodies
MRI	Magnetic Resonance Imaging
PD	Parkinson's Disease
PTZ	Pentylenetetrazole
SANTE	Stimulation of the Anterior Nucleus of the Thalamus for Epilepsy
SC	Superior Colliculus
STN	Subthalamic Nucleus
TFA	Time-Frequency Analysis
TFD	Time-Frequency Distribution
TLE	Temporal Lobe Epilepsy
VA	Ventral Anterior
VL	Ventrallateral Nucleus
VLm	Ventrolateral Pars medialis
VLo	Ventrolateral Pars oralis
VPL	Ventral Posterolateral
VPM	Ventral Posteromedial
WT	Wavelet Transform
WTP	Wavelet Packet Transform

Chapter 1

Introduction

1.1 Context

The International League Against Epilepsy (ILAE) describes epilepsy as a neurological disease consisting of a predisposition to generate recurrent and unpredictable epileptic seizures. In order to diagnose this disease, one or more conditions must be verified. These factors are the occurrence of at least two unprovoked seizures within more than one day, one unprovoked seizure, and a probability of further seizures of at least 60% after the second unprovoked seizure, occurring within ten years, or the diagnosis of an epilepsy syndrome (1; 2).

Epileptic seizures, which are characteristic of this disease, are a consequence of altered normal functioning of neuronal activity in the brain. In these cases, electrical discharges occur that make neuronal activity excessive or synchronous. These episodes manifest themselves through signs or symptoms that last a few seconds or minutes (3). The location at the onset of abnormal neuronal activity allows seizures to be classified, which manifest differently depending on their classification. Seizures can be focal, generalized, or unknown. The former occurs when electrical discharges initially happen in one or more localized regions of the brain. On the other hand, generalized seizures occur due to abnormal neuronal activity in both brain hemispheres and have a generalized location. Finally, when there is not at least 80% confidence that the seizure corresponds to one of the previous classifications, it is classified as unknown. Regardless of its classification, an epileptic seizure can manifest itself in either motor or non-motor forms (see figure 1.1) (4; 2).

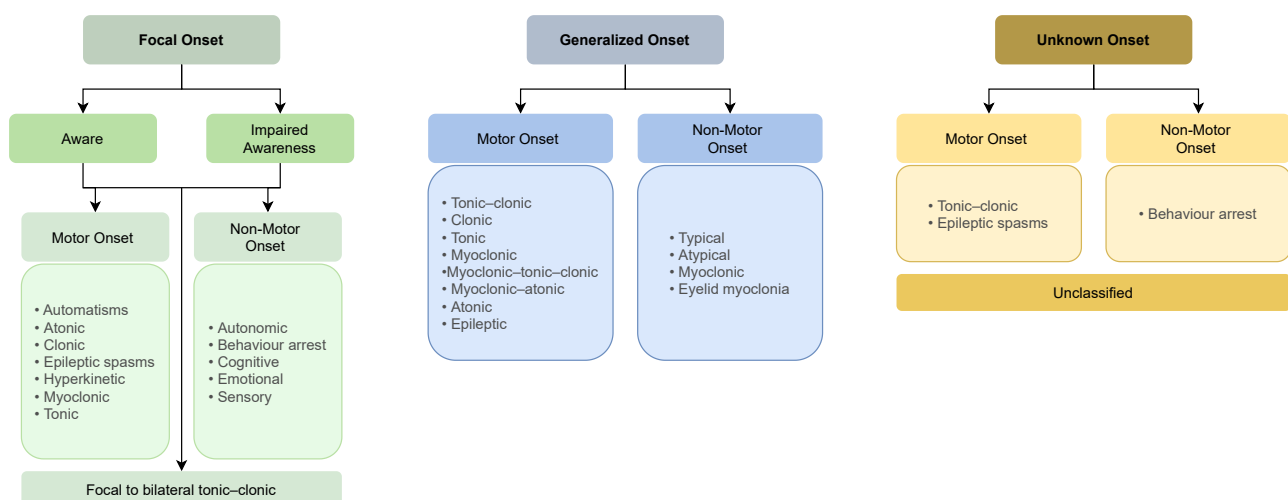


Figure 1.1: Seizure Classification according ILAE - Expanded version . Adapted from (4).

The least invasive and most common treatment for epilepsy is the use of one or more antiepileptic drugs

(AEDs). This solution is adequate for most epileptic patients. However, some patients report continuing recurrent seizures, limiting their quality of life (5). More often, resective surgery is used to treat patients with drug-resistant epilepsy (DRE). However, many of these patients cannot undergo this type of surgery, therefore creating the need for other alternatives to arise (6; 7).

Deep brain stimulation (DBS) is an invasive technique involving the implantation of electrodes that deliver electrical impulses to specific locations in the brain (8). This neuromodulation technique is effective and safe in treating neurological movement disorders, such as Parkinson's disease (PD) or dystonia. The promising results in treating these diseases have reportedly encouraged researchers to extend its application to drug-resistant epilepsy, representing 30% of the epileptic population (5). Several studies have shown the effectiveness of this treatment in reducing the frequency of seizures (9; 10).

The anterior nucleus of the thalamus (ANT) connects to the subicular and retrosplenial cortexes and the mammillary bodies via three constituent subnuclei (11). Several animal studies have shown that ANT plays an important role in seizure propagation. Since then, the interest in ANT-DBS for the treatment of refractory epilepsy has increased (11).

Stimulation of the anterior nucleus of the thalamus for epilepsy (SANTE) is the only clinically controlled trial of ANT-DBS. The results of this bilateral trial have proven its safety and effectiveness in reducing seizure frequency, showing its potential in treating patients with DRE (12).

1.2 Motivation

Although in most cases, the epilepsy treatment is simple and non-invasive, patients with drug-resistant epilepsy still constitute a considerable portion of epileptic patients and see their lives limited by the consequences of the disease and the lack of effective treatments (5). In addition to the adverse effects that recurrent seizures have on their quality of life (13), this disease causes psychological conditions (14) and an increased mortality risk (15; 16). Thus, alternative treatments to medication such as ANT-DBS are of great interest for the treatment of these patients.

In January 2020, Medtronic launched the novel Percept™ PC neurostimulator in the European Union. This is the first certified DBS neurostimulator that, in addition to stimulating, can read signals from deep brain structures simultaneously. This deep brain stimulation system is a promise in adaptive DBS. It allows neuronal monitoring activity in the deep brain nuclei, as the ANT, and defines symptoms or side effects (17).

In June 2020, the Percept™ PC neurostimulator was first implanted, in an epileptic patient resistant to anti-epileptic drugs, at the São João University Hospital in Porto, Portugal ¹.

For the first time, the monitoring of electrical signals in deep brain areas, as well as on the surface, through conventional electroencephalography, while programming different levels of brain stimulation has been made possible for the first time. This opened up the possibility of better detecting or even predicting the occurrence of epileptic seizures.

Thus, the Percept™ PC could be used to investigate the existence of seizure-related biomarkers, namely motor-related potentials, in the ANT to be later able to detect and predict seizures utilizing this system.

¹Portugal is the first in the world to implant neurostimulator with long-term monitoring in epileptic patients. Available at: <https://www.inesctec.pt> (Accessed 18-04-2021)

1.3 Contributions

An epileptic seizure can manifest itself through both motor and non-motor phenomena. Although this type of seizure may be accompanied by loss of consciousness or emotional and cognitive processes, this dissertation will focus more on motor-related seizure semiology. Motor manifestations may include, for example, automatisms or epileptic spasms (4).

The main goal of this project is to understand if there are biomarkers associated with epileptic seizures in the ANT by performing a motor paradigm with movements characteristic of these same seizures. To do this, we intend to use the Percept™ PC neurostimulator to stimulate and monitor the electrical activity of ANT in epileptic patients.

The main contributions of this project are thus described below.

1. Create an experimental protocol based on movements characteristic of an epileptic seizure in ANT-DBS patients with drug-resistant epilepsy undergoing video-electroencephalography (vEEG) monitoring;
2. To assemble a simple experimental setup designed to study the neurophysiological signals associated with specific movements;
3. To validate the experimental paradigm with healthy volunteers and an epileptic patient, replicating the results from the literature about the electrophysiological signals associated with movement;

1.4 Dissertation Outline

This dissertation will address the background, methodologies, and results of the project developed to evaluate biomarkers associated with epileptic seizures in ANT and how their stimulation may influence the previous ones. Therefore, this dissertation is divided into the following chapters:

- Chapter 2 - [ANT-DBS for Epilepsy Treatment](#): Overview on deep brain stimulation of the anterior nucleus of the thalamus.
- Chapter 3 - [Studying the Motor Factors in Epilepsy](#): Presentation of processing motor factors in the brain and their relation to the anterior nucleus of the thalamus and epilepsy.
- Chapter 4 - [Understanding the Role of the ANT in Motor Function: A Study Protocol Design](#): Presentation of the developed protocol and the employed motor paradigm.
- Chapter 5- [Results and Discussion](#): Report of the obtained results concerning the developed studies.
- Chapter 6 - [Conclusions and Future Work](#): Presentation of the final critical observations to retain the key points of the carried out work, as well as the obtained results.

Chapter 2

ANT-DBS for Epilepsy Treatment

2.1 Anterior Nucleus of the Thalamus

2.1.1 Basic Concepts of the ANT

The thalamus is part of the diencephalon and is its most prominent element. This portion has an oval shape and has three different types of nuclei: relay nuclei, association nuclei, and nonspecific nuclei. The former have well-defined inputs and connect to nuclei that relay general sensations, such as the ventral posterolateral (VPL) and ventral posteromedial (VPM). The signals received by the relay nuclei are also transmitted to the ventral lateral nucleus (VL), which is involved in the feedback of cerebellar signals, to the ventral anterior nucleus (VA), responsible for feedback of the output of the basal ganglia, and finally to the special sensory nuclei of the medial and lateral geniculate. On the other hand, the association nuclei receive information from the cerebral cortex and project back to it, connecting to the association areas regulating multimodal input in the cerebral cortex-pulvinar nuclei. Finally, the nonspecific nuclei, of which the intralaminar and midline thalamic nuclei are a part of, have extensions across the cerebral cortex, and these may be involved in functions such as alertness (18).

The thalamus consists of the dorsal thalamus or simply thalamus, ventral thalamus, and epithalamus. It is further divided into several nuclei: anterior, medial, midline, intralaminar, lateral, posterior, reticular, and metathalamus. Figure 2.1 shows a schematic representation of the anatomy of the thalamus and its nuclei (18).

The Anterior Nucleus of the Thalamus is located in the most rostral part of the thalamus. It consists of the anteroventral (AV), anterodorsal, and anteromedial (AM) sub-nuclei that connect differently with other elements of the brain (18). The connective patterns and function of the most significant ANT subnuclei are detailed in the table 2.1.

The AM subnucleus connects through extensive and reciprocal interactions to the anterior cingulate and orbitomedial prefrontal cortex. These connections transmit information to involved areas of the medial frontal lobe, thus interfering with emotional and executive mechanisms. On the other hand, the AV's most extensive interactions connect it to the subiculum and the retrosplenial cortex. This sub-nucleus and the medial mammillary nucleus promote synaptic plasticity in the hippocampal area by transmitting theta rhythm activity. Finally, the anterodorsal helps in mammalian spatial navigation by connecting with the lateral nucleus, the subiculum and the retrosplenial cortex (18).

The ANT is part of the hippocampal system and is primarily known for its importance for episodic memory. The main causes for the latter's deficit are likely to be damage to the ANT and its extensions to the mammillary bodies. However, this target has increased study interest due to evidence showing its possible involvement in seizure propagation (11).

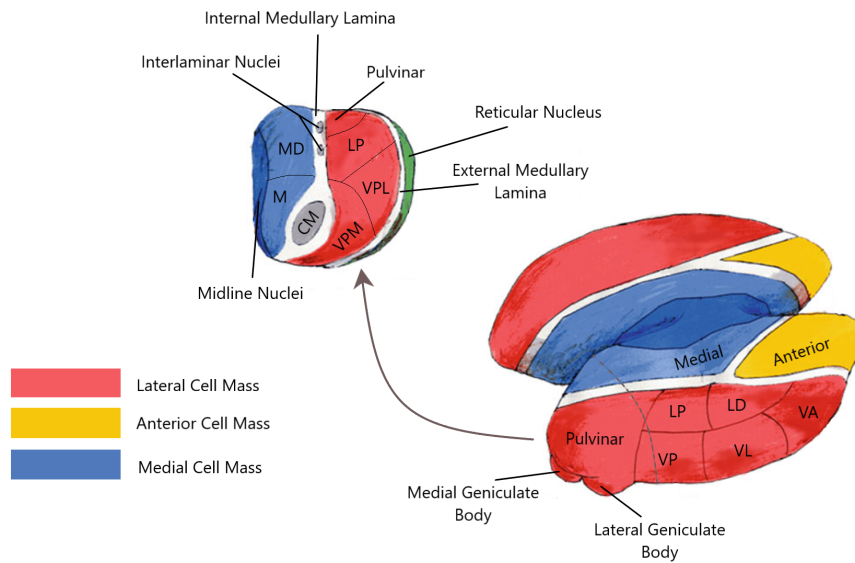


Figure 2.1: Schematic representation of the Thalamic Nuclei. Extracted from (18).

Table 2.1: Patterns and function of the subnucleus of the anterior nucleus of the thalamus. Adapted from (11).

Subnucleus	Cortical input	Mammillary input	Cortical output	Function
Anteromedial	Subiculum retrosplenial cortex	Medial mammillary nucleus	Anterior cingulate and medial prefrontal cortices	“Feed-forward” system conveying integrated hippocampal signals to prefrontal areas involved in emotional and executive functions
Anteroventral	Subiculum retrosplenial cortex	Medial mammillary	Subiculum, presubiculum, and parasubiculum	“Return loop” system conveying theta activity critical for plasticity in the hippocampal circuit
Anterodorsal	Postsubiculum retrosplenial cortex	Lateral mammillary	Postsubiculum retrosplenial cortex	Head-direction signal (supporting mental navigation)

2.1.2 The Role of the ANT in Seizures Propagation

In 1971, Kusske *et al.* (19) conducted a study to understand the effects of ipsilateral lesions on ANT. For this purpose, animal models with focal cortical epilepsy were used. By the fourth week after the lesions, their results were already visible: the frequency and duration of epileptic seizures decreased in the five rhesus monkeys under study compared to the control group. The primates were monitored during this period, and there were no changes in their behavior or neurological function.

Later, Mirski *et al.* (20) conducted an experiment where they applied microinjections of neuroactive compounds into the ANT. Bilateral muscimol microinjections of a selective GABA-transaminase inhibitor injected into the guinea pig ANT inhibited both behavioral seizure action and synchronous high-voltage electroencephalography (EEG) discharges induced by pentylenetetrazole (PTZ). Following this experiment, another one reinforced the efficacy of bilateral injections into the ANT of GABA-transaminase enzyme suicide inhibitor in combating PTZ-induced seizures in rats (21).

The association of ANT and its connections with the spread of seizures became more evident when a study showed that the perturbation between mamillary bodies (MB) and ANT inhibited behavioral action, EEG activity, and lethal effects of PTZ. To do this, they caused bilateral electrolytic lesions in the mammillothalamic connection (22). Similar results were reported after high-frequency electrical stimulation of the MB of rats. In order to obtain these results, specific bilateral stimulation of 100 Hz (1-5 V, 30-200 PA) was used (23). The influence of low dose PTZ-induced cortical bursting was not altered by reproducing high-frequency stimulation in the ANT of rats. However, it inhibited the triggering of clonic seizures while low-frequency stimulation with 8 Hz lowered the threshold for the first paroxysmal EEG bursts proving to have an opposite role of high-frequency stimulation (24).

Although high-frequency stimulation of the ANT effectively inhibits seizure propagation, a study in animal models found that unilateral stimulation of this target does not contribute to decreasing seizure development. On the other hand, this same study proved the efficacy of bilateral high-frequency thalamic stimulation in achieving the proposed goal. Thus, the need to use bilateral ANT stimulation was concluded to prevent seizure propagation (25).

Therefore, ANT has become a focus of interest in epilepsy, and ANT-DBS has proven to be a safe and effective treatment for patients with refractory epilepsy (10).

2.2 Deep Brain Stimulation for Drug-Resistant Epilepsy

DBS is a neuromodulation procedure in which it is necessary to implant electrodes in target points of the brain. This procedure allows the brain to be provided with small electrical stimuli from a battery source, usually called an implantable pulse generator (IPG), which is key to treating some neurological diseases. This battery is usually implanted through minimally invasive surgery in the chest area near the clavicle and establishes a connection with the brain electrodes through extension wires. The electrical impulses emitted are programmed for a given frequency, amplitude, and width depending on the disease to be treated and the desired procedure (8). These adjustments can be made externally, allowing a more effective response to the patient's changes and optimizing the treatment.

Although the knowledge around DBS is still limited, it is possible to prove that it is a safe and effective procedure and very promising. For this reason, it has been explored to treat several neurological conditions. PD, epilepsy, essential tremor, and dystonia are the best-known examples. However, some studies use this technology to treat depression, obsessive-compulsive disease and Alzheimer's, among others (8; 26).

2.2.1 The Fundamentals of Deep Brain Stimulation

Although DBS's mechanisms are not yet well known, studies indicate that this method has an inhibitory action on neuronal circuits. The blocking of depolarization and inactivation of voltage currents or the activation of GABAergic afferents of the stimulated nucleus should be the key to this phenomenon. Likewise, the therapeutic potential of DBS is not yet fully understood. Scientists are still unable to state whether the effects arise from stimulation neurons, glial cells, passage fibers, or afferent inputs to target neurons. The stimulation targets vary from disease to disease, and many authors have different theories. This stimulation can be done through direct application in the suspect areas of initiation of seizure, through an indirect application on deep subcortical structures to interrupt the epileptic nets, or even on deeply located fiber bundles connected to different systems inside the brain. The former alters the excitability of the tissue and the synchronization of the neurons, which can have an inhibitory effect. Direct targets include the hippocampus, amygdala, hypothalamus or specific cortical zones. The second cancels neuronal circuits that favor the emergence of apprehension. These targets include the cerebellum, basal ganglia and thalamus. Finally, the latter changes the threshold of apprehension induction.

In order to apply DBS in the patient's brain, it is necessary to resort to electrode implantation surgery. Before surgery, through magnetic resonance imaging (MRI) of the patient's brain, the target region's stereotactic coordinates are obtained. During the surgery, the image orientation is used to place permanent microelectrodes in the patient's brain.

The neuro-stimulation can be open or closed cycle depending on the method applied. In open-loop stimulation, there is chronic, intermittent, or continuous stimulation that inhibits the occurrence of seizures without taking into account either the patient's symptoms or EEG activity. Closed-loop neurostimulation uses an implantable device that detects seizures and adjusts to the changes occurring from the EEG. This second approach has proven to be more efficient in the treatment of epilepsy (10).

2.2.1.1 Electrode and IPG Design

The IPGs are pulse generators used in DBS and are responsible for providing small electrical impulses in the brain targets. These electrodes must have as the main features of biocompatibility, good conductivity and electrical properties, and appropriate current delivery and spatial configuration to fully fulfill their function.

The most used IPG configuration on DBS is the quadripolar one. This configuration consists of four electrode contacts at the tip of the probe to be equally spaced apart. This is used as it allows for shaping the electric field, hence overcoming some of the conventional electrodes' limitations. The quadripolar arrangement is an example of directional electrodes that would enable the electric field's modeling and increase the treatment's effectiveness while reducing the undesirable effect (27).

However, this type of electrode is not simple to implement or program. Furthermore, this configuration only allows the electrical field to be shaped in the vertical direction when applying high current amplitudes (8).

2.2.1.2 Stimulation Methods

The shape of the stimulation current or voltage function as a function of time is called a stimulation waveform. When this form is repeated, stimulation patterns are created (28).

Studies with patients with Parkinson have shown symmetric biphasic stimulation to be more effective than conventional asymmetric DBS in reducing the motor symptoms of this disease. However, this method requires an extra battery drain. Some studies demonstrated the same in patients with Essential Tremor (ET) as symmetric biphasic activates a larger number of neurons (29).

Another study with PD patients treated with STN DBS revealed that the adverse effects increased and the reduction in motor symptoms was less significant when anodic stimulation with threshold amplitudes was used. On the other hand, when decreasing the amplitude values below this threshold, anodic stimulation proved to be more effective in reducing undesirable symptoms than cathodic stimulation (30).

Selecting the optimal pattern is very challenging, especially in conditions that concur with transient and isolated albeit significant results and a limited observation. This is the case of epilepsy, as the frequency of seizures is very unpredictable (31).

2.2.2 Deep Brain Stimulation Targets in Epilepsy

DBS can be used in the treatment of epilepsy when patients do not respond well to anti-epileptic medication. Although the most common alternative is resective surgery, it is impossible to identify a susceptible focus to undergo resection in some patients.

To date, there has been little evidence regarding the parameters that should be used for epilepsy stimulation. Moreover, these parameters are dependent on the target to be stimulated (26).

In the treatment of epilepsy based on DBS, there are commonly chosen target regions. Among those are the subthalamic nucleus, hippocampus, cerebellum, cortex, and thalamus, specifically the ANT, as illustrated in figure 2.2. Some studies have shown a higher incidence of this type of treatment in ANT (10).

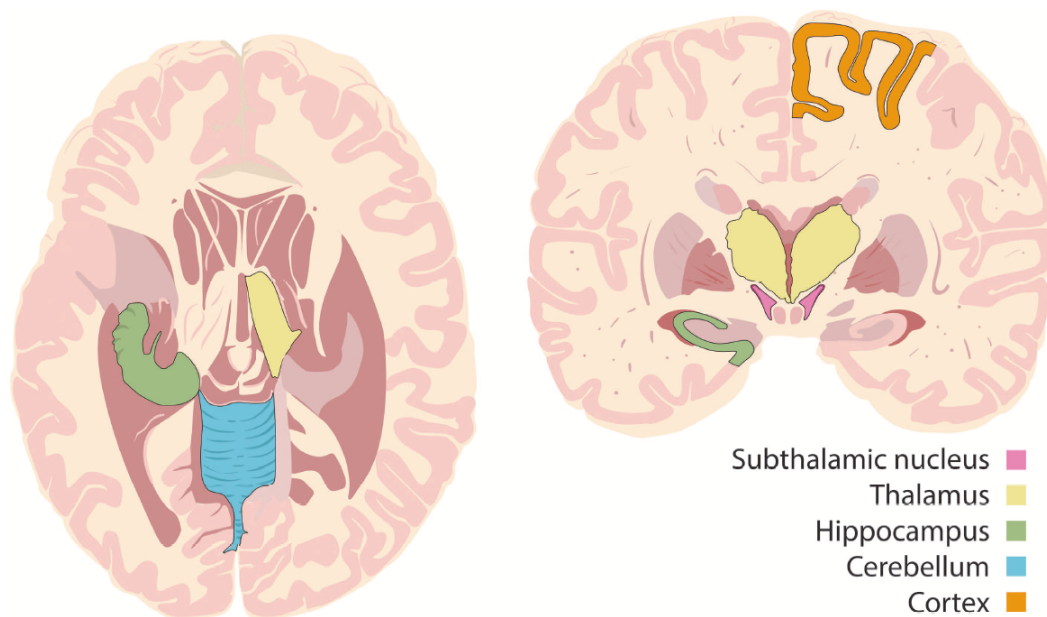


Figure 2.2: Targets of deep brain stimulation. Extracted from (10).

2.2.2.1 Anterior Nucleus of the Thalamus

ANT has been increasingly studied and has been the preferred target of researchers since it is an essential region for controlling the spread of seizures. This phenomenon is due to ANT's connections with the limbic system and generalized projections with areas involved in the pathogenesis of focal epilepsy, such as the hippocampus.

Some studies have found a reduction in seizure frequency in a large proportion of patients studied. ANT-DBS has short-term results that remain or become more effective in the long term. Despite this, the most common adverse symptoms are sleep disturbance and neuropsychiatric symptoms. The studies and their results led to a clinical trial in 2010 called SANTE. This study involved 110 patients, and bilateral implantation was performed at ANT. One month after the start of the double-blind trial, the patients were randomly selected

for a stimulation or non-stimulation regimen. At the end of the three-month blind phase, all patients received stimulation (32). After the 25th month of follow-up, there was a significant reduction in the frequency of seizures and even more promising results in patients with focal seizures and altered consciousness. Transient stimulus-induced seizures were reported in 2 patients. However, no cases of symptomatic hemorrhage or death were reported. Depression and memory loss are adverse effects most commonly reported by stimulated patients. SANTE will be explained in more detail in the [SANTE trial](#).

ANT-DBS is even more effective when ANT-DBS is done simultaneously with EEG recording to monitor EEG desynchronization (10).

2.2.2.2 Centromedian Nucleus of Thalamus (CMNT)

Some animal studies have shown that CMNT is a crucial target at the beginning of seizures (33; 34). In a controlled pilot study of CMNT stimulation, Fisher *et al.* demonstrated a 50% reduction in the frequency of seizures in three of the seven patients under investigation. These had been treated with continuous 24 h/day stimulation trains (35).

In another study with eleven patients with frontal lobe DRE or generalized epilepsy, bilateral DBS treatment targeting CMNT was successful in 64% of cases. Only one of the five patients with frontal lobe epilepsy presented more than a 50% reduction in seizure frequency during the blind period. Only two obtained the same result in the long-term extension phase. However, the six patients with generalized epilepsy resulted in a significant reduction in the frequency of seizures in the first phase, and five showed to maintain this improvement. DBS treatment with stimulation in CMNT proved to be a safe and effective treatment in patients with generalized refractory epilepsy, not useful in frontal lobe epilepsy (10).

2.2.2.3 Hippocampus

The central role of the hippocampus in epilepsy is related to hippocampal sclerosis. In turn, this condition is correlated with the seizures caused by Temporal Lobe Epilepsy (TLE). However, this disorder is quite prevalent in DRE patients whose alternative treatment involves surgery to resection the temporal lobe. The big problem with this treatment is that it cannot be performed in patients with specific features or pathologies. Thus, in these cases, DBS becomes the treatment of choice for the treatment of patients (36).

Velasco *et al.* were the pioneers of systematic studies of hippocampus stimulation with humans. The study involved ten patients before their surgeries to resect the temporal lobe's anterior portion (37). More recently, this group conducted another study to identify anatomical and functional changes in the hippocampus's amygdala in patients with TLE after being submitted to DBS (38). In this study, the researchers extended the follow-up period from 18 months to 7 years, which allowed them to verify patients with normal and abnormal MRIs. Although only about 60% of patients whose MRI detected hippocampal sclerosis obtained improvements with DBS treatment, it proved to be effective in virtually all patients with non-lesional epilepsy (95%). No patient undergoing treatment suffered neurophysiological lesions. However, some microlesions were caused in some patients whose deep electrodes were implanted in the temporal lobe.

On the other hand, Boon *et al.* (39) conducted a study with ten patients, but this time to study the effect of stimulation of the medial temporal lobe in a patient with DRE. After the follow-up period, which lasted about 31 months, the observed results were quite different among tested patients: a single patient had no seizures during the entire period; half of the individuals tested decreased the frequency of attacks by 50%. Of the remaining patients, there was one case that did not respond to treatment and only one case with a seizure reduction of more than 90%, while the remaining showed a decrease of seizure frequency of less than 50%. One patient

had asymptomatic intracranial bleeding after treatment, this being an exception as all other patients reported no severe side effects.

Although it proves to be a safe alternative for patients with TLE drug resistance, it should not be the priority alternative for treating these patients.

2.2.2.4 Caudate Nucleus (CN)

The caudate nucleus head is the best known and most studied structure of this target concerning the study of epilepsy. Studies have found that stimulation of this structure can decrease or suppress seizures due to inhibition resulting from cortex stimulation (40).

The low-frequency stimulation of the central zone of the head of the CN (4 - 8 Hz) supports this hypothesis since it showed to inhibit the decrease of the seizure activity in the neocortex, the reduction of focal discharges, and significant suppression of the generalized discharges (10).

On the contrary, high-frequency stimulation (30-100Hz) from the same region of the CN showed increased epileptic activity through the ipsilateral hippocampus, and amygdala (41).

Šramka and Chkhenkeli (42) conducted a study in which they used caudate and toothed nucleus stimulation with 74 patients. The results showed a decrease in epileptic activity.

In another study with 38 patients, Chkhenkeli *et al.* (43) stimulated ventral crown-rump length at low frequency. This stimulation resulted in improvements in 35 of the patients, and 21 were free of seizures. This investigation used a theory related to the output balance between pro-convulsant and anticonvulsant structures. The group pioneered studies in cases of TLE resistant to drugs with striatal stimulation (40). Considering the primary hypothesis, the results are contradictory, which proves the basal ganglia's capacity in modulating the cortex's epileptogenicity.

Although the results are promising, controlled trials are needed to ensure this method's effectiveness and safety. Furthermore, this target is not currently used in the treatment of DRE.

2.2.2.5 Subthalamic Nucleus (STN)

Cortical synchronization can be the pathological cause of motor seizures. In this sense, STN stimulation has been in vogue as an option to treat this condition. Studies done to treat Parkinson's Disease (PD) with DBS have shown that STN is compact and distinct, making it a target for electrode stimulation (44).

In a study involving three patients with DRE, Benabid *et al.* (45) investigated the consequences of implantation with STN-DBS. The entire study group showed a decrease in the frequency of seizures. Among the improvements, the reduction of cluster seizures (89%) and daytime seizures (88%) stand out (46).

In another study with patients aged from 5 to 38 years (17.6 ± 12.7), Chabardes *et al.* (46) showed that about 80% of patients reduced the frequency of seizures by about 60%. The procedure proved to be effective. However, a device infection was reported in one patient and a subdural hematoma in a second patient.

STN-DBS can be a procedure to be applied in some instances and pathologies related to epilepsy. However, more controlled tests are needed to prove its safety and effectiveness.

2.2.2.6 Cerebellum

The cerebellum is one of the DBS targets to be studied first through the cerebellar nuclei (47). Its effectiveness is because the stimulation of this structure causes a decrease in cortical excitability. In turn, the latter is the key to cease generalized spike-and-wave discharges, as evidenced by studies with rats (48).

Velasco *et al.* (49) conducted a study with DRE patients and motor seizures. The control study was double-blind and randomized. At the end of 6 months, the entire study group showed a reduction of about 41% in the frequency of seizures versus the control group. At the end of 2 years, the patients who continued and were followed up showed a decrease in seizure rate of 24%. This study proved not to be promising since the electrodes' migration led to a new surgery in most of the patients (60%). Also, about 20% of the patients revealed a severe infection.

Thus, the effectiveness and safety of this technique have not been confirmed.

2.2.2.7 Hypothalamus

The mammillary bodies are an integral part of the hypothalamus. This structure has been studied due to the discovery of its epileptiform activity. Thus, the hypothalamus became a potential target for DBS (50). Stimulation of the mammillo-thalamic structure demonstrated a reduction in the frequency and severity of crises (51).

In a study conducted by Franzini *et al.* (52), two patients in the study reported an improvement in the frequency of seizures by about 80% after the 9-month follow-up.

Another study targeting the posteromedial hypothalamus demonstrated a 90% reduction in seizures in patients with DRE and intractable aggressive behavior. The follow-up was carried out over five years (53).

However, it is essential to note that the hypothalamus regulates functions such as the sleep-wake cycle. Any damage such as bleeding resulting from the electrode's placement can alter these functions and the consequent quality of life for the patient. Therefore, this target is not advisable (54).

The parameters used when using DBS for each target depend on the target's features and functions. Besides, there are several distinct values documented in the literature. Thus, table 2.2 presents the most common parameters and respective values for some of the targets shown.

Table 2.2: Parameters most frequently used in DBS for epilepsy (10).

	Parameter	Value
ANT	• Frequency	$\geq 100\text{Hz}$
	• Voltage	1-10V
CMNT	• HFS	1-10V
	• Voltage	1-5V
Hippocampal and STN	• Frequency	$\geq 130\text{Hz}$
	• Voltage	1-5V
Cerebellum	• Low stimulation	10Hz
	• High stimulation	200Hz

2.2.3 Adaptive and Closed-Loop DBS

Adaptive DBS has been increasingly sought after due to its effectiveness and decrease in adverse symptoms. This type of stimulation has become necessary in treating diseases such as PD and epilepsy since it allows a dynamic stimulation that follows the patient's needs.

Local Field Potentials (LFPs) are generated in the extracellular space in a local region where the implanted electrode occurs in which neuronal reactions occur. These potentials are the most commonly chosen biomarkers to close the feedback loop on the DBS. However, the used biomarkers are dependent on the patient and his condition. For example, in treating some PD-related symptoms, beta frequencies are used, while for other signs of the same disease, gamma frequency is used (8).

In 2018, Swann *et al.* (55) conducted a study of only two patients with PD involved using innovative brain-sensing technology (Activa PC+S) to mitigate the adverse symptoms of dyskinesia. In this way, they used a gamma frequency directly related to the mentioned symptom. The results of this study showed its effectiveness in the short-term attenuation of dyskinesia.

Concerning the treatment of epilepsy, the most studied and promising technology is the Neurospatial Neurostimulator. This device allows a stimulation before the seizure that is detected through the alteration of neuronal activity. This type of neurostimulation has proven to be effective and safe in reducing partial-onset seizures. Elder *et al.* (56) demonstrated that the combination of responsive neurostimulation systems, such as NeuroPace, with ANT stimulation is also useful for multifocal or generalized-onset seizures.

Although Closed-Loop DBS is a technique increasingly used, studies with this method focus mostly on PD treatment.

Published studies with proven results in epilepsy use the RNS System (NeuroPace, Inc, Mountain View, CA). This system contributes to reducing the frequency of seizures in adult DRE with partial-onset seizures with a maximum of 2 epileptic foci and it is approved by FDA (57). To do so, it uses the programmable RNS neurostimulator, which is implanted in the skull and connected to one or two profound and/or subdual cortical clues placed according to the focus, as represented in figure 2.3.

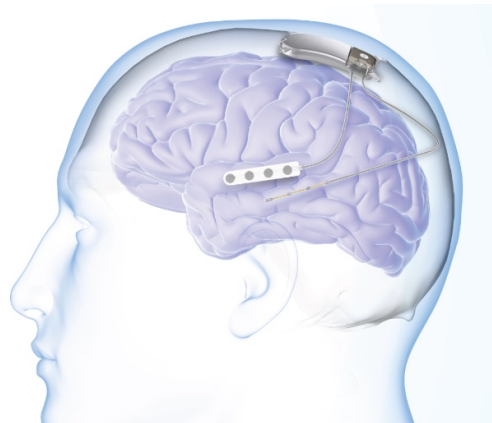


Figure 2.3: RNS neurostimulator and NeuroPace cortical strip and depth leads. Copyright © 2020 NeuroPace, Inc.

In a study carried out over nine years, Nair *et al.* intended to evaluate the safety, efficiency, and quality of life when brain-responsive neurostimulation with the RSN System. After 2-year feasibility or randomized controlled trial, 230 out of 256 patients treated with neuro-stimulation participated in a 7-year open-label trial. In order to evaluate safety, efficacy, and quality of life during treatment, the first one was assessed according to the adverse effects that occurred, the second corresponded to the median percentage change in the frequency of crises and response rate, and the last one was based on Quality of Life in Epilepsy (QOLIE-89) inventory (58). During the entire study period, no serious adverse events directly associated with stimulation occurred. At the end of the study, it was found that both the median percent reduction in seizure frequency and the responder rate presented auspicious values, being their percentages, respectively, of 75% and 73%. Besides, 35% of patients saw their seizures reduced by at least 90%, and 47 of them had no seizure during the minimum period of one year. More than half of them were seizure-free at the end of the last follow-up. Finally, the quality of life of the patients has generally improved (58).

Other older studies, aiming to evaluate the same brain-responsive stimulation parameters but in partial-onset seizures of neocortical or mesial temporal lobe originated, showed relatively similar results to the study mentioned above (59; 60). However, Geller *et al.* (60) demonstrated that mesial temporal sclerosis, bilateral

mesial temporal lobe onsets, prior resection, prior intracranial monitoring, and previous vagus nerve stimulation did not influence the seizure reduction in the subjects under study. Likewise, this parameter was not affected by the location of depth leads relative to the hippocampus. Similarly, Jobst *et al.* (59) showed that the results were the same regardless of whether prior epilepsy surgery or vagus nerve stimulation occurred.

Thus, the studies conclude that brain-responsive neurostimulation is an effective and safe procedure and that it has improved people's quality of life, being therefore very promising. However, the scarcity of closed loop DBS studies aimed at the treatment of epilepsy highlights the importance of further studies in this direction.

2.2.4 Percept™ PC

Percept™ PC is a neuro-stimulator launched in 2020 by Medtronic, initially in the European Union and later in the USA. This device is the only certified stimulator with the particularity of its primary stimulation function, reading signals from deep brain targets. Its novel BrainSense technology allows associating deep brain signals with the state and changes in the patient (61).

In the Adaptive DBS study, the LFPs registered from DBS electrodes were pointed out as possible biomarkers in this stimulation type. Despite the few studies in the area, the investigations on LFPs reported from ANT showed the potential effectiveness of a closed cycle in ANT.

Thus, Percept™ PC intends to be an added value in this sense. This device has several different forms of sense-data whose features are highlighted in table 2.3.

The BrainSense™ Survey intends to provide an extended spatial field of LFP signals while there is no stimulation. In all Sensing types presented, the data comes from both brain hemispheres, but the Survey, in particular, uses 12 channels that are divided into two passes. Half of the electrodes are responsible for compatible pair data collection, while the other six simultaneously use immediately adjacent pairs. A graph is displayed at the user interface, where each LFP graph shows the differential signal between two contacts. The results allow to conclude about the similarity between the two brain regions.

The Timeline analyzes data regarding the activity of LFP signals that occur outside the clinical office. BrainSense™ records LFP power domain data when active. Initially, the stimulator measures raw time-domain data, which is converted to a frequency domain. Then it calculates the power in a specific band of approximately 5 Hz wide. LFP power and stimulation amplitudes are measured in a ten-minute interval and recorded in the neuro-stimulator memory.

BrainSense™ Events refers to LFP snapshots and displays the magnitude of the LFP over a range of frequencies at a given time. The register happens when the patient registers an event configured by the clinician. After the snapshot, the 30 seconds of measured LFP time domain is converted to a frequency domain, and only the data concerning the average of the frequency domain is stored.

Finally, BrainSense™ Streaming allows real-time observation of the LFP power on a chosen band frequency. This enables the statement of LFP changes during the active stimulation or instructing programming and verifying the patient's activities. This type of sensing can be used to record time-domain data of selected channels for signal processing, for example. Usually, the time domain data measured and recorded by the neuro-stimulator is sampled at 250 Hz, and the user must complete the BrainSense™ Setup before moving on to any of the other Sensing modes, except the Survey.

Table 2.3: Type of LFP data collected for each BrainSense™ feature. Adapted from (UC202013068EE© MEDTRONIC2020).

	LFPs Signals	Features
BrainSense™ Survey	LfpMontageTimeDomain (LfpMTD)	Domain: Time Use: In-clinic Stimulation: off Time Length: 20 s Channels: 12 (6 in Pass1 and 6 in Pass2)
	LfpMontage (LfpM)	Domain: Frequency Use: In-clinic Stimulation: off Time Length: 20 s Channels: 12 (6 in Pass1 and 6 in Pass2)
	IndefiniteStreaming (IS)	Domain: Time Use: In-clinic Stimulation: off Time Length: up to 15 min Channels: 12 (6 in Pass1 and 6 in Pass2)
BrainSense™ Timeline	BrainSenseTimeline (BST)	Domain: Power Use: In and out-clinic Stimulation: on/off Time Length: indefinite Channels: 2
BrainSense™ Events	LfpSnapShot (LfpSnap)	Domain: Frequency Use: In and out-clinic Stimulation: on/off Time Length: 15 min Channels: 2
BrainSense™ Streaming	BrainSenseStreaming (BSS)	Domain: Time Use: In-clinic Stimulation: on/off Time Length: up to 15 min Channels: 2

2.3 ANT-DBS Studies for Drug Resistant Epilepsy Treatment

2.3.1 SANTE trial

The SANTE trial is a promising study performed in a controlled, multicenter, double-blind, and randomized way. This study focused on bilateral stimulation of ANT in order to treat epileptic patients (12).

The individuals who participated in the trial corresponded to a total of one-hundred and included adults with partial or secondarily generalized drug-resistant seizures. In an initial blind-phase lasting three months, only half of the patients received stimulation, and the selection was randomized. This phase began one month after implantation in patients. The information regarding the stimulation or non-stimulation received by the patient is detailed in the table 2.4. After this period, all patients received stimulation in an unblinded phase lasting nine months. During this phase, only small and limited parameter changes could be made. However, at the end of this period, a follow-up was initiated. In this phase, it was allowed to change the stimulation parameters freely (12).

As expected, in the last month of the blinded phase, the group that underwent stimulation had a more significant decrease in the frequency of seizures being this decrease 29% greater than the group that was not stimulated. Similarly, the unadjusted median percentage will have been significantly more prominent in the controlled group. Even in the more complex and severe seizures, a significant reduction was reported (12).

Moreover, in two years, the median percent reduction in seizure frequency was 56%. There was a seizure reduction in at least 50% (response rate) in 54% of patients tested, and no episode was reported for at least half a year in 14 patients (12).

Salanova *et al.* (62) reported the SANTE trial's long-term efficacy and safety in a study published five years after the trial began. This study consisted of the follow-up of patients for five years. The results revealed that the median percent reduction in seizure frequency reached 69% in the fifth year, and the response rate reached 68% in the same year. During the entire follow-up period, 16% of the sample had no seizures for at least six months.

Thus, this trial confirmed the effectiveness and safety of ANT-DBS.

Table 2.4: SANTE trial stimulation parameters.

	n	Voltage	Other Stimulation Parameters
Estimated Group	54	5 V	<ul style="list-style-type: none"> • 90 μs pulses • 145 pulses/s
Control Group	55	0 V	<ul style="list-style-type: none"> • "ON" 1 min • "OFF" 5 min

2.3.2 Noncontrolled Studies

Both before and after the SANTE trial, several open-label, uncontrolled, and pilot ANT-DBS studies were conducted to treat epileptic patients.

Kerrigan and colleagues (63) coordinated a study with bilateral intermittent electrical stimulation of the ANT applied to 5 individuals with DRE. The study had a follow-up of 6 to 36 months, and all patients had intractable partial epilepsy, whereas of them also suffered from secondarily generalized seizures. About 80% of patients reported a significant decrease in seizure severity, and one patient reported a considerable reduction in total seizure frequency.

In 2012, Lee *et al.* (64) conducted another study on 15 patients with DRE. In this study, ANT-DBS was used bilaterally, and it was possible to compare the seizures with the preimplantation baseline. The results showed a reduction of about 70% in the frequency of seizures during the follow-up period and a particularly high decrease in the frequency of seizures in 2 patients. The results obtained in the short term showed to be a reflection of what would happen in a long time.

More recently, Jarvenpaa *et al.* (65) investigated the effect of ANT-DBS in 16 epileptic patients. The patients were responders or non-responders if there had or had not been a $\geq 50\%$ reduction in the frequency of the most frequent seizure type in the last six months. The results showed that three-quarters of the patients were respondents. Besides, the entire study population had to perform neuropsychological tests that were more successful by respondents, especially those requiring executive functions and attention.

These studies led to the conclusion of the safety and efficacy of ANT-DBS in epileptic patients. In the table A.1, there are detailed studies done with ANT-DBS for the treatment of DRE.

Chapter 3

Studying the Motor Factors in Epilepsy

3.1 Understanding the Brain Mechanisms in Motor Processes

3.1.1 The Role of Motor Cortex in Movement

After the emergence of interest in the influence of the cerebral cortex on motor functions, several theories were proposed, and several studies started to be developed. In 1870, Gustav Theodor Fritsch and his colleague Eduard Hitzig showed that electrical stimulation of one side of the cerebral cortex produced muscle contraction on the opposite side of the body in an animal model. Later, Roberts Bartholow conducted a study in which he applied electrical stimulation to a specific cortical area and again found involuntary muscle contraction upon stimulation. These two experiments validated the theory that the neurologist John Hughlings Jackson had put forward years before. The brain was proposed as a sensory-motor model, whose various areas had sensory or motor centers. Thus, the brain area stimulated by Bartholow in his experiment came to be called the motor cortex (66).

Besides the study of movement mechanisms, Jackson put special effort into studying movement in focal epileptic seizures. Thus, he showed that the localized actions characteristic of a seizure resulted from muscle contractions triggered by electrical discharges in specific areas in the brain. They proposed that localized movements result from excessive nerve discharges in localized areas of the cortex (66).

Evarts *et al.* (66) developed an experiment with a monkey to determine the motor cortex's primary output. To do this, they trained the monkey to perform tasks in which the direction of force and movement were varied independently. This study showed that the motor cortex activity was related to the amount and pattern of muscle contraction, not to displacement.

Although some studies showed that the basal ganglia and the cerebellum also mediate movement, lesions to the cerebellum did not cause paralysis, unlike lesions to the motor cortex. In addition, it was understood that the motor cortex is involved in both slow and fast motor functions. However, this is not the case with the other two structures, so they were considered complementary structures regarding the processes involved in motor activities (66).

More recently, in order to better understand the mechanisms of movement in the brain, Yeomet *et al.* (67) tried to understand which areas of the brain were activated as the movement progressed. After this study, they found that the major transitions in the neuronal network happened between the states of motor planning and execution. While most areas involved in motor activity were activated during planning, only the connections with the cerebellum and basal ganglia were activated during the performance. On the opposite, the other motor areas decreased their activity. Thus, it was found that the brain mechanisms involved in movement are almost

all completed during the planning phase. It was also shown that the brain created a feedback network during movement execution rather than a motor decision.

3.1.2 Neuronal Activity During Motor Functions

The neuronal processes responsible for motor activity induce changes in brain potentials. These changes manifest themselves through variations in the rhythmic components of the EEG and the occurrence of the Bereitschaftspotential (BP), a negative cortical potential (68). The changes in EEG activity can be demonstrated by decreased or increased power in specific frequency bands. The decrease in power is called event-related desynchronization (ERD), while its increase is named event-related synchronization (ERS). These phenomena occur, respectively, due to decreased or increased synchronization of neighboring neurons (69).

3.1.2.1 Brain Oscillations Frequency

The frequency of the oscillations in the brain is dependent on the number of synchronized neurons, and the former is smaller the greater the number of neurons in synchronization.

On the other hand, the amplitude of the oscillations is directly proportional to the number of synchronized neurons. For this reason, when comparing, for example, the lower alpha and upper alpha components, the former presents a spectral peak with greater magnitude compared to the element with higher frequency (70), as shown in figure 3.1. It only takes 10% of the total neurons to be synchronized for their amplitude to be ten times greater than the amplitude of the remaining neurons.

Furthermore, due to cross-talk between neighboring neurons, when a finger is moved, for example, several areas of the cortex are activated synchronously but at different frequency bands (71).

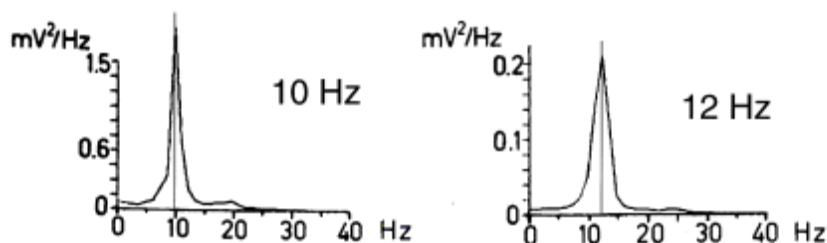


Figure 3.1: Relationship between amplitude and frequency of brain oscillations in lower alpha and upper alpha bands. Adapted from (70).

3.1.2.2 Event-Related Desynchronization/Synchronization

Interpretation of ERD and ERS

The activation of neurons in the cortex causes a desynchronization of the EEG and, thus, ERD's appearance. This happens because an event triggers a population of neurons to function in a desynchronized way. A mu desynchronized rhythm can be observed during a motor or sensorimotor process, while during visual information processing, the desynchronization happens in the occipital alpha rhythm (71; 69).

On the other hand, the appearance of a large-amplitude synchronized alpha rhythm may indicate reduced information processing. In this case, it can be said that the brain may be in 'idling' mode. That is, at the time of this process, the cortical neurons are deactivated (71).

It is also verified that immediately after the end of a finger, arm or foot movement, there is the appearance of a synchronized beta rhythm, that is, a post-movement beta ERS. This happens due to the deactivation of

cortical neurons right after the execution of the event. However, the alpha band needs more time to recover and the ERS appears a little later (see figure 3.2) (71; 69).

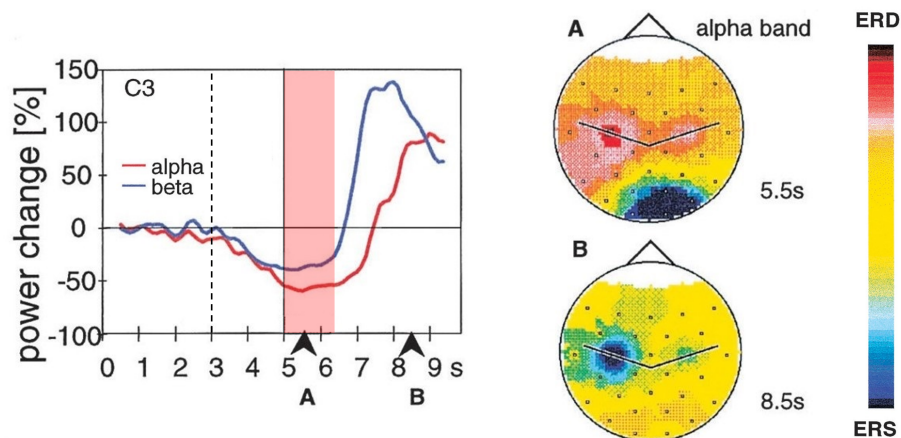


Figure 3.2: On the left side of the image is the grand average ERD curves calculated from the individual ERD curves of nine individuals during the execution of a right-handed movement. The data reflect the acquisition of EEG information from the electrode at position C3 in alpha and beta frequency bands. The red band corresponds to the duration of the action. The grand average maps on the right side of the image are calculated in the alpha band for a 125 ms interval during movement (A) and after movement offset (B). The blue color indicates power decrease (ERD), and the red color represents power increase (ERS). Adapted from (72).

However, it should be noted that an ERD is only significant if the baseline, which should be measured a few seconds before the event begins, represents a prominent peak in the power spectrum. Similarly, it is only considered an ERS if the spectral peak, resulting from the formation of a new rhythmic component, appears during the event (72), as shown in figure 3.3.

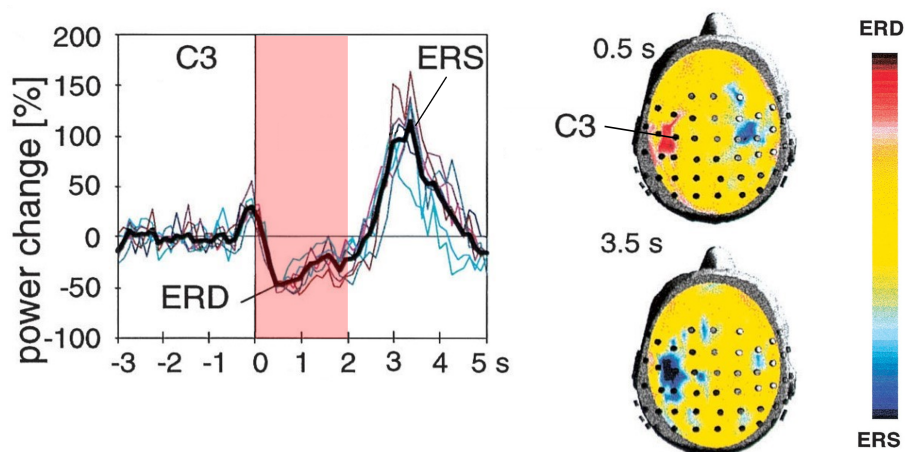


Figure 3.3: On the left side are the individual ERD curves from 8 sessions of right motor imaginary of an individual and the grand average ERD curve (black curve). The data reflect the acquisition of EEG information from the electrode at position C3 in a beta frequency band. The red band corresponds to the imaginary motor time. On the right side of the image are the maps of contralateral ERD and ipsilateral ERS during and contralateral ERS after motor imagery. The blue color indicates power decrease (ERD), and the red color represents power increase (ERS) Adapted from (72).

ERD and ERS in Movement Tasks

Voluntary movements generate desynchronization in both the upper alpha and lower beta bands. The resulting

desynchronization of sensorimotor processes in the brain starts about 2 seconds before the movement onset in the contralateral region and becomes symmetrical immediately before movement execution (68).

However, it is essential to emphasize that these mechanisms are only valid for healthy subjects. Derambure *et al.* (73) demonstrated that mu rhythm desynchronization appears only 0.5 seconds in epileptic patients with frontal lobe epilepsy and focal motor seizures (FMS). Furthermore, the amplitude of the observed desynchronization was increased in the frontocentral region. Also, in patients with TLE, the amplitude of the ERD was increased, although there was no change relative to healthy subjects concerning the onset of desynchronization.

Although the mechanisms in the cortex are different for brisk and slow movements, the contralateral desynchronization starts at approximately the same time for both types of movement. While slow movements require feedback from the periphery, the same is not valid for brisk movements. However, immediately before the onset of movement, the desynchronization becomes symmetrical (68; 72). Thus, the contralateral ERD that occurs before the movement happens due to a neuronal pre-activation in the motor zone is independent of the movement's speed. Furthermore, it was also found that this desynchronization happens similarly for the finger, thumb, and wrist movement (72; 74), as illustrated in figure 3.4.

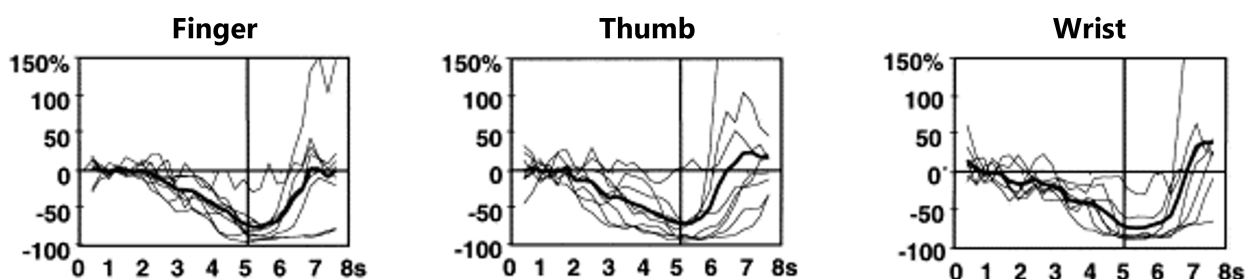


Figure 3.4: Individual ERD curves (thin lines) in the alpha frequency band of eight subjects and the respective grand average ERD curves (thick line). The data recorded at electrode C3 represent the movement of the right finger, thumb, and wrist. The horizontal line indicates 0% power change, and the vertical line represents the beginning of the movement in seconds. Adapted from (74).

On the other hand, during foot movement, desynchronization occurs in the central area of the brain regardless of each foot. However, ERD only occurs in the alpha band. Thus, desynchronization in this frequency band is considered generalized and independent of the region of movement (68).

Interestingly, the process of imagining movement execution involves brain areas and mechanisms very similar to those of movement execution itself. During the motor imagery, there is a desynchronization in mu rhythm. Similar to what happens during the execution of the hand movement, the ERD appears in the region contralateral to the event. However, this desynchronization does not become bilateral as it happens during execution. Despite this, the differences between execution and motor imagination are predominantly found in the sensorimotor region (68; 72).

If there is an ERD at the execution or imagination of a voluntary movement, after the end of this motor process, there is the appearance of an ERS. However, this synchronization only occurs in the beta band in the first and second post-movement since the Rolandic mu rhythm still exhibits a desynchronization (68; 72).

As found for the ERD during the movement's preparation and execution or imagination, the post-movement beta ERS is independent of the movement speed. However, it shows some differences in actions performed with different body parts (68; 72). When comparing the beta ERS after movement of the wrist, fingers, and thumb, was found that the amplitude achieved by synchronization in the wrist is almost double compared to the other two elements (see figure 3.5) (72; 74).

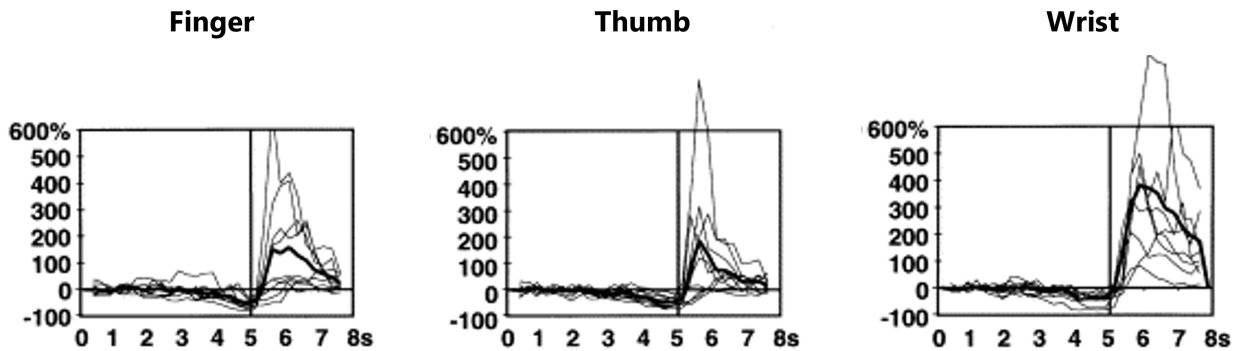


Figure 3.5: Individual ERS curves (thin lines) in the beta frequency band of nine individuals and the respective grand average ERS curves (thick line). The data recorded at electrode C3 represent the end of the right index finger, thumb, and wrist movement. The horizontal line indicates 0% power change, and the vertical line represents the movement offset in seconds. Adapted from (74).

It turns out that after the movement is finished, the brain areas activated are the same ones used during motor execution or imagination. The synchronization phenomenon in the beta band happens after movements with the fingers, hand, arm, or foot and reaches its maximum amplitude 1 second after the event ends. However, it is essential to point out that the beta ERS components are specific to each individual and vary depending on which part of the body is performing the movement (72).

By way of conclusion, figure 3.6 represents a summary of the evolution of the desynchronization and synchronization throughout the process of motor execution and imagination in the right hand and foot, in alpha frequency band.

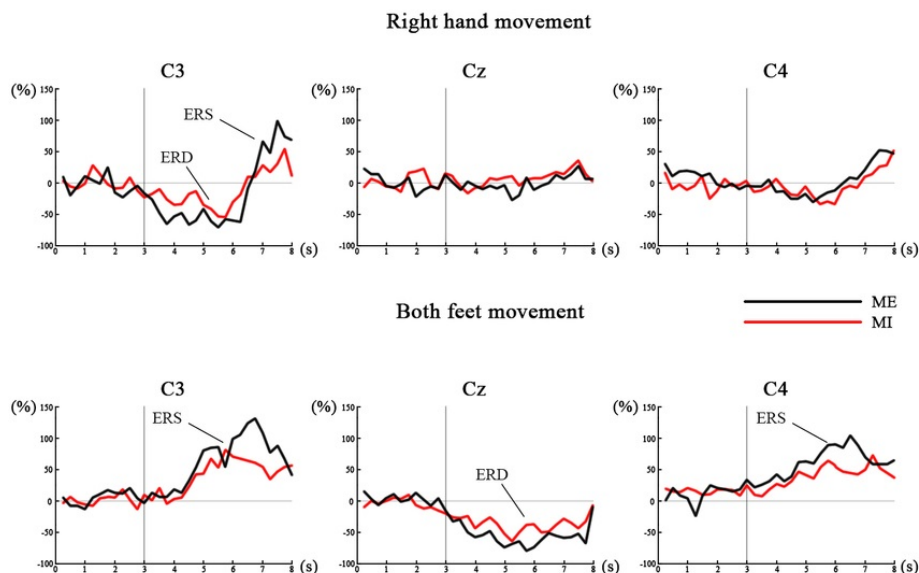


Figure 3.6: Example of ERD/ERS time course for movement with right hand and both feet. The EEG power of C3, Cz, and C4 in the alpha frequency band during the 3 s before, and the 5 s after the onset of movement for various trials in various subjects are depicted. The top panel shows ERD/ERS patterns that occur in right hand movement, and the bottom panel shows ERD/ERS patterns that occur in both feet movement. The red signals represent the imaginary motor, while the black signals represent the motor execution. The horizontal line indicates 0% power change, and the vertical line represents the movement onset in seconds. Adapted from (75).

3.1.3 Recording Neurophysiological Signals

3.1.3.1 EEG Signals

Electroencephalography is a brain signal acquisition technique through invasively placed electrodes or placed in the scalp surface zone. However, the latter approach is the most frequently used. Generally, the placement of the electrodes is done according to the ten-twenty standards. For this purpose, each electrode is identified with a letter according to the corresponding position (F: Frontal, T: Temporal, C: Central, P: Parietal, and O: Occipital). In addition, each electrode also has an associated number, with the left hemisphere corresponding to odd numbers while the right hemisphere is assigned even numbers, and the medial zone is labeled with 'z', as shown in figure 3.7 (76).

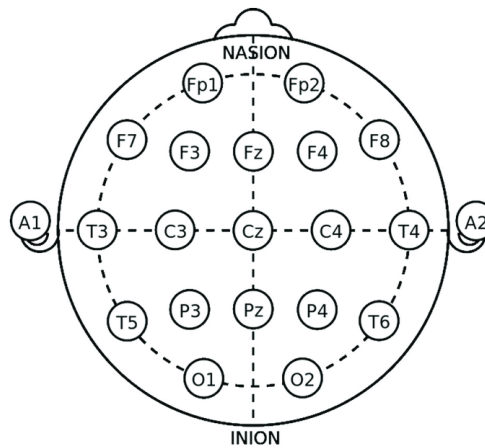


Figure 3.7: 10-20 system of electrode placement. Adapted from (77).

After the signals' acquisition, it is possible to classify the EEG waveforms according to their frequency, amplitude, shape, and the electrode position in question. The frequency, measured in Hz, is the key to differentiate the various waves corresponding to different states and behaviors. Among the various types are Delta, Theta, Alpha, Beta, and Gamma waves, with an increasing frequency, respectively. In the table 3.1, it is possible to find detailed information about each type of eeg rhythm's features (76).

Table 3.1: EEG rhythms and its features. Adapted from (76)

Rhythm	Frequency	Psychological State
Delta	0-4 Hz	<ul style="list-style-type: none"> • Deep rest • Dreamless sleep
Theta	4-8 Hz	<ul style="list-style-type: none"> • Deeply relaxed
Alpha	8-12 Hz	<ul style="list-style-type: none"> • Day dream • Calm
Beta	12-30 Hz	<ul style="list-style-type: none"> • Alert • Active thinking • Anxiety • Panic attack • Focus • Concentration
Gamma	30-100 Hz	<ul style="list-style-type: none"> • Combination of two senses

Due to its characteristics related to the detection and measurement of brain signals and the low cost associated with its use, EEG is widely used to study patients with epilepsy. It allows unambiguous identification of

seizure occurrence and provides information about the patient's type of seizure and epilepsy (78).

Regarding the study of motor tasks, the motor and somatosensory cortex are the most relevant. Considering the location of these regions in the brain, when studying motor functions with EEG signals, the electrodes of most significant interest rely on the central and parietal areas. The figure 3.8 represents the locations of the motor and somatosensory regions and the predominant body part along each of the cortex.

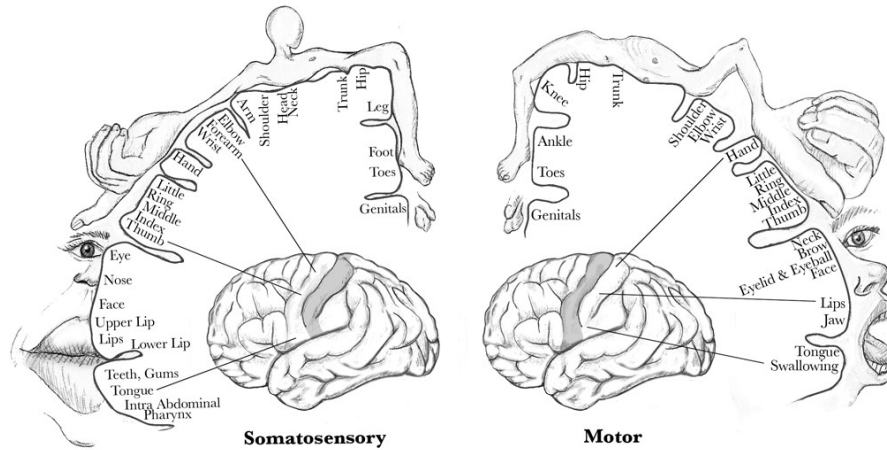


Figure 3.8: Cortical homunculus representation. Extracted from EBM Consult. ¹

Several studies using EEG are dedicated to studying the motor-cognitive complex and have obtained very satisfactory results (79).

3.1.3.2 LFP Signals

Local Field Potential, or depth EEG, measures brain activity from various sets of neuronal cells. For this purpose, small low impedance electrodes are implanted in the intracerebral region in opposition to what happens with the EEG electrodes (80; 81). The signals obtained are complex and demonstrate the spatially weighted electrical activity around the electrodes present in the skull's deep area (82). Despite the electrodes' location, LFP signals are easily subject to external interference that can be diminished by the grounding of the electrodes. Furthermore, the movements can cause a decrease the signal-to-noise ratio, so it is essential to associate systems capable of combating external noise. There are also suspicions that cellular populations outside the recruited network may also introduce noise (82).

The use of deep LFPs is a common practice in the treatment of neuropsychiatric conditions. Typically, electrodes are implanted in basal ganglia (81). Most of the studies are focused on PD and have shown that signals coming from areas such as basal ganglia are a reflection of oscillations due to movement, behavior, cognition, and emotions. Although opinions are divided among scientists, there is evidence that it is possible to precisely modulate these oscillations through DBS, adjusting the stimulation voltage (81). Even though there is not much information about LFPs used in human epilepsy, a recent study recorded LFPs from the first epileptic patient implanted with ANT-DBS Percept™ PC neurostimulator, which will be detailed in section [Percept™ PC](#). This study opened the door for further investigation of their use in patients with DRE (61).

Considering that the LFP signals recorded by the neuro-stimulator need to be synchronized with other equipment, this last study also uses vEEG. This technique has proved to be the key to diagnosis in the treatment of epilepsy (61).

¹ Homunculus: Somatosensory and Somatomotor Cortex. Available at: <https://www.ebmconsult.com/articles/homunculus-sensory-motor-cortex> (Accessed 18-04-2021)

3.2 The Role of ANT on Motor Functions

3.2.1 Motor Experimental Paradigms

For both motor activity studies with EEG and intracerebral signal recording, the applied paradigms are very similar (83).

Typically, paradigms involve three essential phases: task preparation, the task itself, and rest. The rest phase is vital for restoring the baseline state of the subjects. However, it is also necessary since, during the remaining stages, the individuals must avoid blinking or making any eye movement, adjusting their position, or swallowing, and are only allowed to do so during rest. These requirements prevent artifacts in the acquired electrophysiological signal. As a rule, the entire paradigm process is accompanied by visual and/or auditory stimuli to be more intuitive for the volunteers and ensure repeatability between trials. The visual stimuli appear on a monitor positioned before the subject, comfortably seated and still. To ensure that the subject is ready to start the task, the screen displays a cross that must be fixed by the subject a few seconds before the movement begins. Some paradigms are also accompanied by a cue that usually translates into a beep one second or just before the event's start to indicate that the motor task is approaching the start (75; 84).

Figure 3.9 shows a general representation of a motor paradigm.

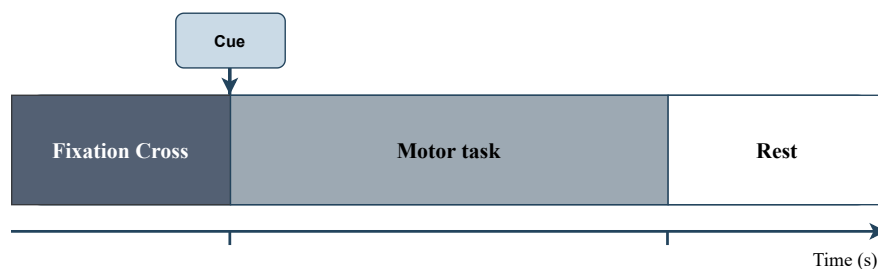


Figure 3.9: General schematic of an experimental motor paradigm.

The duration of each phase depends on the motor paradigm (number of tasks and type of movements, for example), the state of the subject, and from author to author. However, in motor tasks, since after executing or imagining an activity, it takes a few seconds for the brain signals to return to their baseline state, it is recommended that the rest time be no less than 10 seconds (72).

Also, the number of tasks, type of movement, and the number of trials varies greatly depending on the purpose of the study in question. However, the most common exercises are done with the fingers, hands, or feet and range from fast to slow movements or simple to more complex movements (69; 72). In some studies, the tasks are performed a few times. However, the greater the number of performed repetitions, the more significant the study sample will be and the more reliable the results obtained. However, it is always necessary to consider the duration of the paradigm so as not to tire the subjects in the study too much.

3.2.2 Motor-Cognitive Factors Processed in the ANT

3.2.2.1 The Motor Thalamus

As the name implies, the motor thalamus corresponds to the set of regions of the thalamus involved in motor mechanisms, more specifically in pathways originating in brain regions with motor function. The motor thalamus consists of 3 essential regions, and each of them receives input from the cerebellum, the basal ganglia, or the superior colliculus (SC) (85).

The involvement of the cerebellum in motor and sensory functions is known. Thus, it is believed that the VL and the VPL nuclei, by being part of the pathway originating in the cerebellum, may also have some involvement in these mechanisms. Similarly, the ventrolateral pars oralis and medialis (VLo and VLm) and the VA nuclei receive afferents from the basal ganglia's output nodes believed to be involved in the generation of willful movements. Finally, some areas of the lateral border of the mediodorsal nucleus are part of the pathway originating in the SC, so it is thought that this region may be related to eye movements. All the three pathways involved in the motor thalamus ascend to the motor-related cortex. Thus it is hypothesized that the motor thalamus acts as a passive relay. However, more studies in this direction are needed to get concrete conclusions (86).

3.2.2.2 Studies on the Role of ANT on Motor-Cognitive Functions

Bočková *et al.* (87) conducted the only currently existing study based on the role of ANT in motor-cognitive processes in humans. Three patients with pharmaco-resistant epilepsy implanted with ANT-DBS electrodes participated in this study. Each of the subjects performed a paradigm consisting of 2 tasks: copying the letters displayed on a screen and writing any letter not seen on the monitor. The letters appeared on the screen for 200 ms with a 16s interval between visual stimuli.

Intracerebral EEG signals were used to analyze the brain mechanisms during the performance of the paradigm. For the recordings of this signal, a monopolar montage was used, with an ear lobe reference attached.

After preprocessing the neurophysiological signal, both the event-related potentials and the Time-Frequency Analysis (TFA) of the ERD/ERS were processed and evaluated. The power changes analyzed in a range of 2-80 Hz showed some differences between the two tasks performed by the subjects. While there was no significant change in the first task, there was a large amplitude ERD in the alpha and beta bands in the second task. These differences were due to the greater complexity of the second task. In the lower frequencies, there were no differences between the two tasks. Both tasks showed desynchronization resulting from the mental effort required.

This study showed that ANT is involved in the processing of visuomotor tasks.

However, very little is known about the influence of motor mechanisms on ANT, so further studies on this topic should be conducted.

3.3 Event-Related Desynchronization/Synchronization Analysis

3.3.1 Preprocessing

Before ERD/ERS processing is performed, the neurophysiological signals initially acquired must be analyzed and processed so that the results obtained are reliable. Thus, one of the essential steps in the processing of these signals is bandpass filtering. Namely, in movement task analysis, the frequency bandwidth varies between 4-8 Hz to 30 Hz for non-invasive EEG signals (88), between 0.015 and 75Hz for invasive EEG (iEEG) signals (89) and between 1-2 Hz and 80-250 Hz (90; 87) for LFP signals. Applying a bandpass filter in this frequency band automatically eliminates some eye, muscle, and heartbeat-related artifacts.

Although much of the irrelevant data for the study is eliminated after the filtering step, some artifacts remain in the selected frequency band, and some procedures should be applied to detect and destroy them. This can be done by visual inspection and elimination of contaminated epochs or using appropriate algorithms for detection and removal. The simplest artifact detection algorithms are based on the application of thresholds. However,

the most commonly used and effective methods rely on Regression and Blind Source Separation techniques (91).

A prevalent Blind Source Separation method is the Independent Component Analysis (ICA) algorithm. This method can separate and eliminate artifacts from EEG signals by decomposing them into independent components (ICs). These components correspond to the signal sources that are extracted through some assumptions of their statistical properties (92). These sources may or may not be of interest in solving the problem under study, so one must carefully identify and select which components to keep and which to eliminate. Eye and muscle artifacts, for example, are easy to detect since they have specific amplitudes and shapes. For this reason, these sources can easily be visually detected and manually eliminated. However, if it is used EEG signal, there are also tools for analyzing and processing this type of signal that automatically identifies the components, such as EEGLAB (see figure 3.10).

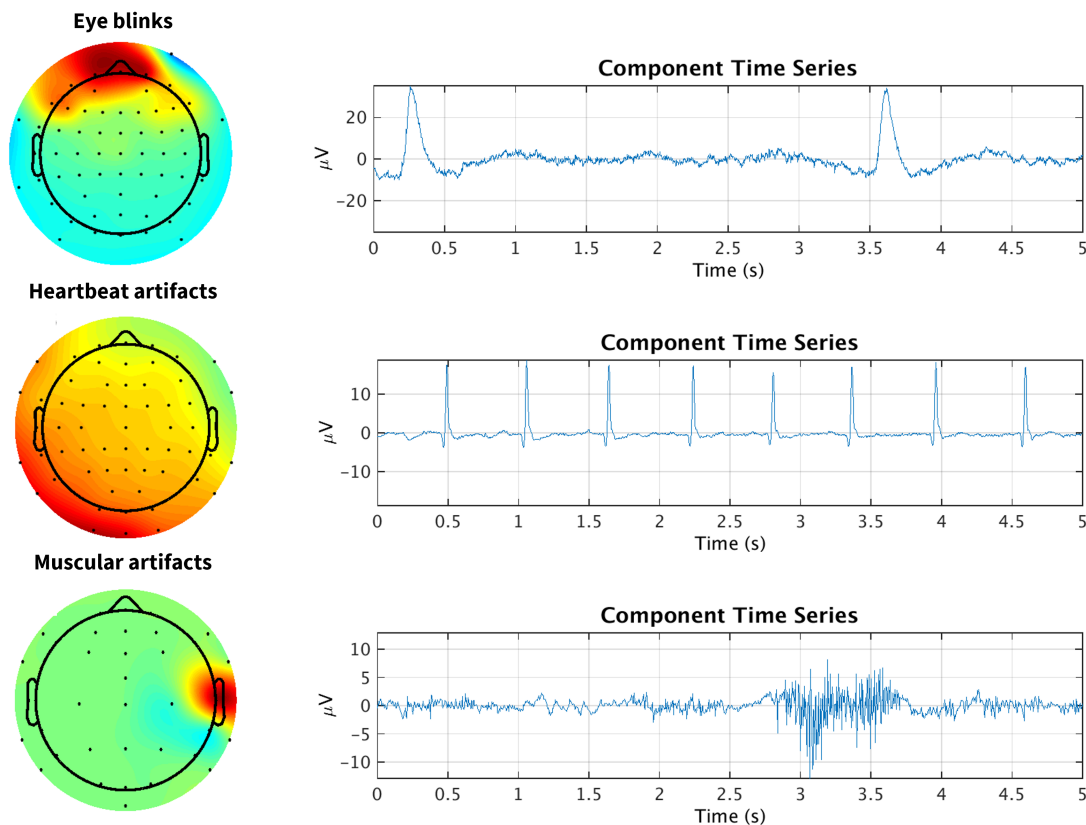


Figure 3.10: Examples of ICs correspondent to artifacts. Eye blinks, heartbeat, and muscular artifacts are evident in both component time series (right side) artifacts and respective scalp topographic maps (left side). Adapted from ICLabel Tutorial. ²

ICA can be processed in various ways, so its several algorithms include *FastICA*, *projection pursuit*, and *Infomax* (93).

Although this technique is recommended only for continuous signal acquisitions and requires considerable data analysis, some studies use ICA to study ERD/ERS with small samples.

Finally, the ERD/ERS study involves a set of trials of multiple events, so it is crucial to resort to extracting epochs from the signal involving the appropriate information. In the study of motor tasks, each epoch should include, in addition to the entire period of execution or imagination of the movement itself, at least 3 seconds

²ICLabel Tutorial: EEG Independent Component Labeling.

Available at: <https://labeling.ucsd.edu/tutorial/labelst> (Accessed 18-04-2021)

before the movement onset and at least 2 seconds after the movement offset. These periods allow us to verify the changes in synchronization and timing that occur in the preparation and completion of the motor activity.

3.3.2 Quantification of ERD/ERS in Time and Space

In order to be able to quantify ERD/ERS, it is necessary to perform several event trials using EEG, and these data should include a few seconds before and after the onset of the event. Therefore, ERD/ERS is presented as the EEG power relative (in percentage) to the power of the reference EEG derivations a few seconds before the onset of the action. The relative power percentage shown in the ERD/ERS time course corresponds to the percentage increase (ERS) or decrease (ERD) of the average power corresponding to the selected reference. The desynchronization and synchronization, that occurs during the selected event execution, require time to develop and return to their baseline state after the event ends, mainly when the elected frequency band includes alpha rhythms. For this reason, when conducting studies involving voluntary movements, there should be a rest interval of at least 10 seconds between actions (69; 72).

In the band power method, after selecting the most appropriate frequency band for the study in question, the ERD/ERS calculation must follow four essential steps, as illustrated in figure 3.11 (69) :

1. bandpass filtering of each event-related trial;
2. squaring of each amplitude sample to obtain power samples;
3. averaging over all trials;
4. averaging over a few consecutive power samples to smooth the data and reduce the variance.

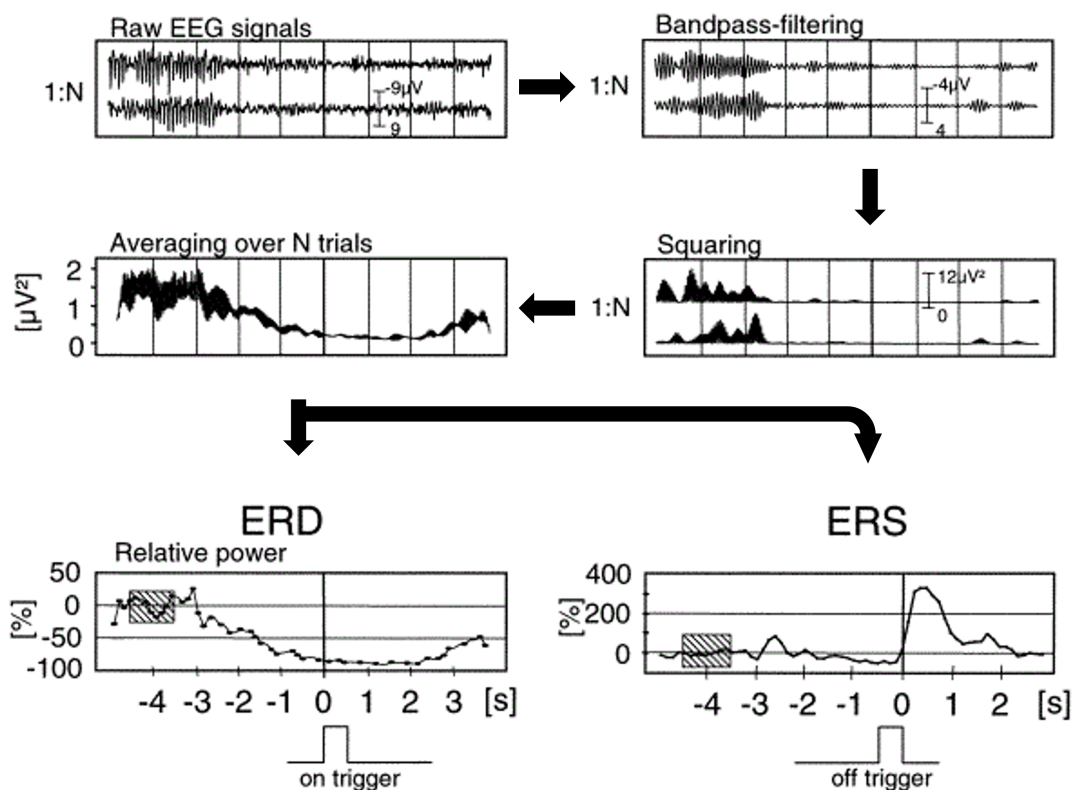


Figure 3.11: Schematic for processing ERD and ERS. The power reduction corresponds to the ERD, and its increase represents the ERS. Adapted from (72)

Another common method can be used to discriminate between phase-locked and not phase-locked power changes. This alternative method is based on the calculation of the intertrial variance and can complement the first one by the following steps (72):

1. bandpass filtering;
2. point-to-point intertrial variance calculation;
3. averaging over time.

To calculate the power change, in percentage, the power in the period after the event onset is given by A, while that of the reference period is given by R. Therefore, ERD/ERS is given by the equation (3.1).

$$ERD/ERS(\%) = \frac{A - R}{R} \times 100 \quad (3.1)$$

, where if the values obtained from this equation are negative, it is considered the presence of ERD while positive values are attributed to ERS.

In order to facilitate the interpretation of the time course of ERD/ERS, a horizontal line should be drawn that represents 0% power change and on which the baseline values should approximate (72).

In addition to ERD/ERS time course representation, spatial mapping is also possible. The most common methods to perform this mapping are surface Laplacian calculation, cortical imaging, and distributed source imaging (72).

A representation of the ERD/ERS time course and its spatial mapping is shown in the figure 3.12.

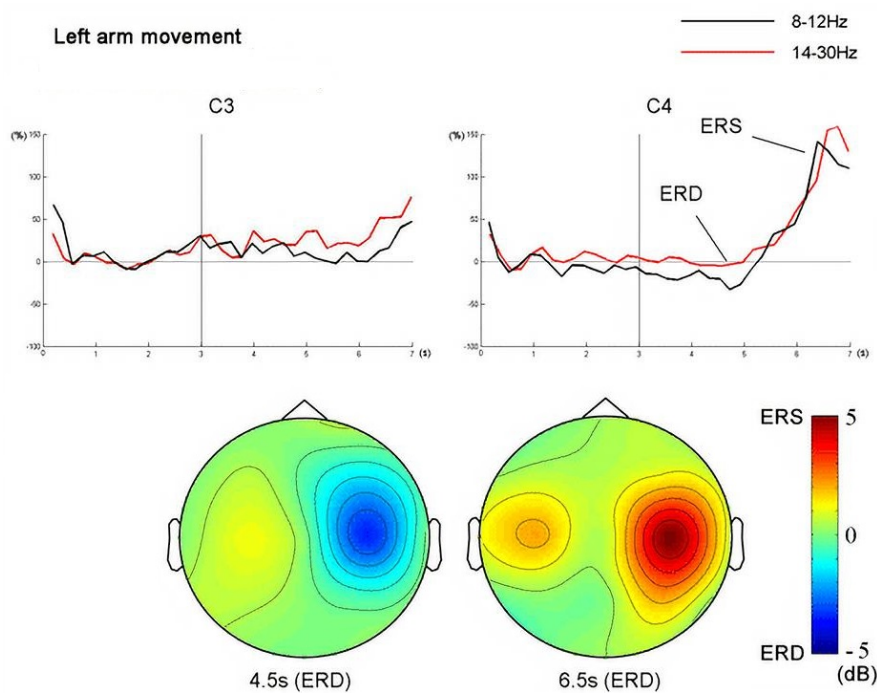


Figure 3.12: ERD/ERS curves representation in alpha and beta frequency bands (upper panel) and ERD/ERS spatial maps (bottom panel) of left arm movement. The blue color represents power decrease (ERD), and the red color represents power increase (ERS). Adapted from (84).

3.3.3 Determination of Subject-Specific Frequency Bands

In order to proceed to the bandpass filtering step for the ERD/ERS calculation, it is necessary to determine which frequency band is best to apply for the event and subject in question. Three different methods can do this: (i) detection of the most reactive frequency band based on the comparison of two short-term power spectra, (ii) continuous wavelet transform (CWT), or (iii) definition of frequency bands relative to the spectral peak frequency (72).

If the first method is chosen, two 1-second power spectra calculated over a set of event-related EEG trials should be compared. Each of the spectra should be related to different phases of the event. One spectrum should include 1-second corresponding to the reference period, while the other should represent the period corresponding to the event itself. Suppose the event under study is the execution of a voluntary movement. In that case, the execution period chosen may check the activity's planning, the move itself, or the recovery period right after the end of the action (72).

After correctly selecting the reference and activity periods, a curve should be drawn that corresponds to the difference between the log power spectra of the reference and activity periods. Furthermore, this curve should also be accompanied by a 95% confidence interval to facilitate the identification of the increase and decrease of power corresponding to the ERS and ERD, respectively (72).

The second method compares a signal $x(t)$ with dilated and shifted components of a wavelet ψ and is defined by the following equation:

$$X_w(a, b) = \frac{1}{|a|^{1/2}} \int_{-\infty}^{\infty} x(t) \overline{\psi} \left(\frac{t-b}{a} \right) dt \quad (3.2)$$

, where a represents the wavelet dilation and b corresponds to the wavelet shifting (72).

Time and frequency resolution in CWTs is performed at the specific scale a . This translates into analyzing high frequencies with high temporal resolution and analyzing low frequencies with low temporal resolution. These features have proven to be very useful in the analysis of EEG signals (72; 94).

Finally, the last method mentioned suggests using an average frequency of the peak alpha centroid $f(i)$ to adjust each frequency band. Thus, four frequency bands, in a 2Hz range, should be defined concerning $f(i)$. These bands should fall on the theta and alpha frequencies of about 4 ± 12 Hz and are designated (72; 94):

- theta for $f(i) - 6$ to $f(i) - 4$;
- lower 1 alpha for $f(i) - 4$ to $f(i) - 2$;
- lower 2 alpha for $f(i) - 2$ to $f(i)$;
- upper alpha for $f(i)$ to $f(i) + 2$.

The ERD must be calculated in each of these ranges individually. In addition, the frequency bands should be given in Hz instead of using the term "alpha", for example (72).

3.3.4 Time-frequency Domain Analysis

As the name suggests, time-frequency domain analysis operates on signals in both the time and frequency domains. The most commonly used methods are based on the time-frequency distribution (TFD) and the wavelet transform (WT) (95).

The TFD provides the energy density or intensity of the signal in both time and frequency. In this way, the energy at a given frequency and the frequency distribution at a given time can be obtained (95).

WT is useful in detecting small details, changes, and similarities in signals, which may be non-stationary. This method starts from a parent waveform and creates the waveform on the scale of magnification and reduction. This method can be classified as either continuous waveform transform or discrete waveform transform (DWT) (95).

The baseline normalized spectrogram or event-related spectral perturbation (ERSP) method is commonly used in studying ERD and ERS. To compute ERSP, it is necessary to obtain the power spectrum over a sliding window that runs through the entire signal. Next, it is also required to obtain the average of all the trials performed. In order to do so, the ERSP is given by (96):

$$ERSP(f,t) = \frac{1}{n} \sum_{k=1}^n |F_k(f,t)|^2 \quad (3.3)$$

, where n represents the number of trials, f corresponds to the frequency, t corresponds to the time, $F_k(f,t)$ represents the spectral estimate. For this calculation, one can use techniques such as the short-time Fourier transform, a sine wave transform, or a multitaper Slepian decomposition (96; 97). Upon completion of this process, a time vs. frequency image is represented in each pixel by a color indicating the power in dB relative to the time-locked event. Usually, the blue color represents the ERD, and the red color represents the ERS.

The method described is used by the EEG signal processing and analysis tool EEGLAB. This tool evaluates the statistical significance of desynchronization and synchronization using the bootstrap technique. In this method, spectral estimates made from randomly selected portions of the trial baseline are selected for each trial of each event. Subsequently, these latency windows from the baseline are averaged. After repeating this process a few hundred times, a distribution amplitude represented by significance thresholds is created.

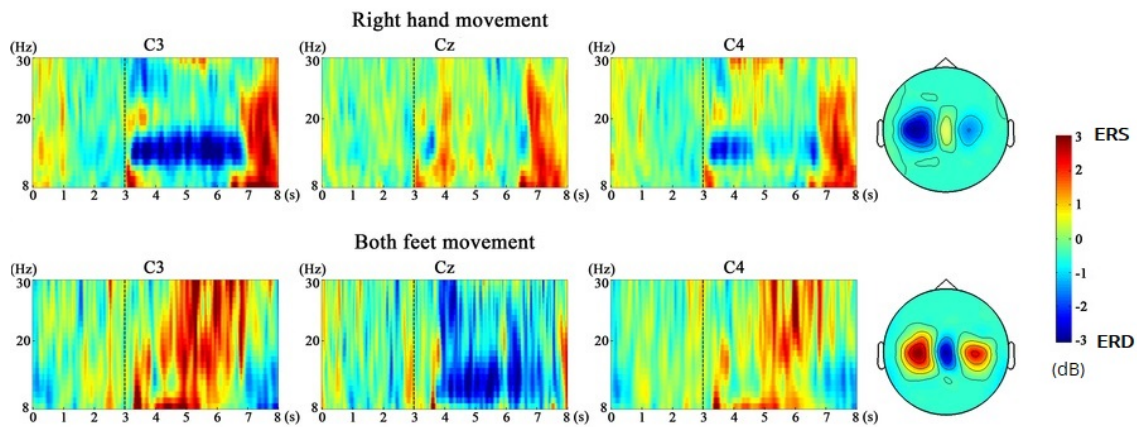


Figure 3.13: A representative example of time-frequency maps, using Fast Fourier Transform, for ME of two movements. The top image shows time-frequency maps of the right hand movement and the bottom image time-frequency maps of the movement of both feet. For each movement, time frequency maps of channel C3 over left sensorimotor cortex, C4 over right sensorimotor cortex, and Cz are illustrated. In all maps, 3 s indicates the onset of the ME. Each of the movements is also represented by the topography of the head corresponding to the best frequency band the seconds 4-7, on the right side of the figure. The blue color represents power decrease (ERD), and the red color represents power increase (ERS). Adapted from (75).

3.4 Epileptic Seizure Semiology

Epileptic seizures are accompanied by various signs and symptoms that are source of diagnosis. Identifying these signs is based on a visual expert opinion that focuses on the predominant ictal features. The ictal phenomenon present in epileptic seizures is divided into four categories (98):

- Sensory sphere;
- Consciousness;
- Motor sphere;
- Autonomic sphere.

An epileptic seizure is usually accompanied by symptoms belonging to more than one of the mentioned categories. However, the predominant symptoms correspond only to one of the categories. There are also seizures whose symptoms do not correspond to any of the spheres mentioned. These kinds of seizures are called 'special seizures'.

The semiological classification of seizures is fundamental as it allows for a more correct and precise classification by specialists. Figure 3.14 shows the semiological variety of epileptic seizures.

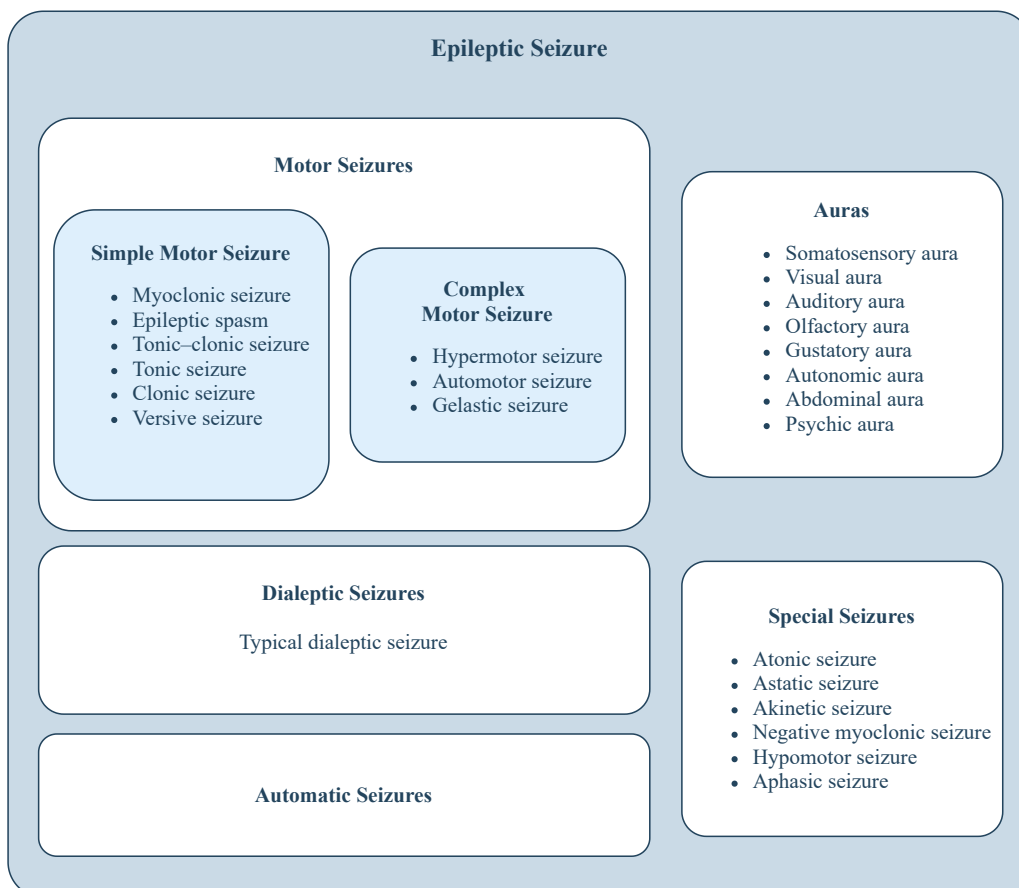


Figure 3.14: Epileptic seizure semiology. Adapted from (98)

3.4.1 Motor Seizures

The occurrence of motor processes accompanies some types of seizures. The symptomatic associated with the episode makes it possible to identify whether they are simple or complex motor seizures (98).

3.4.1.1 Simple Motor Seizures

As the name implies, this type of seizures are characterized by the presence of simple, unnatural movements. There are several subtypes associated with these seizures that are distinguished depending on the duration of the muscle contraction, the rhythmicity of the repetitive movement, and the muscles involved.

Myoclonic Seizures These seizures are accompanied by short-lasting non-rhythmic muscle contractions that can be unilateral or generalized. In the latter case, the limbs most often affected are the shoulders and proximal arms. These types of episodes are probably triggered in the primary motor cortex or premotor areas.

Clonic Seizures Repeated muscle contractions of short duration characterize these seizures. They affect various muscle groups with a more significant influence on the face and distal segments of the extremities. These types of episodes are triggered in the primary motor cortex or premotor areas.

Tonic Seizures Tonic seizures consist of sustained muscle contractions that last at least 3 seconds. The contractions may involve only one or several muscle groups. When focal epilepsy is present, the predominantly affected areas are the proximal muscle groups, with the contralateral area being most influenced by the contractions leading to an asymmetrical posture. Focal tonic seizures are believed to be generated in the cortical motor areas. However, the reticular formation of the stem brain and the thalamus may also be involved.

Epileptic Spasms Epileptic spasms are characterized by a conjunction of tonic and myoclonic features and last between 2 and 10 seconds. The contractions affect the proximal and axial muscles, resulting in flexion of the head and legs and the spreading of the arms. This type of seizure is common in children and focal epilepsies with different epileptogenic zones.

Versive Seizures Vertical seizures are characterized by rolling movements of the eyes and tilting of the head to one side. This happens as a result of electrical discharges in the frontal eye part, causing the eyes to roll to the side contralateral to the release. However, activity from other brain areas can spread to the frontal eye field, leading to this type of seizure.

Tonic-clonic Seizures These seizures are characterized by the occurrence of patterns of generalized tonic contractions and clonic contractions. The total duration of the episode varies between 1 and 2 minutes, and the generalized tonic-clonic seizure can occur in generalized or focal epilepsy syndromes. The origins of the seizure are the same as those presented for tonic and clonic seizures.

3.4.1.2 Complex Motor Seizures

Complex motor attacks are characterized by the execution of automatisms by the patient. These movements are usually complex and involve several parts of the body moving in different planes. The subtypes of this type of seizure depend on the characteristics of the automatisms (98).

Hipermotor Seizures These seizures consist of complex, large amplitude sets of movements lasting less than 60 seconds. These seizures mainly affect the proximal areas of the body. The origin of the seizures occurs in the frontal mesial or supplementary sensorimotor cortex area. However, if the seizure is generated elsewhere, it can spread to these areas, leading to a hypermotor seizure.

Automotor Seizures Automatisms characterize automotor seizures. Oroalimentary automatisms are very frequent and include chewing, deglutition, and lip-smacking. Manual automatisms, also very frequent, involve fumbling, picking up, and gesturing movements (99). This type of seizure is more frequent in patients with temporal lobe epilepsy, accounting for 60% of the epileptic adult population (100). However, seizures can also occur in subjects with frontal lobe epilepsy. Although there is no evidence about the origin of these seizures, it is believed that the anterior cingulate gyrus may be involved in this process as it leads to distal automatisms.

Gelastic Seizures Ictal "laughing" is characteristic of this type of seizure. This symptom corresponds to an exaggerated retort of regular laughter. This type of seizure is common in patients with hypothalamic hamartomas.

Chapter 4

Understanding the Role of the ANT in Motor Function: A Study Protocol Design

Initially, it was intended to develop a protocol including a motor paradigm performed by epilepsy patients implanted with the new Percept™ PC neurostimulator. Thus, the focus of this protocol would be the acquisition and subsequent analysis of LFP signals relative to the ANT target.

Due to some setbacks during the development of this dissertation, it was not possible to conduct experimental trials with patients implanted with Percept™ PC, making it impossible to acquire and analyze LFP signals under the circumstances initially proposed. However, the protocol was adapted so that EEG and iEEG signals could replace the analyzed signal. Thus, a EEG acquisition study was created with healthy pro bono volunteers and another iEEG acquisition study with a single epileptic participant. The only difference between these two studies, other than the number of participants, was the addition of a stimulation phase in the latter, as described below.

In addition to these two investigations, it was possible to complement this work by analyzing LFP signals obtained from ANT under a simple motor paradigm. It is essential to mention that others had already developed the protocol and signal acquisition for this study in the working group. Thus, the following will note the procedure performed by these elements during the performance of another study.

4.1 Setup

4.1.1 Outline

The developed setup is suitable for experiments based on simple and complex upper limb movements.

The experimental setup involves a movie camera to film the movements made by the subjects during the execution of the motor paradigm. It is important to note that the camera did not capture the faces of the volunteers at any time to maintain their anonymity and safety. Depending on the type of signal acquired (EEG, iEEG, or LFP), a suitable acquisition system was also used to record them at the electrodes of interest.

Auditory and/or visual cues indicated the type of movement and the beginning of the exercise to make the process more intuitive for the subjects. However, the volunteers received indications about the type of movement they should perform and feedback about their execution throughout the process.

The data were acquired on the computer whose screen was presented to the subjects and were copied to an external disk.

A representation of the setup for the EEG acquisition study is shown in figure 4.1.



Figure 4.1: Photograph of the experimental setup used to study movement with EEG signals in healthy subjects.

4.1.2 Auditory and Visual Cue

The visual and auditory stimuli belonging to the motor paradigm routine were designed using the Graphical user interface (GUI), available in MATLAB. The experimental routine was developed in an HP Pavilion-14-ce004np laptop with installed Windows 10 and MATLAB (R2020a).

The routine started with a short questionnaire whose information was stored in a text file.

Usually, a fixation cross is displayed on the screen seconds before the cue, indicating the movement's beginning. However, due to the heterogeneity in epileptic patients' cognition, the fixation cross was replaced by displaying the question "Are you ready?" and a "Yes" button that the subject must press to start the test to make the process more intuitive.

In addition to visual stimuli, the paradigm was also accompanied by auditory stimuli that indicated the beginning of a new paradigm phase.

4.1.3 Electrophysiological Signal Recording

4.1.3.1 EEG and iEEG Signals

A micromed SD LTM 64 PLUS headbox (see figure 4.2) was used to acquire EEG signals in healthy subjects. This device is capable of receiving signals from up to 64 different channels. Since it is an amplifier, it can increase the power of the signals, transform the analog input signals into digital signals, and store them in a microcontroller.



Figure 4.2: Photograph of the Micromed SD LTM 64 PLUS headbox.

Video-EEG completed the setup and was acquired through a Sony Hi8 360x Zoom digital video camera (see figure 4.3). Both devices connect to a computer that has SystemPlus EVOLUTION software installed. This system allows you to observe the signal acquisition in real-time, mark events, and analyze the signal itself.



Figure 4.3: Photograph of the Sony Hi8 360x Zoom digital video camera.

The experimental tests performed on the epileptic patient took place at the Epilepsy Monitoring Unit (EMU) of Centro Hospitalar Universitário de São João (CHUSJ). For these tests with iEEG acquisition, the SD LTM 64 EXPRESS amplifier from Micromed was used. This amplifier is similar to the SD LTM 64 PLUS amplifier. However, it is portable, unlike the latter. The video-EEG is acquired through a filming system inherent to the hospital. In one of the iEEG signal acquisition phases, stimulation was performed, and for that, an SD LTM cortical stimulator (see figure 4.4) add-on was connected to the amplifier. The connection between these two devices is possible by connecting a wire. Using the BRAIN QUICK®EEG software, it is possible to configure the stimuli and stimulated channels. Similar to the SystemPlus EVOLUTION, this software allows you to observe the signal acquisition and process it, and this is possible for both EEG and iEEG signals.



Figure 4.4: Micromed SD LTM 64 EXPRESS headbox and SD LTM Cortical Stimulator. Extrated from ¹

The data was exported to an EDF file and stored on an external disk at the end of the experimental tests. In both cases, synchronization of the signals and the video was automatically done by the software used.

4.1.3.2 LFP Signals

Acquisition of LFP signals was made using the Percept™ PC (see figure 4.5). This system has a DBS electrode, an extension wire, and an IPG. During stimulation, an electrical current is generated in the IPG that reaches the target after passing through the extension wire and the DBS electrode. These signals were acquired in all BrainSense modes and sampled at 250 Hz.

This acquisition is usually accompanied by the acquisition of EGG and video-EEG signals to make the analysis of the signals richer and more reliable.



Figure 4.5: Percept™PC neurostimulator. Provided by Medtronic, Inc.

¹BRAIN QUICK®LTM LINE. Available at: <https://micromedgroup.com/brain-quick-egg/brain-quick-ltm-line/> (Accessed 24-09-2021)

Although video-EEG and EEG were automatically acquired using appropriate software, this is not the case with LFP signals. Thus, it is necessary to synchronize the LFP and EEG signals. To this end, the tapping technique is used. This maneuver consists of making light touches on the DBS electrodes before and after the execution of the paradigm. Tappings generate artifacts in both the EEG and LFP signals, which allow them to be synchronized. This technique showed an accuracy of approximately 0.5 s (17).

4.2 Experimental Protocol

In order to verify the existence of biomarkers related to epileptic seizures in the ANT, a never-before-used motor paradigm was developed, however, based on simpler motor paradigms performed in previous studies.

The developed paradigm is divided into simpler motor coordination movements and related-seizure activities. For motor coordination, two types of movements were chosen: finger to nose and hand tap. The first type of movement should be performed with the right hand, while the hand tap is divided into two movements. The first is performed with the right hand and the second with the left hand.

With the help of Dr. Ricardo Rego and Dr. António Campos from the EMU of the CHUSJ, four movements, that are frequently automated during seizures with motor expression, were chosen. These movements consist of hand rubbing, circling both hands on the legs, non-repetitive actions that correspond to interactions with objects around the patient, and chewing.

The set of movements associated with the paradigm is shown in figure 4.6.

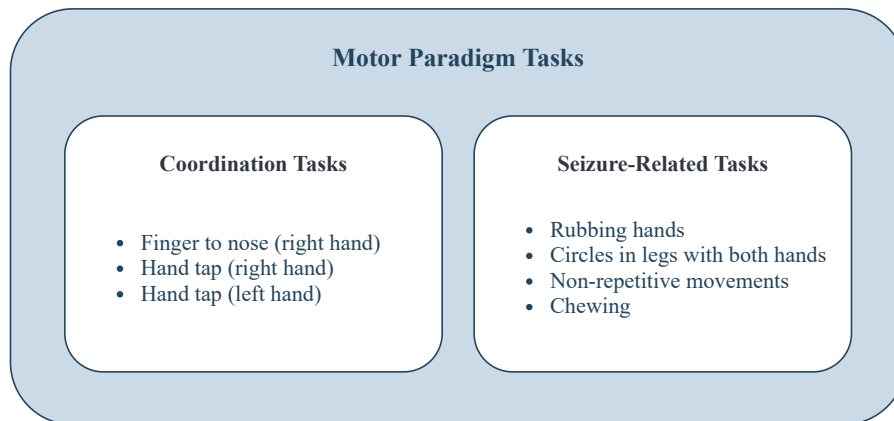


Figure 4.6: Motor paradigm tasks.

The experimental routine associated with the proposed paradigm is displayed on a screen in front of which the participant must be seated. In order to obtain all the necessary information for the subsequent processing of the data and interpretation of the results, before the beginning of the paradigm itself, a short questionnaire is presented to the subject. This includes information such as the volunteer's age and gender, their dominant hand, and whether or not the subject has ever undergone deep brain stimulation.

After this step, and the subject indicates that they are ready to start the test, a beep sounds 3 seconds before the indication to initiate movement. The indications about the type of movement to perform and its illustrative image are presented to the volunteer. The activity period lasts for 30 seconds. Likewise, the auditory cue is emitted to indicate the end of the movement and the beginning of the rest period, which has the same duration as the activity period. After this sound signal, a window with the expression "Rest!" is displayed on the screen. The entire process from the audible cue indicating the approaching start of the movement to the end of the rest period is performed for all tasks in several blocks. Figure 4.7 represent the developed paradigm.

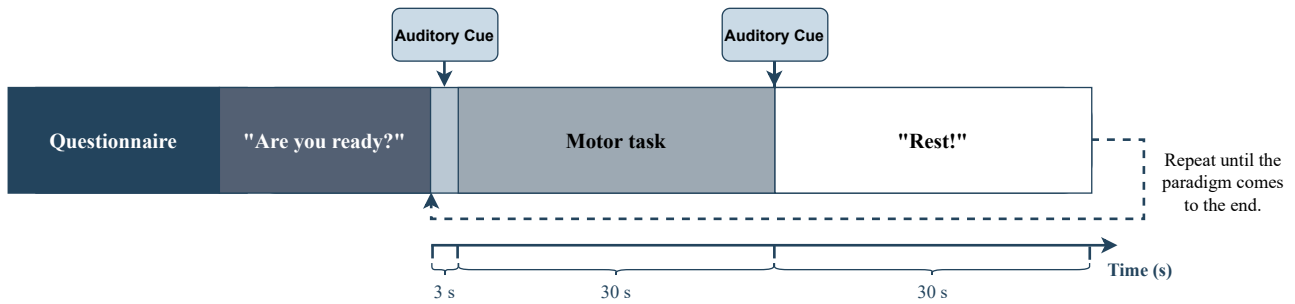


Figure 4.7: Developed motor paradigm.

The choice of the number of blocks to be executed is dependent on the cooperation of the volunteers. However, it is known that a more significant number of motor task blocks are likely to produce more reliable results.

During the entire execution of the paradigm, the volunteers should be in a room with the door closed and technological equipment such as cell phones and television turned off to avoid noise and interference with the signals being recorded.

In studies with iEEG or LFP signals, the same paradigm should be repeated after stimulation of the selected target with 2 mA and 4 mA.

4.3 Methods

4.3.1 Non-invasive EEG Movement Study

4.3.1.1 Setup

Both the EEG signals acquired from an SD LTM 64 PLUS headbox and the video were recorded simultaneously by the SystemPlus EVOLUTION software. This software was installed on a computer that displayed the visual and auditory stimuli indicative of the various phases of the paradigm.

After each session, the acquired EDF and AVI files were saved on an external disk that would later be connected to a laptop with MATLAB installed. A routine to calculate the ERD/ERS curves and perform TFA on the events of interest was created on the laptop.

A schematic of the setup used for this study is shown in figure [4.10](#).

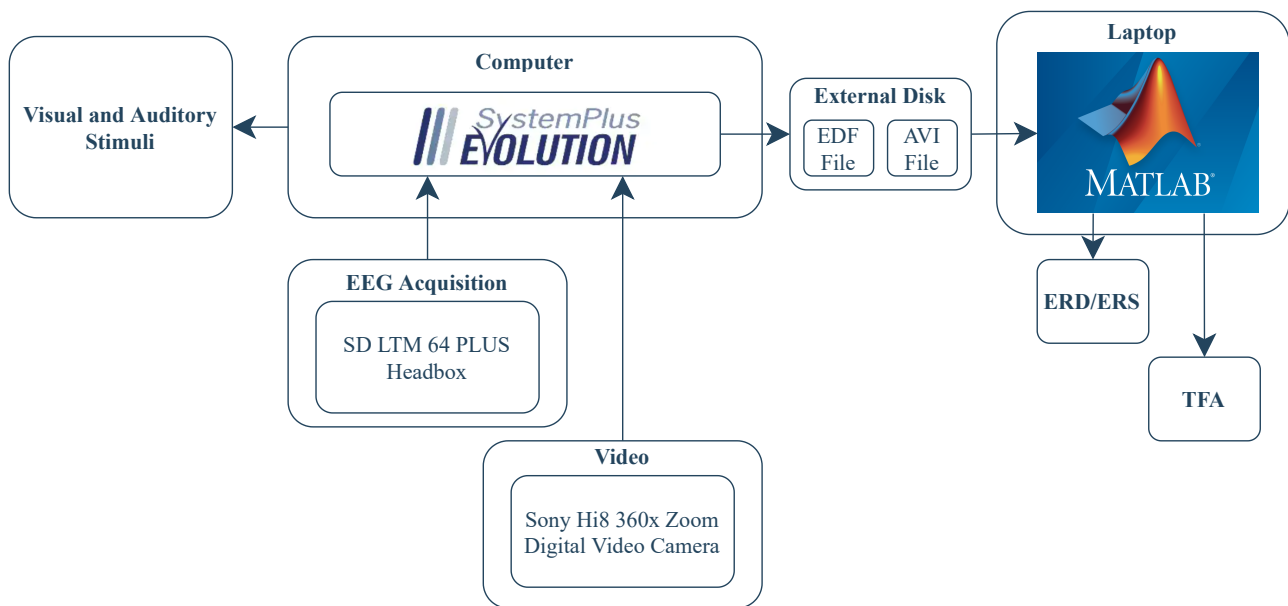


Figure 4.8: Developed setup for non-invasive EEG movement study.

4.3.1.2 Subjects

Fifteen healthy subjects (8 women; mean age: 22.9 ± 1.9 years) participated in this experimental study. However, data acquired from 6 healthy volunteers were excluded due to the poor quality of recording EEG signals. About 78% of the participants were right-handed. All participants were informed about the purpose and conditions of the study and gave written informed consent.

4.3.1.3 Procedure

For the experimental trials, the volunteers were seated on a chair in a room with low light and no interference from noise or electronic equipment. Before the beginning of the experimental paradigm, it was ensured that the subjects were sitting comfortably. Each subject performed seven blocks of the paradigm, including all proposed motor tasks. They were asked to avoid blinking, swallowing, or making any movement other than those requested while performing the exercises. The subjects' performance was being corrected throughout the experiment.

4.3.1.4 EEG Signal Acquisition

The EEG signals were acquired using a Micromed SD LTM 64 PLUS headbox. Elastic caps with 32 and 64 Ag-AgCl electrodes to place the electrodes on the subjects' scalp were used. It is important to note that adjustable caps of different sizes were used depending on the countenance of the subject's scalp. The signals were recorded in a monopolar montage and came from 8 active electrodes at FPz, Fz, C3, Cz, C4, P3, Pz, and P4 according to the international standard 10-20 system. The electrodes at the AFz and CPz locations were used as ground and reference, respectively. The central channels (C3, Cz, and C4) were selected since they retain motor activity and body sensations information. The parietal area channels (P3, Pz, and P4), on the other hand, are related to cognitive processing and some motor areas (101). The recorded signals were observed in real-time and were sampled at 256 Hz.

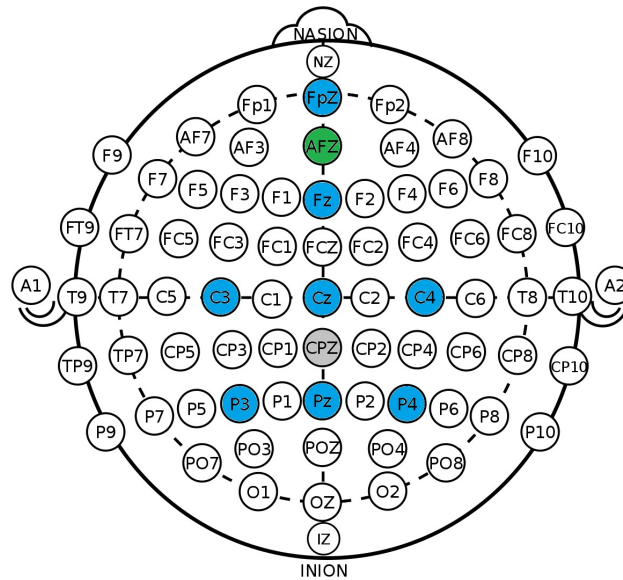


Figure 4.9: Electrode array used in EEG movement study. The ground and reference electrodes are colored in green and gray respectively. The remaining used electrodes are colored in blue.

4.3.1.5 Preprocessing

The preprocessing of the EEG data was performed using the EEGLAB toolbox (v2020.0) integrated into MATLAB. By inspecting the vEEG, the events were marked in the obtained data. The data was re-referenced to common average reference. After removing the DC component, the signals were filtered between 8 and 30 Hz using a 4th order Butterworth filter.

The events were extracted in the form of epochs. Their information included the data from 4 seconds before the beginning of the movement until the end of the movement ([-4000 30000] ms). In order to observe the behavior of the data after the end of the action, some epochs were also acquired between 4 seconds before the beginning of the movement and 4 seconds after the end of the movement.

The ICA method was applied to all epochs by using the *infomax* algorithm². This step detected the ICs in the signal and rejected artifacts, but a visual inspection was also performed to remove any artifact that the previous methods had not removed.

4.3.1.6 ERD/ERS and TFA Analysis

ERD/ERS quantification was performed as described in the [Quantification of ERD/ERS in Time and Space](#) section for available electrodes sites. Since EEGLAB did not have this function built-in, a script was developed in MATLAB (R2020a) for this purpose.

Time-frequency maps were obtained for the electrodes of interest in the frequency range 8-30 Hz. A method based on Wavelet decomposition was used for this. To this end, the number of cycles initially chosen was equal to 3 (Hanning-tapered window). This number continued to expand, reaching 20% in the equivalent FFT window at the highest frequency.³ The baseline corresponded to the 4 seconds before the movement onset.

²EEGLAB: runica. Available at: <https://sccn.ucsd.edu/jung/tutorial/runica.htm> (Accessed 03-10-2021)

³EEGLAB: pop_newtimef. Available at: https://github.com/sccn/eeqlab/blob/develop/functions/popfunc/pop_newtimef.m (Accessed 03-10-2021)

4.3.2 iEEG Movement Study

4.3.2.1 Setup

Both the iEEG signals acquired from an SD LTM 64 EXPRESS headboxes and the video were recorded simultaneously by the BRAIN QUICK® EEG software. This software was installed on a computer that displayed the visual and auditory stimuli indicative of the various phases of the paradigm.

After each session, the acquired EDF and AVI files were saved on an external disk that would later be connected to a laptop with MATLAB installed. A routine to calculate the ERD/ERS curves and perform TFA on the events of interest was created on the laptop.

A schematic of the setup used for this study is shown in figure 4.8.

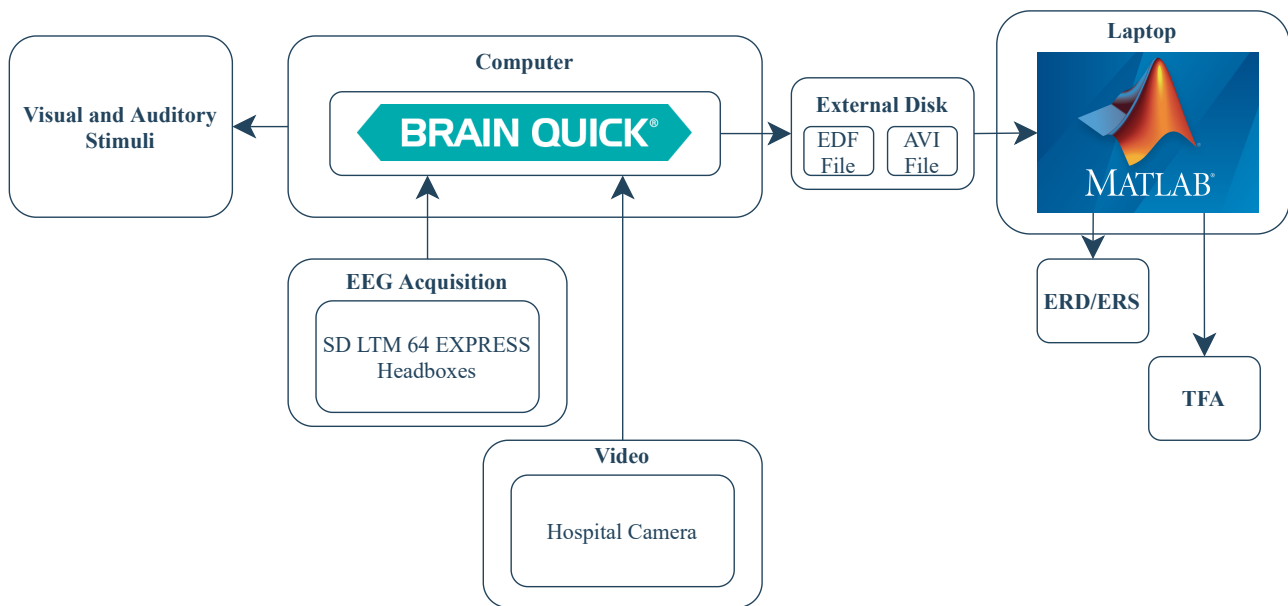


Figure 4.10: Developed setup for iEEG movement study.

4.3.2.2 Subjects

Only one epileptic patient with focal temporal epilepsy (male; 63 years old) and right-handed participated in this experimental study. The participant was informed of the purpose and conditions of the study and gave written informed consent.

4.3.2.3 Procedure

The subject was seated on a bed in a room with low light and no interference from noise or electronic equipment. Before the beginning of the experimental paradigm, it was ensured that the subject was sitting comfortably. Four blocks of the paradigm were performed before stimulation and another four after stimulation. These processes took place on two different days. The volunteer was asked to avoid blinking, swallowing, or making movements other than those requested while performing the exercises. The subject performance was being corrected throughout the experiment.

4.3.2.4 iEEG Signal Acquisition

iEEG signals were acquired using a micromed SD LTM 64 EXPRESS headbox. Data were recorded from electrodes located on body, tail, and head of the hippocampus, the anterior and posterior insula, the anterior

medial and posterior cingulate, the frontal orbital area, and the amygdala shown in figure 4.11, in a bipolar montage. The designations of each electrode, as well as their inputs, are described in table 4.1.

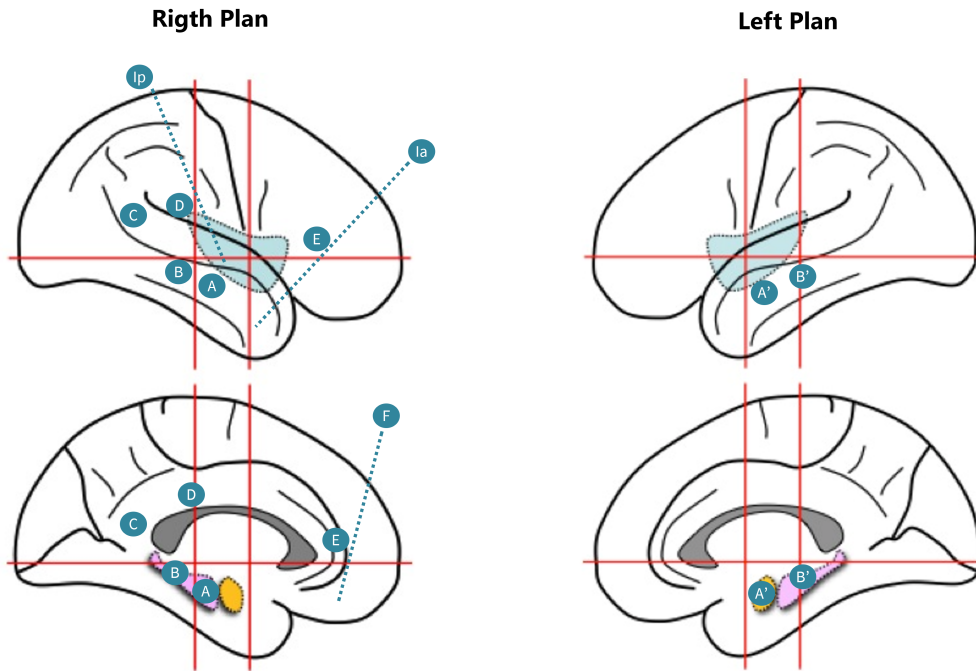


Figure 4.11: Target positions for the movement study with iEEG signals corresponding to the right (left side) and left (right side) plans. The yellow shaded region represents the amygdala, the pink shaded region represents the hippocampus and the blue shaded region represents the insula.

Table 4.1: Targets' details for iEEG movement study.

Name	Input	Target
A	T2	Hippocampus' body
B	T2	Hippocampus' tail
C	Posterior T1	Posterior cingulate
D	P2	Medial cingulate
E	F2	Anterior cingulate
F	F1	Frontal orbital
Ia	F1/2	Anterior insula
Ip	P1	Posterior insula
A'	T2	Amygdala
B'	T2	Hippocampus' head

The recorded signals were observed in real-time and were sampled to 1024 Hz.

4.3.2.5 Stimulation Protocol

Each of the electrodes in a bipolar assembly was subjected to 50 Hz biphasic stimulation for 5 s. Experimental testing was started with an intensity of 1 mA and gradually increased to 4 mA, or 3 mA in the hippocampus, with a 1 mA interval. The interval between stimuli was 5 s. During the procedure, the patient was asked to repeat the hand rubbing movement, and the data and its changes were observed in real-time.

4.3.2.6 Preprocessing

The preprocessing of the iEEG data was performed using the EEGLAB toolbox (v2020.0) integrated into MATLAB. By inspecting the vEEG, the events were marked in the obtained data. After removing the DC component, the signals were filtered between 0.015 and 75 Hz using a 4th order Butterworth filter.

The events were extracted in the form of epochs. Their information included the data from 4 seconds before the beginning of the movement until the end of the movement ([-4000 30000] ms). In order to observe the behavior of the data after the end of the action, some epochs were also acquired between 4 seconds before the beginning of the movement and 4 seconds after the end of the movement.

The ICA method was applied to all epochs by using the *infomax* algorithm⁴. This step detected the ICs in the signal and rejected artifacts, but a visual inspection was also performed to remove any artifact that the previous methods had not removed.

4.3.2.7 ERD/ERS and TFA Analysis

The analysis was the same used in the movement EEG study within the frequency range selected for this study.

4.3.3 LFP Movement Study

4.3.3.1 Setup

In addition to the implantable neurostimulator, the Percept™ PC is also composed of a clinician programming tablet, communicator, and a patient controller (102). The LFP signals acquired from this device were registered on the tablet in JSON file format. When these signals were recorded, the neurostimulator was programmed to stimulate or not the targets of interest. Simultaneously, a 3D Infrared Depth Radar Video and Infrared Video NeuroKinect System were used for vEEG acquisition. The video could be observed in real-time on the computer, while the LFP signals were only recorded on the computer after the end of each session.

Next, the LFP data was saved on an external disk as well as the AVI file. The disk would later be connected to a laptop with MATLAB installed. A routine was created on the laptop to calculate the ERD/ERS curves and perform TFA on the events of interest.

A schematic of the setup used for this study is shown in figure 4.12.

4.3.3.2 Subjects

Only one epileptic patient with focal temporal epilepsy (male; 60 years old) participated in this experimental study. The participant was informed of the purpose and conditions of the study and gave written informed consent.

4.3.3.3 Procedure

The subject was seated on a bed in a room with dim light and no interference from noise or electronic equipment. In this case, the experimental paradigm was to perform outward and inward movements with the hands (automotor automatism), with the arms in the air for about 18 s. The paradigm was performed once without deep brain stimulation and repeated at 2 mA and 4 mA stimulation.

⁴EEGLAB: runica. Available at: <https://sccn.ucsd.edu/jung/tutorial/runica.htm> (Accessed 03-10-2021)

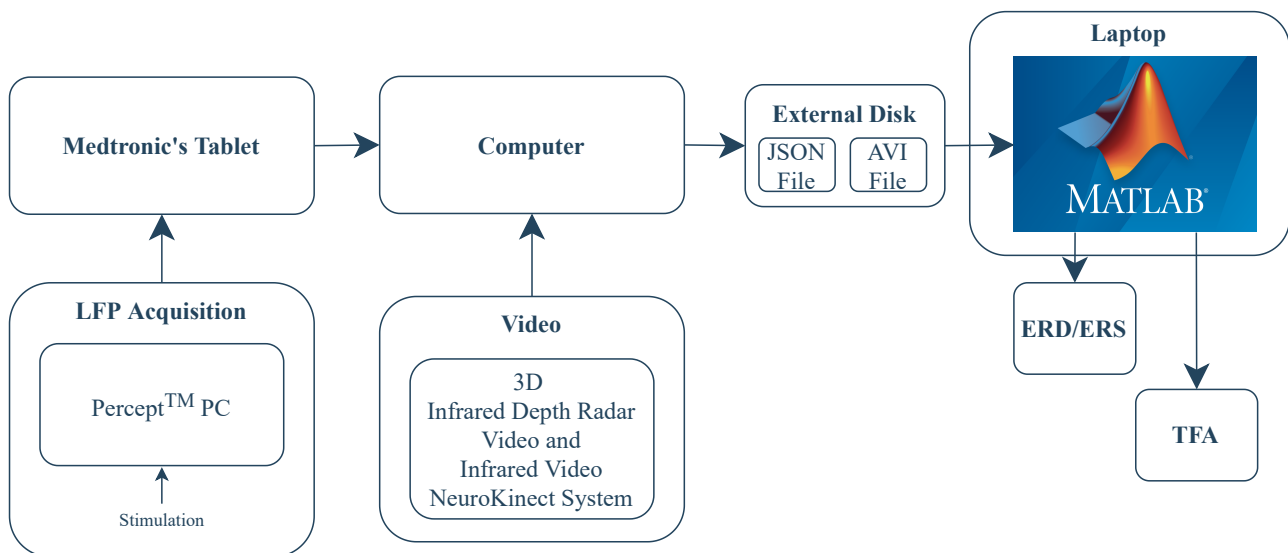


Figure 4.12: Developed setup for LFP movement study.

4.3.3.4 LFP Signal Acquisition

The LFP signals were acquired using the Percept™ PC neurostimulator. During the motor paradigm (described in the [Procedure](#) section), the signal acquisition was performed in BSS mode. The recordings correspond to the signals coming from the electrodes located at 1-3R and 1-3L. It is important to note that channel 1-3R was located in contact with the ANT and other neighboring structures, while electrode 1-3L was in direct contact only with the ANT.

LFP signals were recorded simultaneously with EEG signals and vEEG.

4.3.3.5 Preprocessing

Preprocessing of the LFP data was performed using the EEGLAB toolbox (v2020.0) integrated into MATLAB. After removing the DC component, the signals were filtered between 1 and 90 Hz using a 4th order Butterworth filter.

Based on the method suggested by Islam *et al.* (103) for identifying finger movements in LFP data, the wavelet packet transform (WPT) was used to extract the features of the LFP signals in the frequency range between 1 and 90 Hz. Thus, the discrete Meyer wavelet (demy) was applied with a decomposition level equal to 5. After reconstruction of the signals obtained after this processing, the Welch's power spectral density was estimated (window=500; samples=7250; overlapping=50%; f=1:90 Hz) in order to get the frequency range in which each of the signals is comprised. This entire method was scripted in MATLAB. Next, all signals with different frequency ranges were redirected to EEGLAB. By inspecting the vEEG, the events were marked in the data. The events were extracted in the form of epochs. Their information included the data from 2 seconds before the beginning of the movement to the end of the movement ([-2000 18000] ms). The ICA method was applied to all epochs by using the runica algorithm. This step detected the ICs in the signal and rejected artifacts, but a visual inspection was also performed to remove any artifact that the previous methods had not removed.

4.3.3.6 LFP Analysis

Regarding the LFP data, ERD/ERS quantification was performed as described in the [Quantification of ERD/ERS in Time and Space](#) section for available electrodes sites. Since EEGLAB did not have this function built-in, a

script was developed in MATLAB (R2020a) for this purpose.

Time-frequency maps were obtained for the electrodes of interest in the frequency range 1-90 Hz . A method based on Wavelet decomposition was used for this. To this end, the number of cycles initially chosen was equal to 3 (Hanning-tapered window). This number continued to expand, reaching 20% in the equivalent FFT window at the highest frequency.⁵

For the representation of the frequency map, the 2 seconds prior to the movement in which the patient had his arms in the air without movement were chosen as the baseline. The movement had a total duration of 18 seconds. In addition, frequency maps for the signals resulting from WTP processing were obtained in the calculated frequency range after estimating Welch's power spectral density.

Furthermore, a script was created in MATLAB capable of reading and analyzing a portion of the vEEG corresponding to the movement paradigm in the absence of stimulation. A rectangle in which one of the hands could be visualized was selected and cut away from all the frames of the video. Thus, it was possible to identify the moments corresponding to the onset of movement throughout the video. By convention, it was defined that the movement started with the hands facing outward. The average duration of the movement as well as its frequency were obtained.

⁵EGLAB: pop_newtimef. Available at: https://github.com/sccn/eeglab/blob/develop/functions/popfunc/pop_newtimef.m (Accessed 03-10-2021)

Chapter 5

Results and Discussion

5.1 EEG Movement Study

5.1.1 ERD/ERS Quantification and TFA

5.1.1.1 Results

The obtained ERD/ERS time course for finger to nose (with right hand) movement revealed the onset of desynchronization in the contralateral zone to the movement. The ERD started just over 2 seconds before the action, in the 8-12 Hz band. The desynchronization becomes symmetrical within the first 0.5 seconds before the activity. For the 13-30 Hz frequency range, similar patterns were observed. In both cases, ERD was more significant in the contralateral zone (see figure 5.1).

An example of the time-frequency maps (8-30 Hz) for the same movement made by subject 3 at the electrodes located at C3 and C4 is represented in figure 5.2. The onset of desynchronization in the 2 seconds preceding the movement is evident in electrode C3 and the desynchronization during the movement is observed in both C3 and C4 electrodes.

It was possible to verify a similar behavior concerning the ERD appearance onset in the contra and ipsilateral areas in hand tap movements. In these movements, the ipsilateral desynchronization proved to be more significant than expected. During its execution, these movements were performed with direct contact between the two hands. Besides that, the area of the brain responsible for processing hand movement is located between the central and parietal regions (review figure 3.8). So, the signals corresponding to the electrodes located in P3 and P4 were also analyzed to understand whether the phenomenon observed was due to the overlapping of movement and body sensation processing (see figures 5.3 and 5.4). Our theory was confirmed, as desynchronization was shown to be more significant in the contralateral zones.

For more complex movements made with both hands, such as rubbing hands, circling hands, and making non-repetitive movements, the ERD in C3 and C4 appear approximately a couple of seconds before the activity starts. Concerning rubbing hands, circling hands movements (see figures 5.5 and 5.6), the intensity of the desynchronization was similar on both sides. Nevertheless, higher power was observed in the electrode located at C3. This phenomenon should be related to the fact that most volunteers are right-handed and have more excellent skill in the right hand.

Regarding non-repetitive movements, the desynchronization was not very significant (see figure 5.7). In the alpha rhythmic band, the ERD at the electrode located at C4 showed very low intensity. These phenomena can be due to the difficulty that the volunteers showed in mechanizing these more complex movements and, again, due to the subjects' greater general dexterity in the right hand.

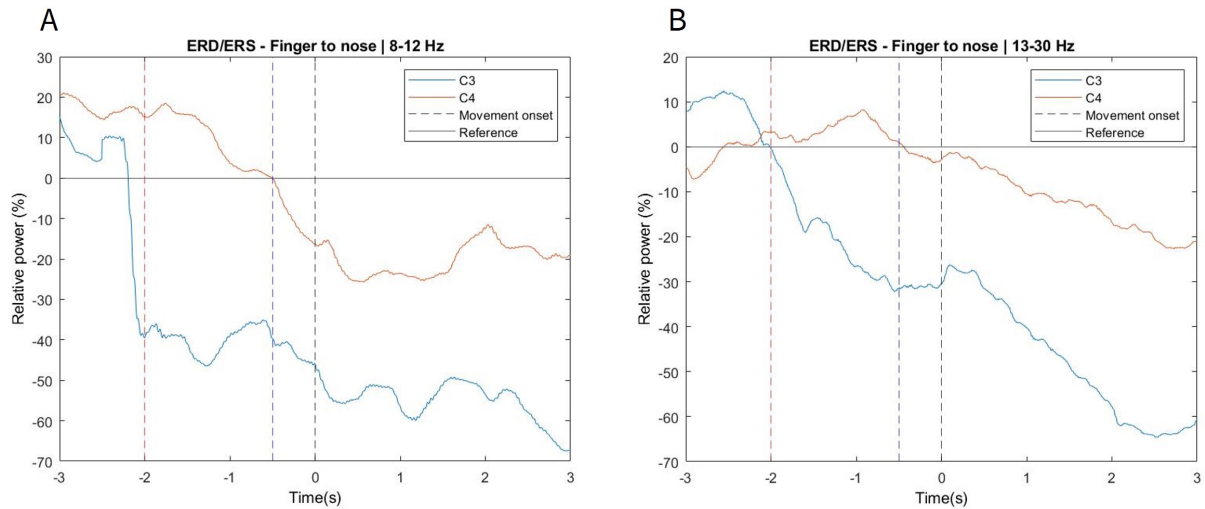


Figure 5.1: ERD/ERS time course for finger to nose movement. The EEG power of C3 and C4 in the alpha and beta frequency bands during the 3 s before, and the 3 s after the onset of movement all the blocks executed for all the subjects are depicted. The left panel shows ERD/ERS patterns that occur in alpha rhythm, and the right panel shows ERD/ERS patterns that occur beta rhythm. The blue signals represent the electrode C3, while the orange signals represent the electrode C4. The horizontal line indicates 0% power change, the black vertical line represents the movement onset in seconds, the red and dark blue vertical lines represent 2 and 0.5 seconds before the movement onset, respectively.

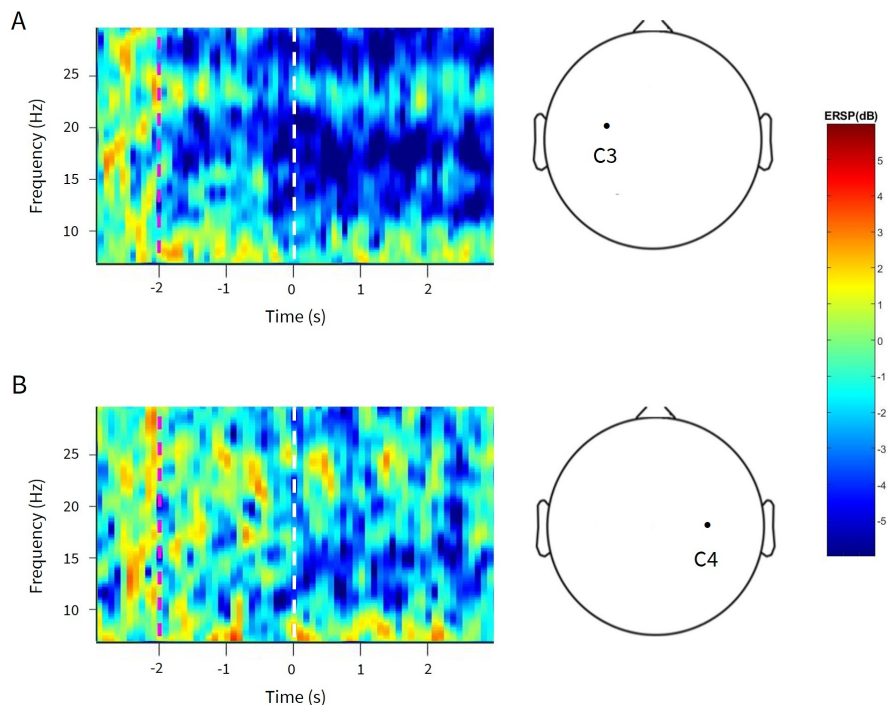


Figure 5.2: Time-frequency maps for finger to nose movement executed by subject 3 in frequency range of 8-30 Hz. The upper panel represents the time-frequency map obtained for electrode C3 and the bottom panel represents the time-frequency map obtained for electrode C4. The dotted magenta line represents 2 seconds before the movement onset and the white dotted line represents the movement onset. The blue color represents power decrease (ERD), and the red color represents power increase (ERS).

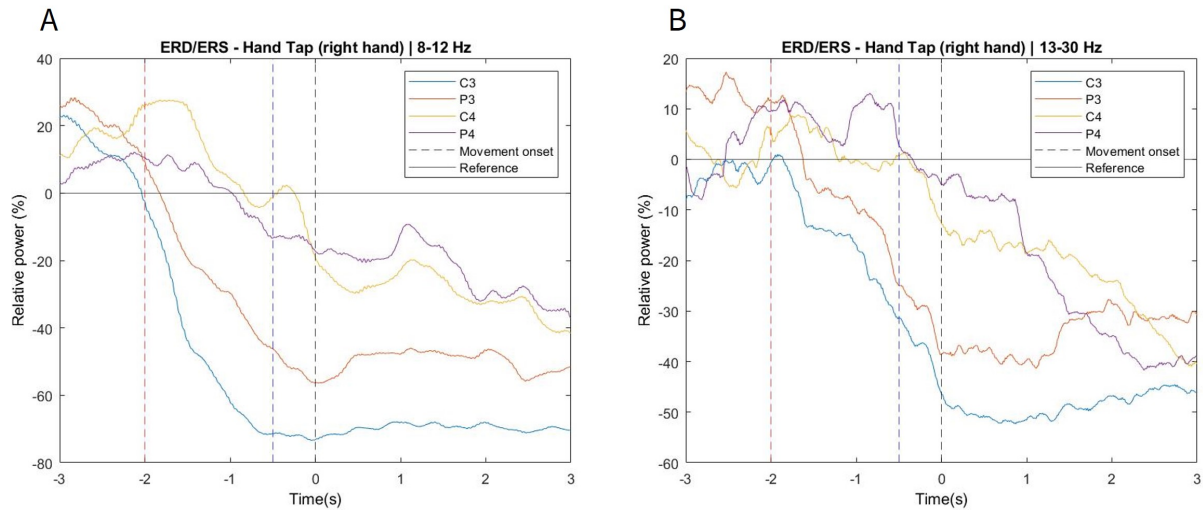


Figure 5.3: ERD/ERS time course for hand tap movement with the right hand. The EEG power of C3,P3,C4 and P4 in the alpha and beta frequency bands during the 3 s before, and the 3 s after the onset of movement all the blocks executed for all the subjects are depicted. The left panel shows ERD/ERS patterns that occur in alpha rhythm, and the right panel shows ERD/ERS patterns that occur beta rhythm. The blue signals represent the electrode C3, the orange signals represent the electrode P3, the yellow signals represent the electrode C4 and the purple signals represent the electrode P4. The horizontal line indicates 0% power change, the black vertical line represents the movement onset in seconds, the red and dark blue vertical lines represent the 2 and 0.5 seconds before the movement onset, respectively.

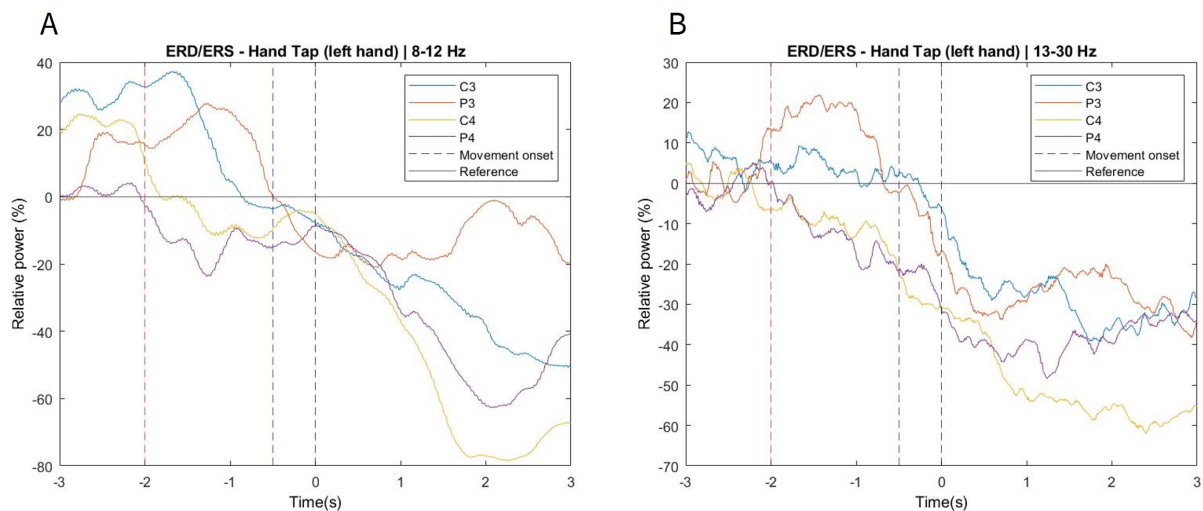


Figure 5.4: ERD/ERS time course for hand tap movement with the left hand. The EEG power of C3,P3,C4 and P4 in the alpha and beta frequency bands during the 3 s before, and the 3 s after the onset of movement all the blocks executed for all the subjects are depicted. The left panel shows ERD/ERS patterns that occur in alpha rhythm, and the right panel shows ERD/ERS patterns that occur beta rhythm. The blue signals represent the electrode C3, the orange signals represent the electrode P3, the yellow signals represent the electrode C4 and the purple signals represent the electrode P4. The horizontal line indicates 0% power change, the black vertical line represents the movement onset in seconds, the red and dark blue vertical lines represent the 2 and 0.5 seconds before the movement onset, respectively.

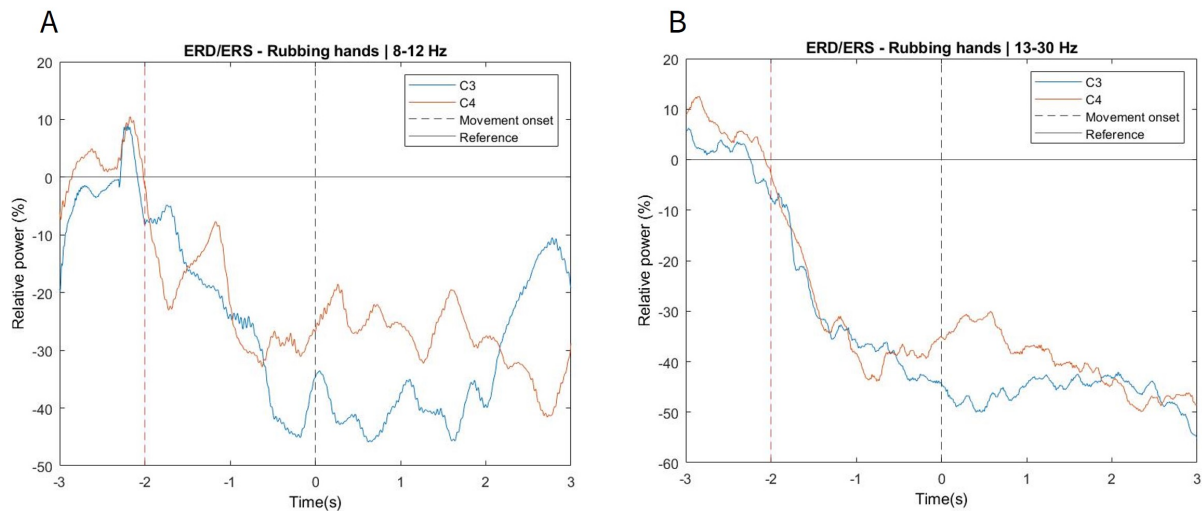


Figure 5.5: ERD/ERS time course for rubbing hands movement. The EEG power of C3 and C4 in the alpha and beta frequency bands during the 3 s before, and the 3 s after the onset of movement all the blocks executed for all the subjects are depicted. The left panel shows ERD/ERS patterns that occur in alpha rhythm, and the right panel shows ERD/ERS patterns that occur beta rhythm. The blue signals represent the electrode C3, while the orange signals represent the electrode C4. The horizontal line indicates 0% power change, the black vertical line represents the movement onset in seconds and the red vertical lines represent 2 seconds before the movement onset.

Finally, although ERD was seen before chewing, immediately after its onset, ERS appeared at the electrodes located at C3 and C4 (see figure 5.8).

5.1.1.2 Discussion

As presented in the [Neuronal Activity During Motor Functions](#) section, Lopes da Silva *et al.* (69) found that motor activity influences brain potentials. These potentials can be observed through EEG signals. Decreased neuronal synchronization in the areas responsible for motor processing, called ERD, leads to the reduced power of EEG signals. In contrast, increased synchronization of neurons, called ERS, leads to the opposite effect on EEG power.

The ERD/ERS curves consist of observing the change in EEG power (in percentage) during the execution of a movement relative to a period chosen as the baseline. The baseline corresponds to the average EEG power a few seconds before the beginning of the event.

Earlier, Hallett *et al.* (68) showed that the execution of a voluntary movement in healthy subjects results in desynchronization, in both alpha and beta rhythm. The ERD starts 2 seconds before the action onset in the contralateral zone and immediately before the movement onset in the ipsilateral area, always with a higher ERD in the contralateral zone. This is valid for any movement performed with the upper limbs.

This study based on the use of LFP signals used the application of a motor paradigm based on movements characteristic of epileptic seizures to reproduce the findings reported in the literature.

As Lopes da Silva *et al.* (69) had reported, all movements performed during the execution of the developed motor paradigm, except chewing, led to the appearance of desynchronization (ERD).

All movements performed with only one side of the upper limbs led to the appearance of ERD in the contralateral zone, 2 seconds before the beginning of the movement. The ERD became symmetrical immediately before the onset of the event for all these cases however, the ERD was always more significant in the contralateral zone. This was true for both alpha and beta rhythms. For example, in the finger-to-nose movement

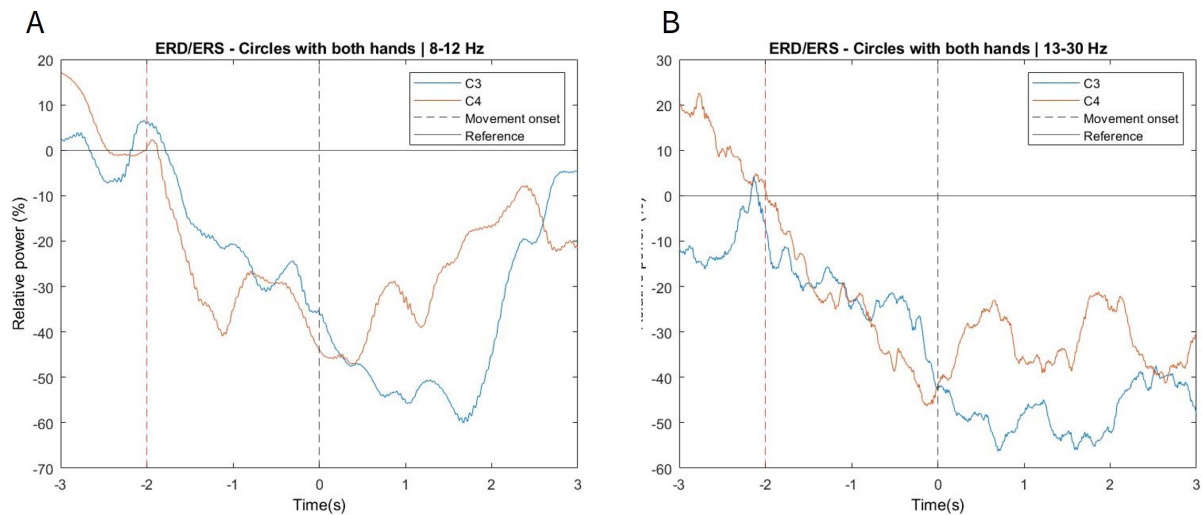


Figure 5.6: ERD/ERS time course for circles with the hands movement. The EEG power of C3 and C4 in the alpha and beta frequency bands during the 3 s before, and the 3 s after the onset of movement all the blocks executed for all the subjects are depicted. The left panel shows ERD/ERS patterns that occur in alpha rhythm, and the right panel shows ERD/ERS patterns that occur beta rhythm. The blue signals represent the electrode C3, while the orange signals represent the electrode C4. The horizontal line indicates 0% power change, the black vertical line represents the movement onset in seconds and the red vertical lines represent 2 seconds before the movement onset.

performed with the right hand, desynchronization was present around 2 seconds prior to the movement at the contralateral electrode C3. Immediately before the movement onset in the ipsilateral electrode C4, it also verified the appearance of ERD, however, with lower power than the one demonstrated in electrode C3. In the movements performed with both sides of the upper limbs, the desynchronization started about 2 seconds before the movement in both electrodes C3 and C4. Once again, it was possible to observe this for both alpha and beta rhythm.

These results are in line with what had been reported by Hallet *et al.* (68), thus validating the results found in the literature.

As for chewing, it was impossible to find any desynchronization pattern at the movement onset in the electrodes C3 and C4. This happens because these electrodes do not receive information from mouth movements.

Hence, it was possible to cross-check the data from this study with those found in the literature. However, it is important to note that it is recommended to perform several blocks of movement, and the ICA method to decompose the signal is only recommended for continuous signal acquisitions. However, a reduced number of blocks (7 blocks) of movements were used to study EEG movements, and the ICA method was applied to non-continuous acquisitions.

5.1.2 Alpha and Beta Rhythms

5.1.2.1 Results

For all the movements performed with the upper limbs, it was possible to verify the appearance of ERS after the termination of the event. However, some differences were observed in the alpha and beta frequency bands. Beta ERS was observed immediately after the end of the movement. In the alpha band, there was a longer period until the appearance of synchronization. An example of this phenomenon is shown in figure 5.9. The figure shows the alpha and beta rhythms 3 seconds before and after the end of the finger to nose movement.

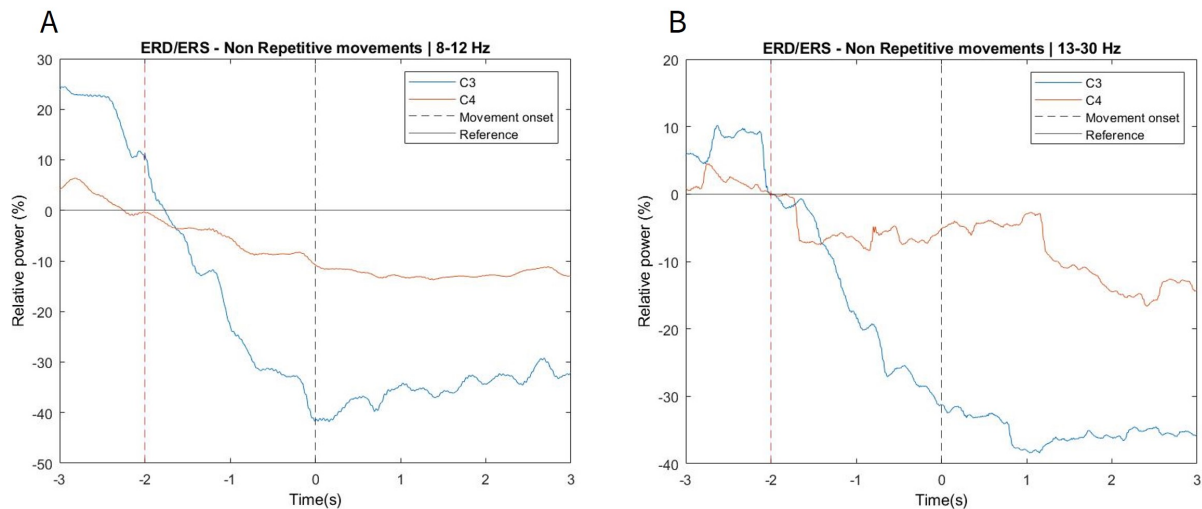


Figure 5.7: ERD/ERS time course for circles with the hands movement. The EEG power of C3 and C4 in the alpha and beta frequency bands during the 3 s before, and the 3 s after the onset of movement all the blocks executed for all the subjects are depicted. The left panel shows ERD/ERS patterns that occur in alpha rhythm, and the right panel shows ERD/ERS patterns that occur in beta rhythm. The blue signals represent the electrode C3, while the orange signals represent the electrode C4. The horizontal line indicates 0% power change, the black vertical line represents the movement onset in seconds and the red vertical lines represent 2 seconds before the movement onset.

5.1.2.2 Discussion

Pfurtscheller *et al.* (72) found that immediately after the end of a finger, arm or foot movement, a synchronized beta rhythm appears. In contrast, the alpha band needs more time to recover, so the ERS appears a little later. Additionally, the beta ERS usually reaches its maximum amplitude about 1 second after the end of the event. However, it is essential to note that the ERS beta components are specific to each individual and vary depending on the part of the body that performs the movement.

In this study, besides some slight differences described in the [ERD/ERS Quantification and TFA](#) section, the big difference observed between alpha and beta rhythms during the entire process of movement execution was in the recovery period after the end of the movement.

As reported in the literature, ERS beta appeared immediately after the end of the movement while the alpha rhythm took longer to recover. However, contrary to what Pfurtscheller *et al.* (72) reported, the maximum amplitude of beta ERS was not around 1 second after the movement.

Despite this contradiction, Pfurtscheller *et al.* (72) had also reported that the time interval in which the maximum ERS amplitude in the beta band was reached was movement-dependent and subject-specific. Thus, as described in (72), a 1-second power spectrum concerning the activity period was compared with another one in the rest period in order to be able to determine the specific frequency bands of subject 5 (see figure 5.10). The chosen activity period corresponded to 1-2 seconds after the end of the movement. A subject-specific frequency band between 13 and 15 Hz was obtained. The ERD/ERS time course plotted for the finger-to-nose movement of subject 5 in this frequency band is shown in figure 5.11. As expected, the ERS beta appeared immediately after the end of the movement and reached its maximum between 1 and 2 seconds after it.

Hence, it was possible to cross-check the data from this study with those found in the literature. However, it is important to note that the sample under study was not significant and the ICA method for identifying artifactual ICs in epochs despite only being advised for use in continuous data.

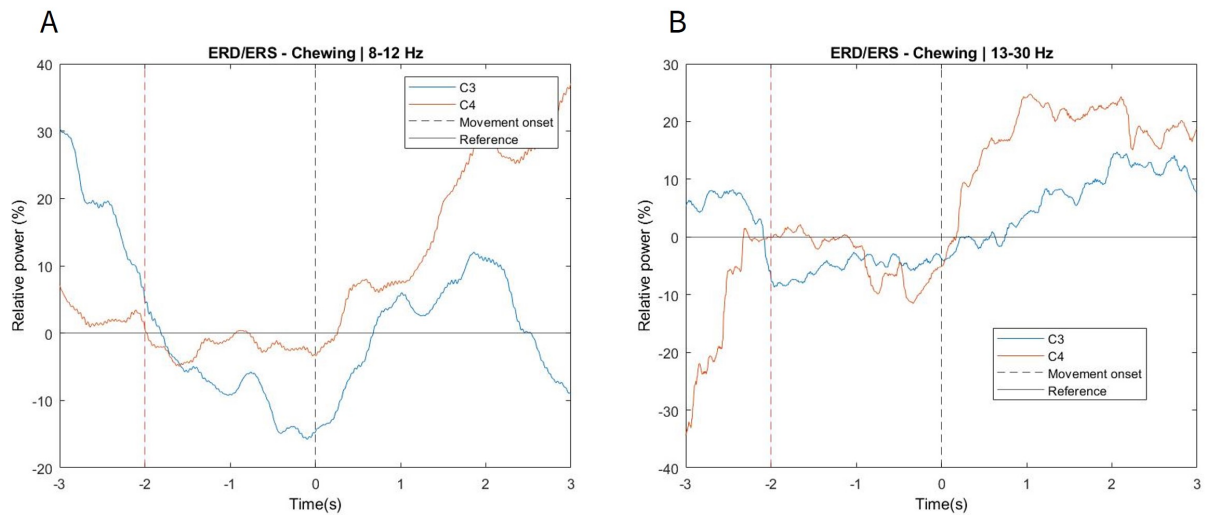


Figure 5.8: ERD/ERS time course for chewing. The EEG power of C3 and C4 in the alpha and beta frequency bands during the 3 s before, and the 3 s after the onset of movement all the blocks executed for all the subjects are depicted. The left panel shows ERD/ERS patterns that occur in alpha rhythm, and the right panel shows ERD/ERS patterns that occur beta rhythm. The blue signals represent the electrode C3, while the orange signals represent the electrode C4. The horizontal line indicates 0% power change, the black vertical line represents the movement onset in seconds and the red vertical lines represent 2 seconds before the movement onset.

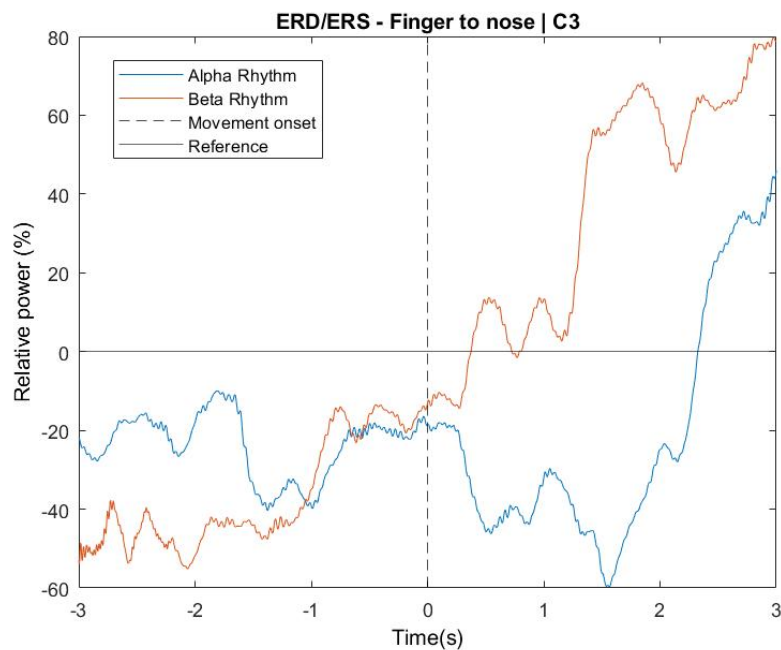


Figure 5.9: ERD/ERS time course for finger to nose movement for alpha and beta rhythms. The EEG power of C3 alpha and beta frequency bands during the 3 s before, and the 3 s after the offset of movement all the blocks executed for all the subjects are depicted. The blue signal represents the alpha rhythm, while the orange signal represents the beta rhythm. The horizontal line indicates 0% power change and the vertical line represents the movement offset.

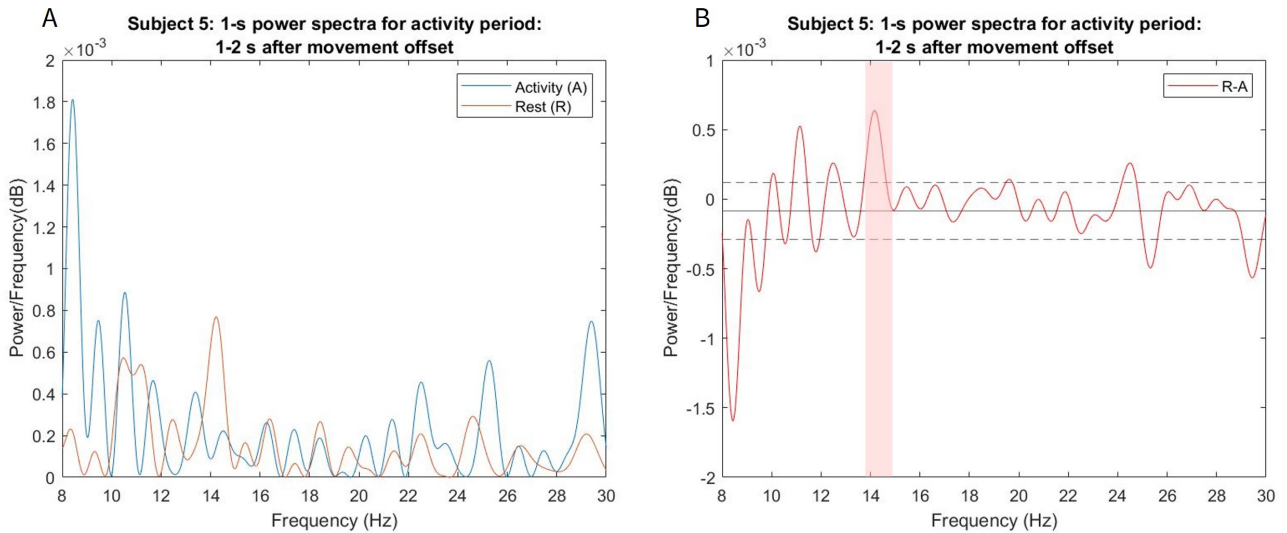


Figure 5.10: 1-second power spectra relative to the activity period 1-2 seconds after movement offset. The selected movement was the finger to nose. The continuous horizontal line indicates 0 power/frequency and the dotted lines indicate the 95% confidence interval. Orange signal represents the activity period and blue signal represents the rest period (left panel). The red signal represents the difference between the two of them (right panel). The red shaded region represents the subject 5 specific frequency band.

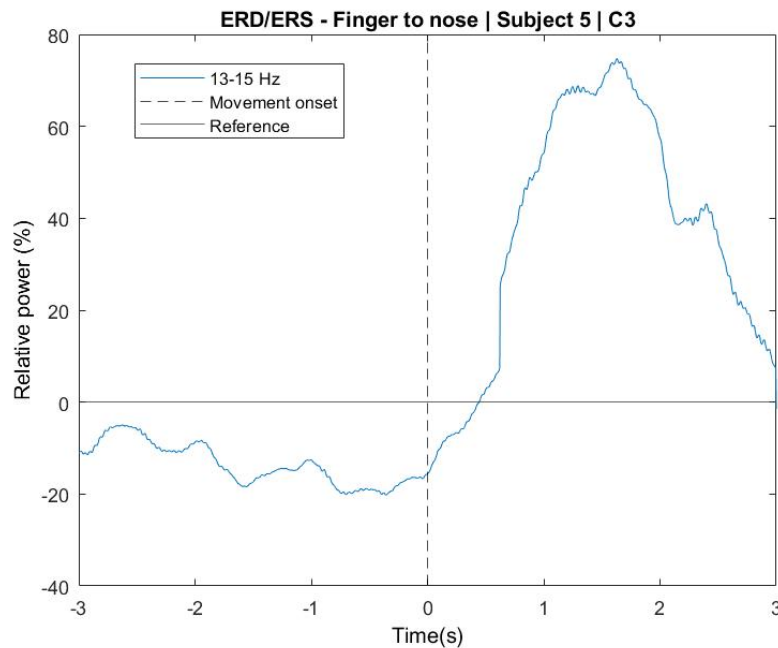


Figure 5.11: ERD/ERS time course for finger to nose movement. The EEG power of C3 in 13-15 Hz frequency band during the 3 s before, and the 3 s after the movement offset in all the blocks executed for subject 5 are depicted. The horizontal line indicates 0% power change and the dotted vertical line represents the movement offset in seconds.

5.2 iEEG Movement Study

5.2.1 Results

For all movements performed during the execution of the developed motor paradigm, temporal frequency maps in the frequency range of 0.5-75 Hz for electrodes located in sites belonging to the hippocampus were obtained.

An example of these maps for 3 of the electrodes of interest and during the execution of the finger to nose

movement is represented in the figure 5.12). As can be seen in the figure, it was impossible to observe patterns of desynchronization and synchronization indicative of movement.

In addition, the ERD/ERS time course for movements performed before and after stimulation application was plotted. Significant differences were not observed before and after the stimulation protocol execution, as noted in the figure 5.13.

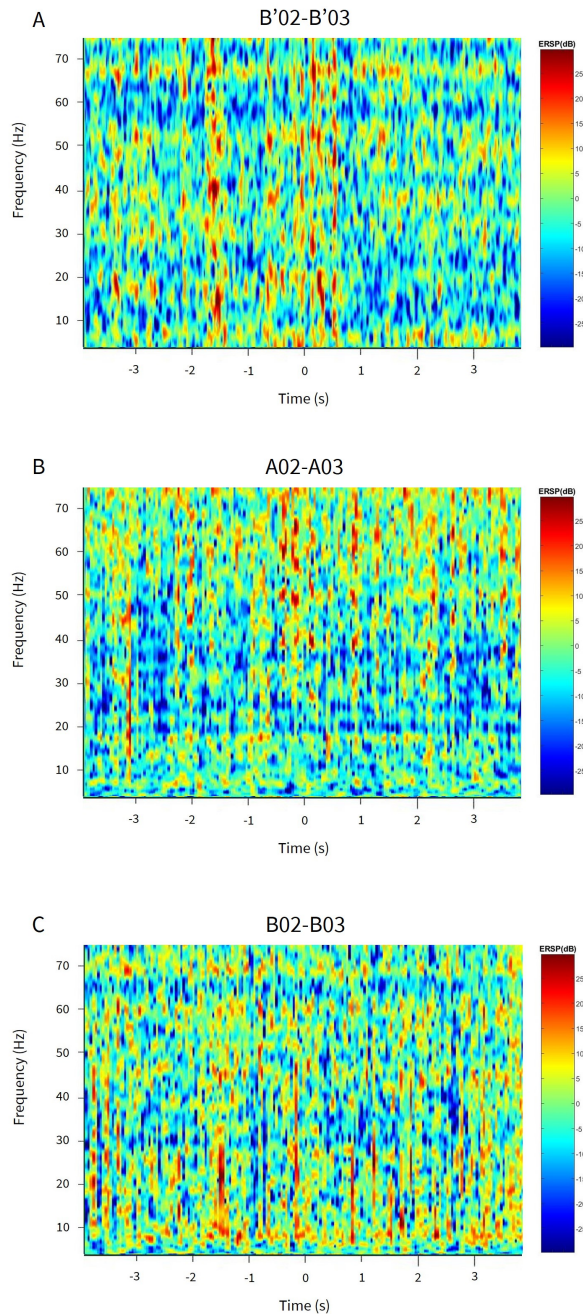


Figure 5.12: Time-frequency maps obtained for finger to nose movement in hippocampus targets. The maps were obtained in 0.5 to 75 Hz frequency range for 4 seconds before and after the movement onset. The upper panel represents the B'02-B'03 electrodes acquisitions, the middle panels represents the A02-A03 electrodes acquisitions and the bottom panel represents the B02-B03 electrodes acquisitions. The blue color represents power decrease (ERD), and the red color represents power increase (ERS).

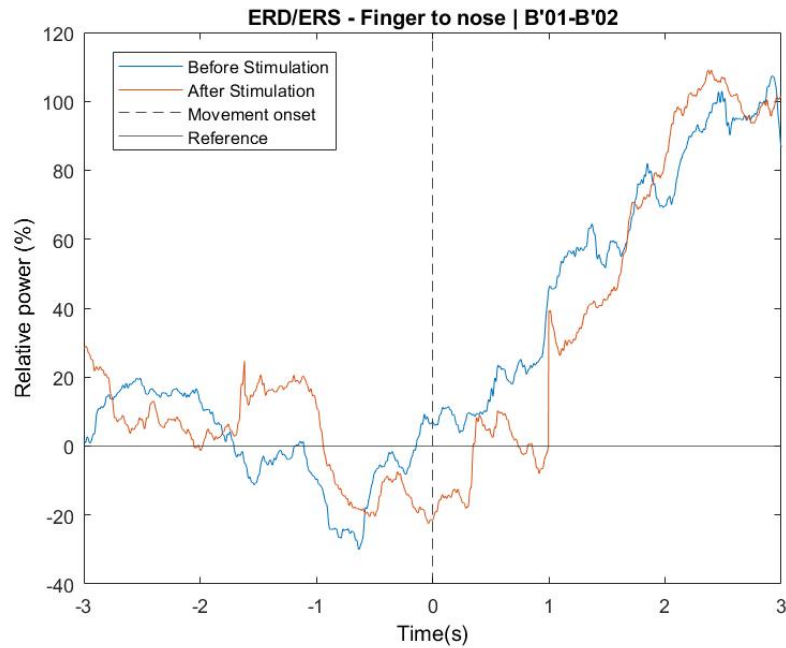


Figure 5.13: Time course ERD/ERS for finger to nose movement executed before and after the stimulation. The data represents the signals acquired from B'01-B'02 electrodes 3 seconds before and after the movement onset. The blue signal represents the finger to nose movement before the stimulation while the orange signal represents the same movement after the stimulation. The horizontal line indicates 0% power change, the black vertical line represents the movement onset in seconds.

5.2.2 Discussion

Sochurkova *et al.* (89) conducted the only current ERD/ERS-based study during motor task performance when acquiring iEEG signals from the hippocampus. Only a 28-year-old right-handed man suffering from drug-resistant mesiotemporal lobe epilepsy participated in this study. A paradigm with a brisk self-paced flexion of the fingers was used. The ERD/ERS time course did not verify the occurrence of synchronization or desynchronization indicative of movement performance. This study did not address the differences found in the execution of movements before and after stimulation.

Kerr *et al.* (104) conducted a study that revealed the existence of movement-related powers in the hippocampus. These potentials have been observed through the analysis of Event-Related Potentials (ERPs).

In our study, the ERD/ERS patterns were analysed. In order to do so, the time-frequency maps for the electrodes located in locations belonging to the hippocampus were obtained. These maps did not reveal patterns of desynchronization and synchronization during the movement execution. This was true for all types of performed movements.

Therefore, these results were similar to those related in (89). However, it is relevant to note that the existing literature lists observations for a single trial and our data were acquired in a bipolar setup unlike the study reported in the literature, which may influence the results obtained. Additionally, the sample under study was not significant for both studies and the ICA method for identifying artifactual ICs in epochs, although it is only advised for use in continuous data. In addition, different types of mounts were used in the two studies which may make it impossible to compare them.

5.3 LFP Movement Study

Bočková *et al.* (87) conducted the only currently existing study involving ERD/ERS and using LFP signals from the ANT of humans. This investigation involved motor-cognitive tasks, and the patterns of synchronization and desynchronization found were attributed exclusively to cognitive function.

In our study, as a result of applying the WPT method, for each stimulation intensity, six new signals were obtained (details 1-5 and approximation 5) with different frequency bands. The estimation of Welch's power spectral density revealed that the signals resulting from this process relied on 1-5 Hz, 3-9 Hz, 7-17 Hz, 14-34 Hz, 27-56 Hz, and 50-90 Hz.

In the time-frequency map corresponding to the LFP signal in the range from 1 to 90 Hz, obtained in the 1-3L contact, a pattern of zones synchronized at a very similar frequency between them was observed. Such phenomenon did not occur for the 1-3R electrode (see figure 5.14).

The time-frequency map obtained for the contact located in the ANT in the 7-17 Hz frequency range demonstrated the existence of a synchronization pattern similar to that verified in the signal map involving the more comprehensive frequency range (see figure 5.15). In order to observe this phenomenon in more detail, an ERD/ERS time course was traced in that frequency range (see figure 5.16).

Although the literature indicates that a synchronized alpha rhythm of large amplitude may be indicative of 'idling' (71), it was suspected that the observed synchronization was correlated with the periods corresponding to the performance of the inward and outward hand-turning movement. Thus, the moments corresponding to the positive peaks, during the activity period, of the obtained ERD/ERS curve were detected. Thus, was obtained the frequency appearance of the detected peaks 1.09 ± 0.99 Hz.

The movement frequency was also obtained from the analysis of video frames corresponding to the movement paradigm. For this purpose, the frames corresponding to the position of the hands outwards were marked in order to be able to calculate the duration of each movement and, consequently, its frequency. Therefore, the frequency obtained was 1.27 ± 0.90 Hz, which is why we strongly believe in the proposed theory.

Next, the software MaxTRAQ - Innovision-Systems was used to trace the movement of the thumb of the patient's right hand. For this, the video corresponding to the execution of the requested motor automatism was analyzed with a sampling frequency of 30 Hz. Thus, the target (thumb of the right hand) was manually marked along with each frame, which allowed plotting a Y coordinate graph of that exact point along time and detecting the target's trajectory along with the whole movement (see figure 5.17).

In the graph representing the Y coordinates of the thumb (see figure 5.18) the positive peaks corresponded to the maximum rotation performed in the movement of turning the hands inwards, while the negative peaks corresponded to the same phenomenon but when the patient turned the hands outwards.

Figure 5.19 represents the overlay of the motion signal in the form of Y coordinates of the right thumb and the frequency vs time map obtained in the frequency band 7-17 Hz. The analysis of the superposition of these two signals allowed to verify that not all points of maximum hand rotation are accompanied by synchronization; however, all the movements in which there is synchronization correspond to a movement in which there is full hand rotation.

Furthermore, the video frames representing the peaks detected in the ERD/ERS time course revealed that, at those times, the patient's hands were turned inwards or outwards, as seen in figure 5.20.

It was also possible to investigate the delay between the ERD/ERS curve and the movement signal represented by the Y coordinates through cross-correlation between these two, and a delay of 2.464 s was obtained (see figure 5.21). Thus, it was verified that the ERD/ERS appeared about 2 seconds before the movement onset, as with desynchronization before movement in EEG signals (68).

Finally, figure 5.22 represents the superimposition of the ERD/ERS curve and the signal corresponding to the movement with delay and with the delay set. It was found that the positive or negative peaks of these two signals were mainly coincident.

In conclusion, the relationship between motor automatisms and the appearance of synchronization in the signals from the ANT is confirmed. This finding opens doors to investigate whether there is a relationship between the signals coming from the ANT and the automatisms triggered by epileptic seizures, and therefore whether the ANT has motor biomarkers related to epileptic seizures.

However, it is essential to mention that this experiment was carried out based on only one block in one trial, so a protocol of motor tasks proposed in [Experimental Protocol](#) should be applied, with the execution of the maximum number of blocks possible to validate the results obtained.

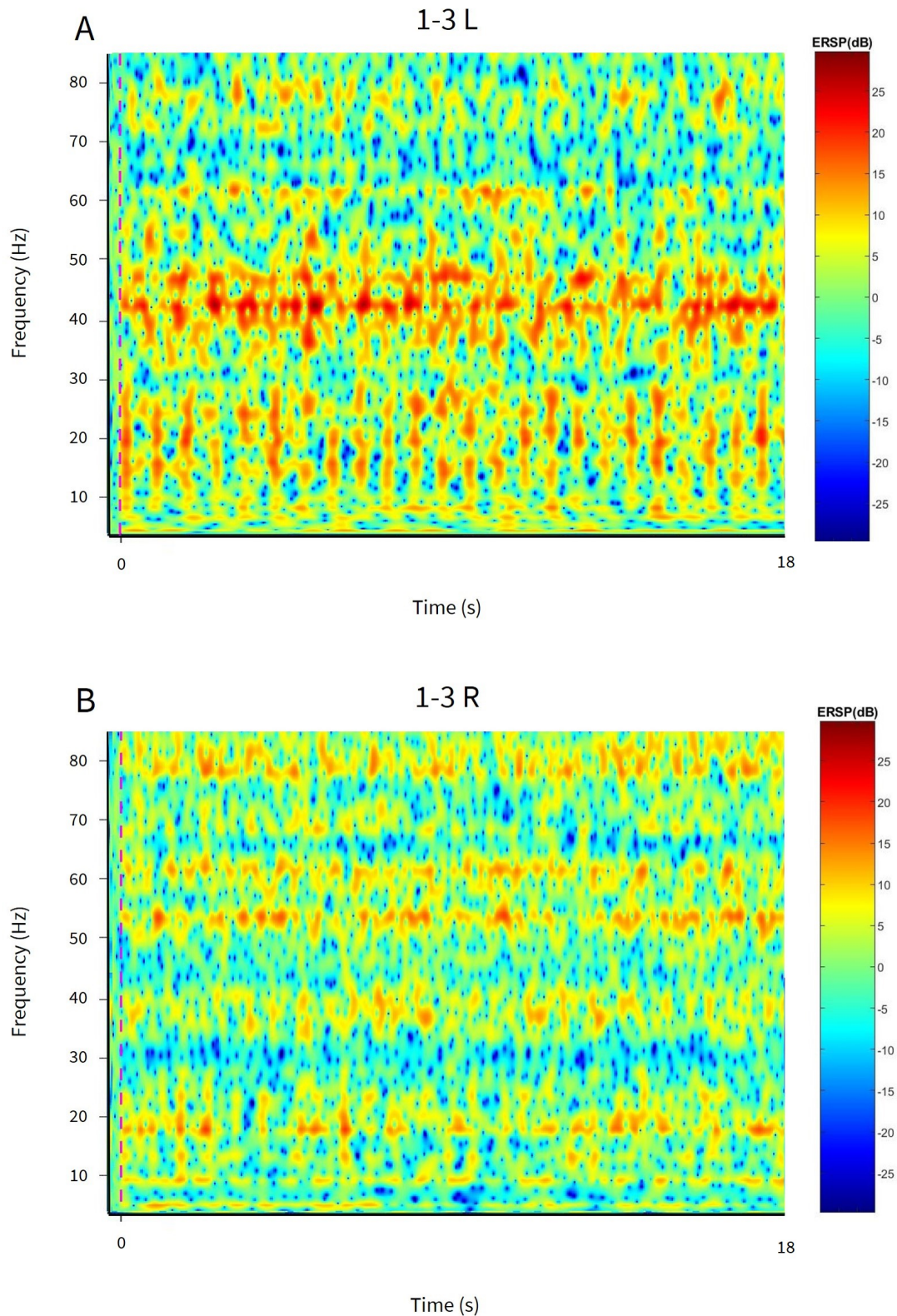


Figure 5.14: Time-frequency maps obtained for movement paradigm executed without stimulation. The maps were obtained in frequency range of 1-90 Hz and between 2 seconds before and 18 seconds after (movement offset) the movement onset. The upper panel represents the time-frequency map obtained for 1-3 L contact and the bottom panel represents the time-frequency map obtained for 1-3 R contact. The dotted magenta line represents the movement onset. The blue color represents power decrease (ERD), and the red color represents power increase (ERS).

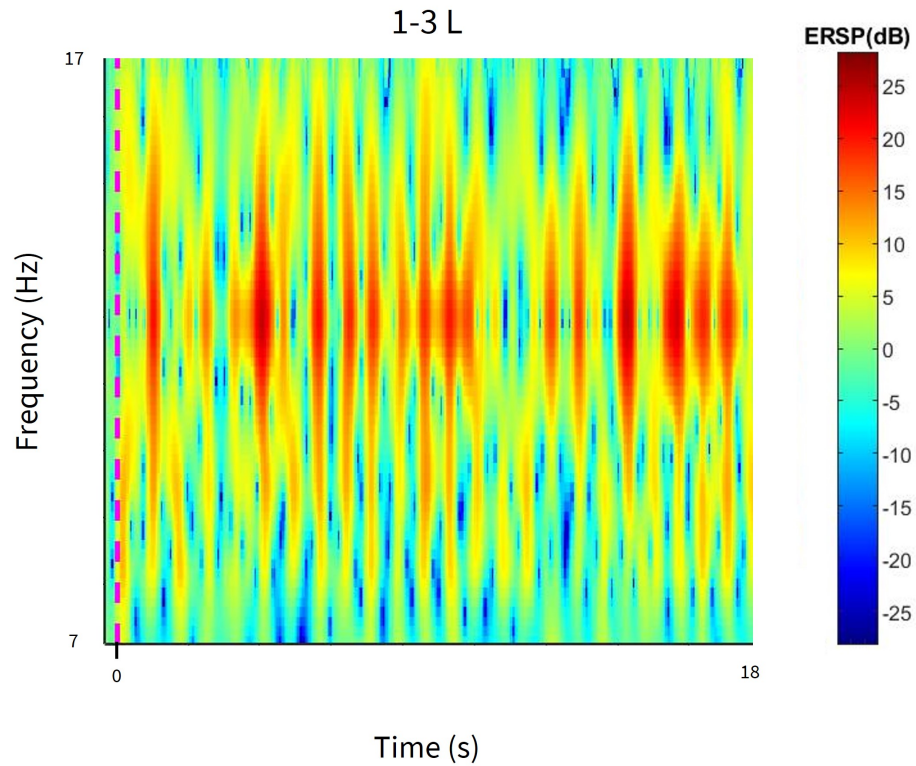


Figure 5.15: Time-frequency map for movement paradigm, executed without stimulation. The map was obtained in frequency range of 7-17 Hz and between 2 seconds before and 18 seconds (movement offset) after the movement onset. The map represents the 1-3 L contact. The dotted magenta line represents the movement onset. The blue color represents power decrease (ERD), and the red color represents power increase (ERS).

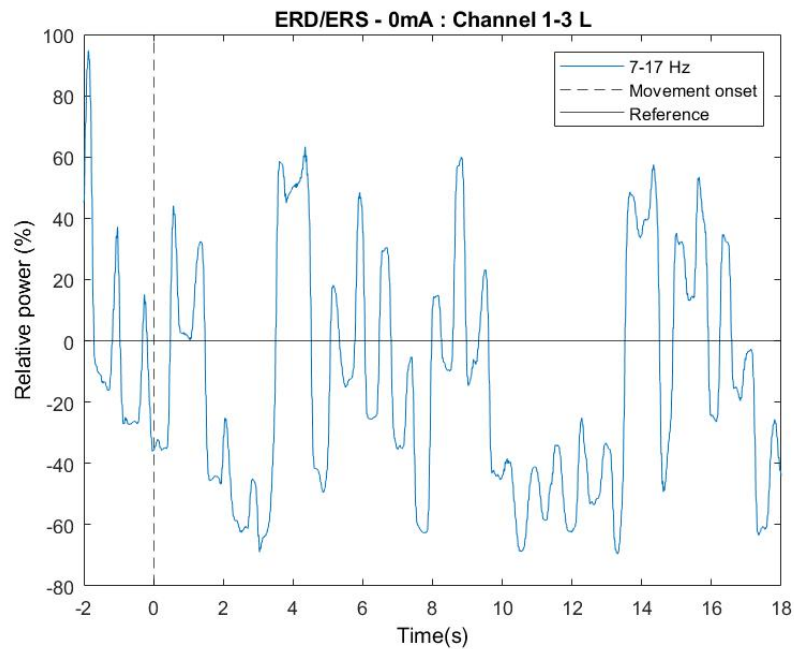


Figure 5.16: ERD/ERS time course for movement paradigm, executed without stimulation. The ERD/ERS pattern was obtained for frequency range of 7-17 Hz and between 2 seconds before and 18 seconds (movement offset) after the movement onset. The curve represents the 1-3 L contact. The horizontal line indicates 0% power change, the dotted vertical line represents the movement onset.



Figure 5.17: Representation of the selected target and its trajectory. The red dot represents the target corresponding to the thumb of the patient's right hand, and the green trace represents its trajectory along the motor automatism execution time.

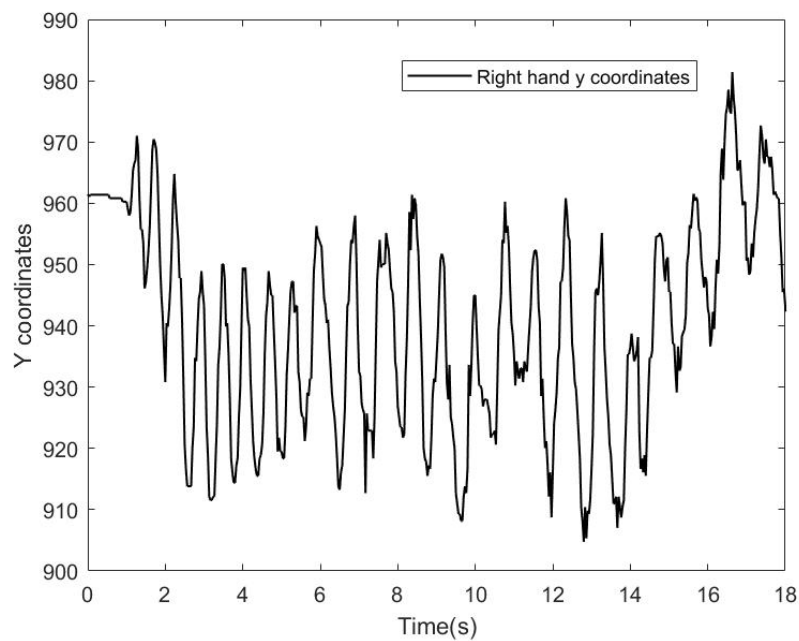


Figure 5.18: Y coordinates of the thumb of the patient's right hand over time. The time interval recorded corresponds to the period of execution of the proposed motor automatism.

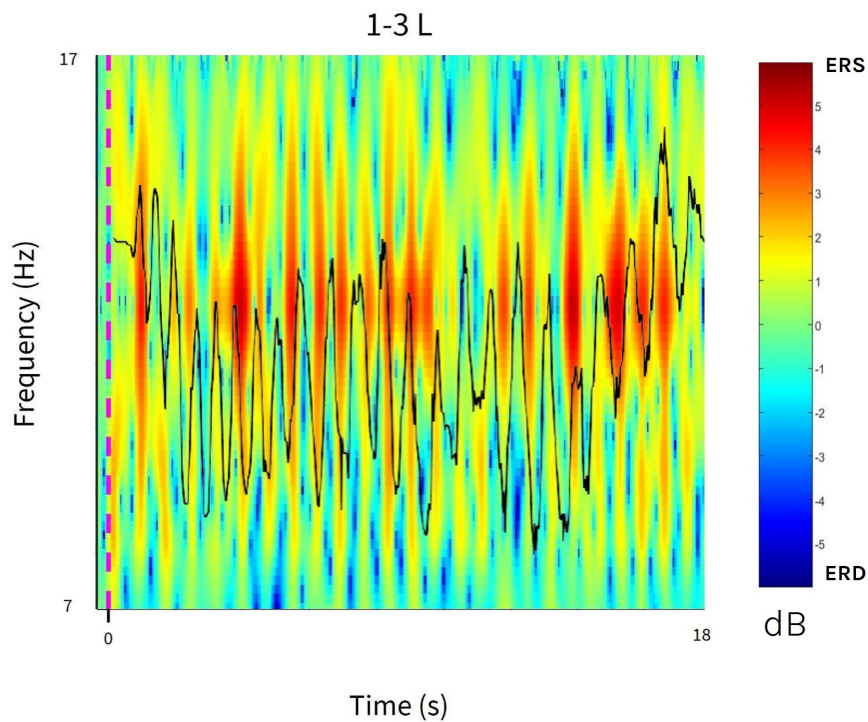


Figure 5.19: Overlay of the time-frequency map in the frequency range 7-17 Hz and the representative movement signal. The time-frequency map represents the period 2 seconds before and 18 seconds (offset movement) after the start of the action. The graph of Y coordinates of the patient's thumb is black and corresponds to the whole movement period. The map represents the 1-3 L contact. The dotted magenta line represents the beginning of the movement. The blue color represents the decrease in power (ERD), and the red represents the increase in power (ERS).

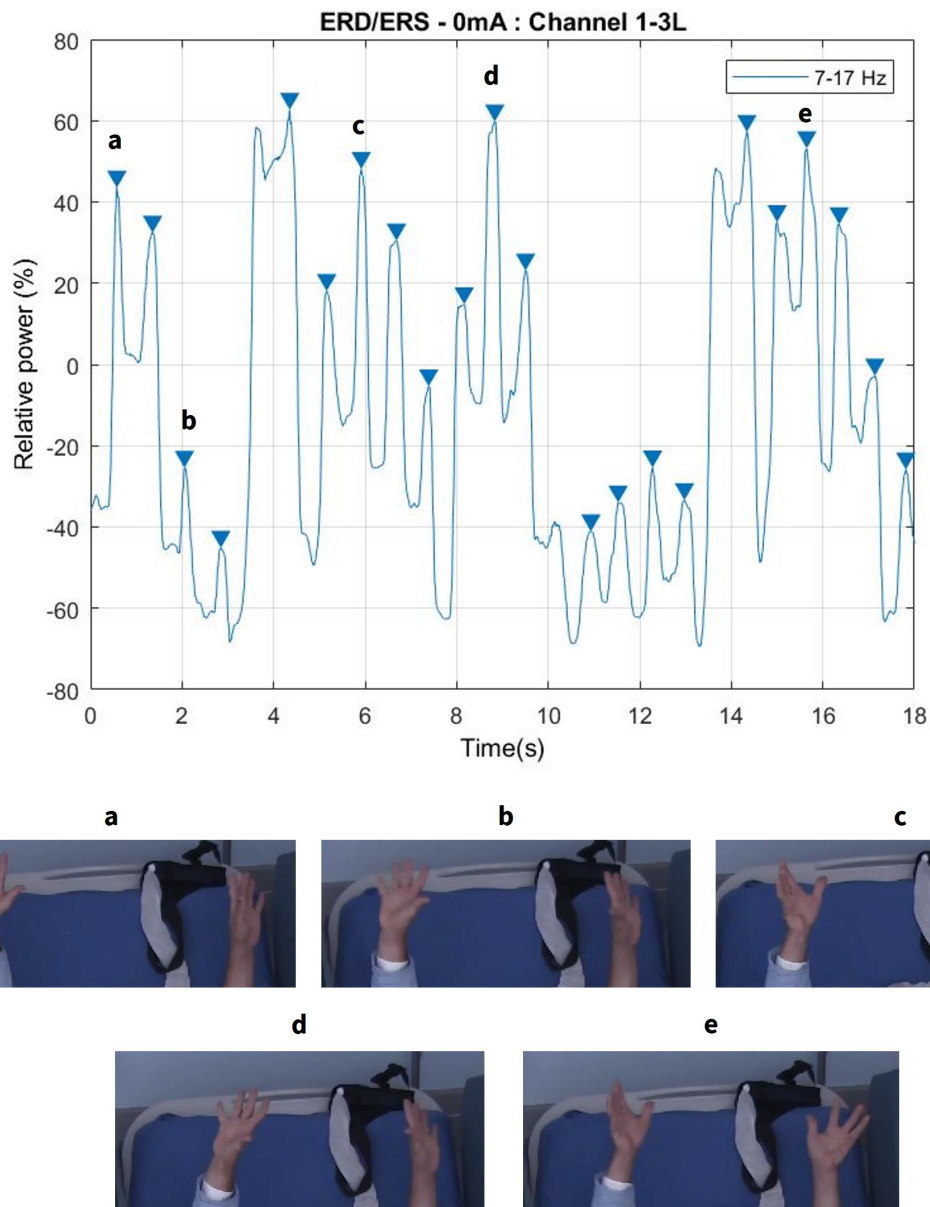


Figure 5.20: Detected peaks in ERD/ERS time course for movement paradigm, executed without stimulation, and some exemplified frames. The ERD/ERS pattern was obtained for frequency range of 7-17 Hz and during the movement execution. The curve represents the 1-3 L contact. Frames a,b and d illustrate the hands outwards while frames c and e illustrate the hands inwards.

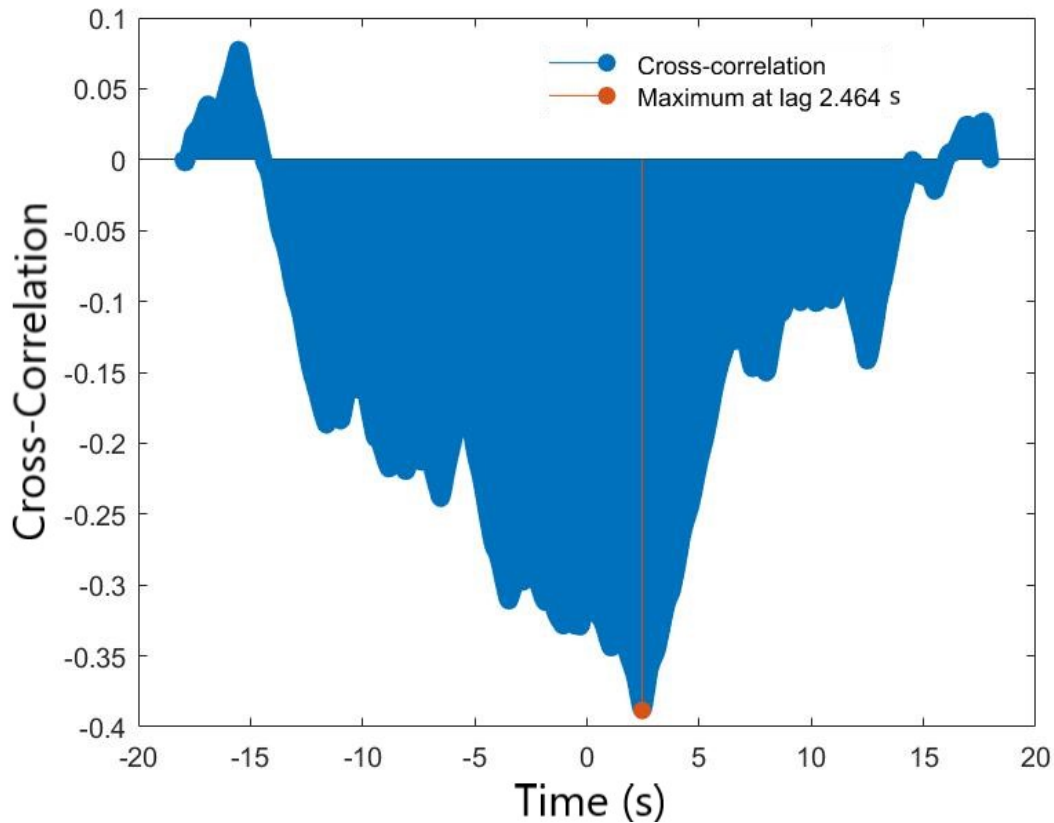


Figure 5.21: Cross-Correlation between the ERD/ERS curve and the movement signal represented by Y coordinates. The orange line corresponds to the maximum peak of the cross-correlation.

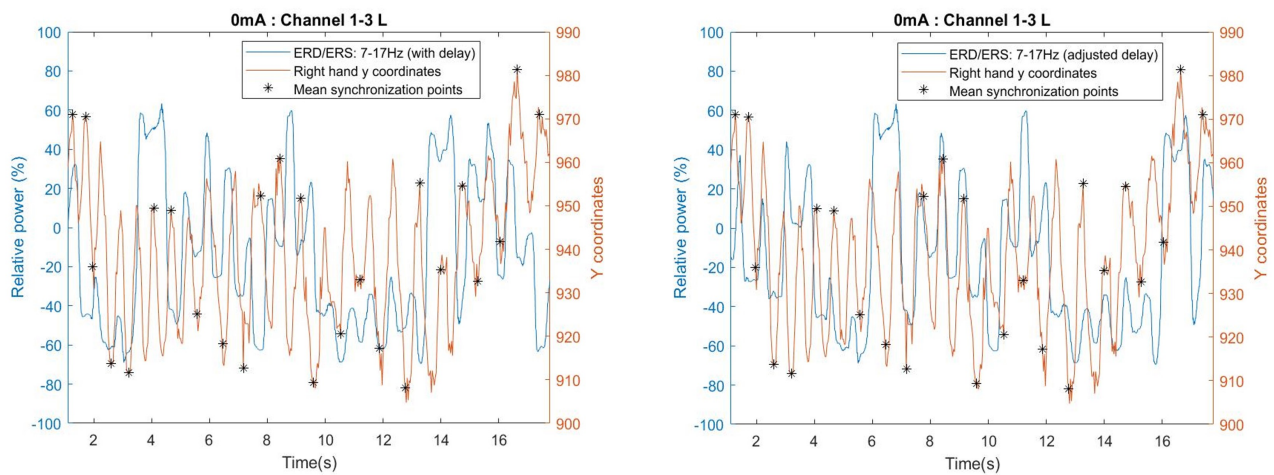


Figure 5.22: Overlay of the ERD/ERS curve and the representative motion signal. The left panel represents these signals still with a delay, while the right panel represents the same signals with the corrected delay. The black asterisks correspond to the moments where synchronization exists (in the time-frequency map).

Chapter 6

Conclusions and Future Work

In carrying out this study, a protocol was developed based on a motor paradigm applied to LFP signals obtained using the Percept™ PC neurostimulator. The main objective of this dissertation would then be to verify the existence of biomarkers related to epileptic seizures, more specifically with movements made during the seizure, in the DBS ANT target.

Due to an infection at the site, where the neurostimulator was implanted, the epileptic patient suitable for this study in Portugal had to undergo a Percept™ PC removal surgery. This setback made it impossible to carry out the proposed protocol for a survey with LFP signals.

Thus, it was proposed to carry out the protocol developed in studying movements using EEG and iEEG signals. In the first study, 15 healthy volunteers participated, and in the last, only one epileptic subject participated.

For the study of movements with EEG related to ERD/ERS patterns, some regions located in the central and parietal parts of the brain were chosen as targets due to their influence on the processing of movements performed with the upper limbs. This experience showed results in agreement with those in the literature. However, some limitations, such as the small number of movement blocks performed, and the use of the ICA method in discontinuous data, were presented in this experiment. In future work, it is recommended that this study be reproduced with a more significant number of activity blocks and choose and a different method of signal decomposition.

For the study performed with iEEG signals, similarly to the study mentioned above, the ERD/ERS patterns were observed during the execution of the movement. In this case, the chosen targets were located in the hippocampus. The results did not reveal any relationship between the movements' performance and the appearance of desynchronization or synchronization in the selected targets. For this reason, in future work, it is recommended to reproduce the methods suggested in the literature to identify the movement relative potentials in hippocampus signals (through the study of ERD/ERS or ERPs).

Finally, it was possible to use the previous patient implanted with the Percept PC to test a motor automatism (turning hands with hands in the air) and study whether any type of activation could be detected in the ANT electrodes. This was performed using LFP data acquired in BSS mode with the Percept PC textmark. Analysis of the ERD/ERS patterns during the implementation of the paradigm allowed us to verify the existence of synchronization possibly associated with motion in the ANT target. In order to confirm this theory, the corresponding vEEG frames were analyzed, and the motion frequency and synchronization patterns were analyzed, revealing very similar values of about 1Hz.

Furthermore, it was possible to verify a relationship between the onset of synchronization and the moments when maximum hand rotation was reached and a delay of about 2 seconds between the ERD/ERS curve

corresponding to the ANT signals and the signal representing the movement. Thus, it was inferred that synchronization occurred approximately 2 seconds before the onset of action, as with desynchronization when studying with EEG signals.

Thus, it was found that the signals from the ANT were related to the motor automatism, characteristic of epileptic seizures, performed by the patient. This novel and innovative study opens doors for studying the relationship between movements associated with epileptic seizures and the LFPs coming from the ANT.

However, it should be noted that we analyzed data that corresponded to a single session of a movement, so additional studies should be carried out with the application of the protocol proposed in this dissertation to validate the conclusions drawn.

Appendix A

Bi-ANT DBS in Epilepsy

Table A.1: Clinical studies of Bi-ANT DBS for the treatment of DRE. Adapted from (10).

Study	n	Seizure type	Follow up (months)	Outcomes (Average seizure reduction)
(105)	6	CPS	>36	4/6 had "significant clinical control"
(106)	5	GTC, DA, CPS, AA, SGTC, PM	48-84	55%
(107)	5	SPS, CPS, SGTC	6-36	48% (57–98%) of "serious seizures"
(108)	3	TS, DA, HM, AM, SGTC	2-30	75.4% (50–90.6%) 3/3 RR
(109)	4	G, P, STGC	33-48	49% (35–76%) 1/4 RR
(110)	4	(Bi- MTLT) SGTC, CPS, SPS, DA	36	75.6% (53–92%) 4/4 RR
(12) (SANTE)	110	CPS, SGTC	3 blind 24 total	26% above controls after 2 months; 56%, 54% RR
(64)	15	CPS, GTC, SPS	24-67	70.5% (0-100%) 13/15 RR
(111)	9	CPS, SGTC	22–60	57.9% (35.6–90.4%) 7/9 RR
(112)	2	SPS, CPS, SGTC	3	53% SR, 80% SR 2/2 RR
(113)	6	(LGS), CPS, SGTC	>36	3/5 RR

Table A.2: Continued - Clinical studies of Bi-ANT DBS for the treatment of DRE. Adapted from (10).

Study	n	Seizure type	Follow up (months)	Outcomes (Average seizure reduction)
(114)	9	CPS, SGTC	28	7/9 RR
(115)	15	NR	9–52	10/15 RR
(116)	1	CPS, GTC	60	100%
(117) (SANTE)	83	SANTE study	60	69% 68% RR
(118)	16	SPS, CPS, SGTC, GTC, MYO, DA	52	65 % at 3 years 11/16 RR
(119)	2	(SBH) CPS, SGTC	18, 12	61% SR, 75% SR 2/2 RR
(120)	1	SPS	12	> 60%
(121)	1	GTC	40	87%
(122)	1	CPS, GTC	60	100%
(123)	16	NR	24	12/16 RR

Seizure Type: G - Generalized; P - Partial; CS - Clonic; SPS - Simple partial seizure; CPS - Complex partial seizure; DA - Drop attack: atonic; DIA - Dialeptic; GTC - Generalized tonic-clonic; AA - Atypical absence; SGTC - Secondly generalized; PM - Partial motor; TS - Tonic; TC - Tonic-clonic; TA - Typical Absence; HM - Hypermotor; AM - Automotor; MYO - Myoclonic; RSE - Refractory status epilepticus; DRA - Dravet Syndrome; SBH - Subcortical band heterotopia; LGS - Lennox-Gastaut Syndrome; NR - Not report;

Outcomes: RR - Responders Rate (Seizure reduction $\geq 50\%$); SR - Seizure Reduction;

References

- [1] Robert S. Fisher, Carlos Acevedo, Alexis Arzimanoglou, Alicia Bogacz, J. Helen Cross, Christian E. Elger, Jerome Engel, Lars Forsgren, Jacqueline A. French, Mike Glynn, Dale C. Hesdorffer, B. I. Lee, Gary W. Mathern, Solomon L. Moshé, Emilio Perucca, Ingrid E. Scheffer, Torbjörn Tomson, Masako Watanabe, and Samuel Wiebe. ILAE Official Report: A practical clinical definition of epilepsy. *Epilepsia*, 55(4):475–482, 2014. doi:10.1111/epi.12550.
- [2] Orrin Devinsky, Annamaria Vezzani, Terence J. O’Brien, Nathalie Jette, Ingrid E. Scheffer, Marco De Curtis, and Piero Perucca. Epilepsy. *Nature Reviews Disease Primers*, 4(May), 2018. doi:10.1038/nrdp.2018.24.
- [3] Robert S. Fisher, Walter Van Emde Boas, Warren Blume, Christian Elger, Pierre Genton, Phillip Lee, and Jerome Engel. Response: Definitions proposed by the International League Against Epilepsy (ILAE) and the International Bureau for Epilepsy (IBE) [4]. *Epilepsia*, 46(10):1701–1702, 2005. doi:10.1111/j.1528-1167.2005.00273_4.x.
- [4] Robert S Fisher, J Helen Cross, Jacqueline A French, Norimichi Higurashi, Edouard Hirsch, Floor E Jansen, Lieven Lagae, Solomon L Moshé, Jukka Peltola, Eliane Roulet Perez, Ingrid E Scheffer, and Sameer M Zuberi. Operational classification of seizure types by the International League Against Epilepsy: Position Paper of the ILAE Commission for Classification and Terminology. *Epilepsia*, 58(4):522–530, apr 2017. doi:10.1111/epi.13670.
- [5] P. Kwan and J. W. Sander. The natural history of epilepsy: An epidemiological view. *Journal of Neurology, Neurosurgery and Psychiatry*, 75(10):1376–1381, 2004. doi:10.1136/jnnp.2004.045690.
- [6] Sean Jeremy Nagel and Imad Michel Najm. Deep Brain Stimulation for Epilepsy. *Neuromodulation: Technology at the Neural Interface*, 12(4):270–280, 2009. URL: <https://onlinelibrary.wiley.com/doi/abs/10.1111/j.1525-1403.2009.00239.x>, doi:<https://doi.org/10.1111/j.1525-1403.2009.00239.x>.
- [7] Barbara C. Jobst, Terrance M. Darcey, Vijay M. Thadani, and David W. Roberts. Brain stimulation for the treatment of epilepsy. *Epilepsia*, 51(SUPPL. 3):88–92, 2010. doi:10.1111/j.1528-1167.2010.02618.x.
- [8] Joachim K. Krauss, Nir Lipsman, Tipu Aziz, Alexandre Boutet, Peter Brown, Jin Woo Chang, Benjamin Davidson, Warren M. Grill, Marwan I. Hariz, Andreas Horn, Michael Schulder, Antonios Mammis, Peter A. Tass, Jens Volkmann, and Andres M. Lozano. Technology of deep brain stimulation: current status and future directions. *Nature Reviews Neurology*, 2020. URL: <http://dx.doi.org/10.1038/s41582-020-00426-z>, doi:10.1038/s41582-020-00426-z.
- [9] Casey Halpern, Howard Hurtig, Jurg Jaggi, Murray Grossman, Michelle Won, and Gordon Baltuch. Deep brain stimulation in neurologic disorders. *Parkinsonism and Related Disorders*, 13(1):1–16, 2007. doi:10.1016/j.parkreldis.2006.03.001.
- [10] Nasser Zangiabadi, Lady Diana Ladino, Farzad Sina, Juan Pablo Orozco-Hernández, Alexandra Carter, and José Francisco Téllez-Zenteno. Deep brain stimulation and drug-resistant epilepsy: A review of the literature. *Frontiers in Neurology*, 10(JUN):1–18, 2019. doi:10.3389/fneur.2019.00601.

- [11] Nicholas D. Child and Eduardo E. Benarroch. Anterior nucleus of the thalamus: Functional organization and clinical implications. *Neurology*, 81(21):1869–1876, 2013. doi:[10.1212/01.wnl.0000436078.95856.56](https://doi.org/10.1212/01.wnl.0000436078.95856.56).
- [12] Robert Fisher, Vicenta Salanova, Thomas Witt, Robert Worth, Thomas Henry, Robert Gross, Kalarickal Oommen, Ivan Osorio, Jules Nazzaro, Douglas Labar, Michael Kaplitt, Michael Sperling, Evan Sandok, John Neal, Adrian Handforth, John Stern, Antonio DeSalles, Steve Chung, Andrew Shetter, Donna Bergen, Roy Bakay, Jaimie Henderson, Jacqueline French, Gordon Baltuch, William Rosenfeld, Andrew Youkilis, William Marks, Paul Garcia, Nicolas Barbaro, Nathan Fountain, Carl Bazil, Robert Goodman, Guy McKhann, K Babu Krishnamurthy, Steven Papavassiliou, Charles Epstein, John Pollard, Lisa Tonder, Joan Grebin, Robert Coffey, Nina Graves, and the SANTE Study Group. Electrical stimulation of the anterior nucleus of thalamus for treatment of refractory epilepsy. *Epilepsia*, 51(5):899–908, may 2010. URL: <https://doi.org/10.1111/j.1528-1167.2010.02536.x>, doi:<https://doi.org/10.1111/j.1528-1167.2010.02536.x>.
- [13] Athanasios Gaitatzis, Anthony L Johnson, David W Chadwick, Simon D Shorvon, and Josemir W Sander. Life expectancy in people with newly diagnosed epilepsy. *Brain*, 127(11):2427–2432, 2004. URL: <https://doi.org/10.1093/brain/awh267>, doi:[10.1093/brain/awh267](https://doi.org/10.1093/brain/awh267).
- [14] Jane McCagh, John E. Fisk, and Gus A. Baker. Epilepsy, psychosocial and cognitive functioning. *Epilepsy Research*, 86(1):1–14, 2009. doi:[10.1016/j.epilepsyres.2009.04.007](https://doi.org/10.1016/j.epilepsyres.2009.04.007).
- [15] Eugen Trinka, Gerhard Bauer, Willi Oberaigner, Jean-Pierre Ndayisaba, Klaus Seppi, and Claudia A Granbichler. Cause-specific mortality among patients with epilepsy: Results from a 30-year cohort study. *Epilepsia*, 54(3):495–501, 2013. URL: <https://onlinelibrary.wiley.com/doi/abs/10.1111/epi.12014>, doi:<https://doi.org/10.1111/epi.12014>.
- [16] Kenneth D. Laxer, Eugen Trinka, Lawrence J. Hirsch, Fernando Cendes, John Langfitt, Norman Delanty, Trevor Resnick, and Selim R. Benbadis. The consequences of refractory epilepsy and its treatment. *Epilepsy and Behavior*, 37:59–70, 2014. doi:[10.1016/j.yebeh.2014.05.031](https://doi.org/10.1016/j.yebeh.2014.05.031).
- [17] Elodie M. Lopes, Maria Do Carmo Vilas-Boas, Ricardo Rego, Angela Santos, and Joao P.S. Cunha. Video-EEG and Percept™ PC deep brain neurostimulator fine-grained synchronization for multi-modal neurodata analysis. *International IEEE/EMBS Conference on Neural Engineering, NER*, 2021-May:963–966, 2021. doi:[10.1109/NER49283.2021.9441422](https://doi.org/10.1109/NER49283.2021.9441422).
- [18] Stanley Jacobson and Elliott M. Marcus. *Neuroanatomy for the Neuroscientist second edition*, volume 40. 2011. URL: [http://doi.wiley.com/10.1002/1521-3773\(%\)2820010316\(%\)2940\(%\)3A6\(%\)3C9823\(%\)3A\(%\)3AAID-ANIE9823\(%\)3E3.3.CO\(%\)3B2-C](http://doi.wiley.com/10.1002/1521-3773(%)2820010316(%)2940(%)3A6(%)3C9823(%)3A(%)3AAID-ANIE9823(%)3E3.3.CO(%)3B2-C).
- [19] John A. Kusske, George A. Ojemann, and Arthur A. Ward. Effects of lesions in ventral anterior thalamus on experimental focal epilepsy. *Experimental Neurology*, 34(2):279–290, 1972. doi:[10.1016/0014-4886\(72\)90174-4](https://doi.org/10.1016/0014-4886(72)90174-4).
- [20] Marek A. Mirski and James A. Ferrendelli. Anterior thalamic mediation of generalized pentylenetetrazol seizures. *Brain Research*, 399(2):212–223, 1986. doi:[10.1016/0006-8993\(86\)91511-8](https://doi.org/10.1016/0006-8993(86)91511-8).
- [21] John W. Miller, Ann C. McKeon, and James A. Ferrendelli. Functional anatomy of pentylenetetrazol and electroshock seizures in the rat brainstem. *Annals of Neurology*, 22(5):615–621, 1987. doi:[10.1002/ana.410220510](https://doi.org/10.1002/ana.410220510).
- [22] M A Mirski and J A Ferrendelli. Interruption of the mammillothalamic tract prevents seizures in guinea pigs. *Science*, 226(4670):72–74, 1984. URL: <https://science.sciencemag.org/content/226/4670/72>, doi:[10.1126/science.6433485](https://doi.org/10.1126/science.6433485).
- [23] Marek A. Mirski and Robert S. Fisher. Electrical Stimulation of the Mammillary Nuclei Increases Seizure Threshold to Pentylenetetrazol in Rats. *Epilepsia*, 35(6):1309–1316, 1994. doi:[10.1111/j.1528-1157.1994.tb01803.x](https://doi.org/10.1111/j.1528-1157.1994.tb01803.x).

- [24] Marek A. Mirski, Lisa Ann Rossell, John B. Terry, and Robert S. Fisher. Anticonvulsant effect of anterior thalamic high frequency electrical stimulation in the rat. *Epilepsy Research*, 28(2):89–100, 1997. doi:10.1016/S0920-1211(97)00034-X.
- [25] Clement Hamani, Flavio I.S. Ewerton, Saulo M. Bonilha, Gerson Ballester, Luiz E.A.M. Mello, Andres M. Lozano, Imad Najm, Ali R. Rezai, Marcos Velasco, Francisco Velasco, Philip A. Starr, Alim L. Benabid, and Roy A.E. Bakay. Bilateral Anterior Thalamic Nucleus Lesions and High-frequency Stimulation Are Protective against Pilocarpine-induced Seizures and Status Epilepticus. *Neurosurgery*, 54(1):191–197, 2004. doi:10.1227/01.NEU.0000097552.31763.AE.
- [26] Andres M. Lozano, Nir Lipsman, Hagai Bergman, Peter Brown, Stephan Chabardes, Jin Woo Chang, Keith Matthews, Cameron C. McIntyre, Thomas E. Schlaepfer, Michael Schulder, Yasin Temel, Jens Volkmann, and Joachim K. Krauss. Deep brain stimulation: current challenges and future directions. *Nature Reviews Neurology*, 15(3):148–160, 2019. doi:10.1038/s41582-018-0128-2.
- [27] Frank Steigerwald, Lorenz Müller, Silvia Johannes, Cordula Matthies, and Jens Volkmann. Directional deep brain stimulation of the subthalamic nucleus: A pilot study using a novel neurostimulation device. *Movement disorders : official journal of the Movement Disorder Society*, 31(8):1240–1243, aug 2016. URL: <https://pubmed.ncbi.nlm.nih.gov/27241197><https://www.ncbi.nlm.nih.gov/pmc/articles/PMC5089579/>, doi:10.1002/mds.26669.
- [28] Warren M Grill. Model-based analysis and design of waveforms for efficient neural stimulation. *Progress in brain research*, 222:147–162, 2015. URL: <https://pubmed.ncbi.nlm.nih.gov/26541380><https://www.ncbi.nlm.nih.gov/pmc/articles/PMC4772858/>, doi:10.1016/bs.pbr.2015.07.031.
- [29] Sol De Jesus, Leonardo Almeida, Leili Shahgholi, Daniel Martinez-Ramirez, Jaimie Roper, Chris J Hass, Umer Akbar, Aparna Wagle Shukla, Robert S Raike, and Michael S Okun. Square biphasic pulse deep brain stimulation for essential tremor: The BiP tremor study. *Parkinsonism & Related Disorders*, 46:41–46, jan 2018. URL: <https://doi.org/10.1016/j.parkreldis.2017.10.015>, doi:10.1016/j.parkreldis.2017.10.015.
- [30] Anna Dalal Kirsch, Sharon Hassin-Baer, Cordula Matthies, Jens Volkmann, and Frank Steigerwald. Anodic versus cathodic neurostimulation of the subthalamic nucleus: A randomized-controlled study of acute clinical effects. *Parkinsonism & Related Disorders*, 55:61–67, oct 2018. URL: <https://doi.org/10.1016/j.parkreldis.2018.05.015>, doi:10.1016/j.parkreldis.2018.05.015.
- [31] Joachim K Krauss, John Yianni, Thomas J Loher, and Tipu Z Aziz. Deep Brain Stimulation for Dystonia. *Journal of Clinical Neurophysiology*, 21(1), 2004. URL: <https://journals.lww.com/clinicalneurophys/Fulltext/2004/01000/Deep{ }Brain{ }Stimulation{ }for{ }Dystonia.4.aspx>.
- [32] Tim A.M. Bouwens van der Vlis, Olaf E.M.G. Schijns, Frédéric L.W.V.J. Schaper, Govert Hoogland, Pieter Kubben, Louis Wagner, Rob Rouhl, Yasin Temel, and Linda Ackermans. Deep brain stimulation of the anterior nucleus of the thalamus for drug-resistant epilepsy. *Neurosurgical Review*, 42(2):287–296, 2019. doi:10.1007/s10143-017-0941-x.
- [33] Pradeep K. Banerjee and O.Carter Snead. Thalamic mediodorsal and intralaminar nuclear lesions disrupt the generation of experimentally induced generalized absence-like seizures in rats. *Epilepsy Research*, 17(3):193 – 205, 1994. URL: <http://www.sciencedirect.com/science/article/pii/0920121194900507>, doi:[https://doi.org/10.1016/0920-1211\(94\)90050-7](https://doi.org/10.1016/0920-1211(94)90050-7).
- [34] Ali Gorji, Christoph Mittag, Parviz Shahabi, Thomas Seidenbecher, and Hans-Christian Pape. Seizure-related activity of intralaminar thalamic neurons in a genetic model of absence epilepsy. *Neurobiology of Disease*, 43(1):266 – 274, 2011. Autophagy and protein degradation in neurological diseases. URL: <http://www.sciencedirect.com/science/article/pii/S096999611100101X>, doi:<https://doi.org/10.1016/j.nbd.2011.03.019>.

- [35] Robert S. Fisher, Sumio Uematsu, Gregory L. Krauss, Barbara J. Cysyk, Robert McPherson, Ronald P. Lesser, Barry Gordon, Pamela Schwerdt, and Mark Rise. Placebo-controlled pilot study of centromedian thalamic stimulation in treatment of intractable seizures. *Epilepsia*, 33(5):841–851, 1992. URL: <https://onlinelibrary.wiley.com/doi/abs/10.1111/j.1528-1157.1992.tb02192.x>, arXiv:<https://onlinelibrary.wiley.com/doi/pdf/10.1111/j.1528-1157.1992.tb02192.x>, doi:<https://doi.org/10.1111/j.1528-1157.1992.tb02192.x>.
- [36] Samuel Wiebe, Warren T. Blume, John P. Girvin, and Michael Eliasziw. A randomized, controlled trial of surgery for temporal-lobe epilepsy. *New England Journal of Medicine*, 345(5):311–318, 2001. PMID: 11484687. URL: <https://doi.org/10.1056/NEJM200108023450501>, arXiv:<https://doi.org/10.1056/NEJM200108023450501>, doi:10.1056/NEJM200108023450501.
- [37] Ana Luisa Velasco, Marcos Velasco, Francisco Velasco, Diana Menes, Felipe Gordon, Luisa Rocha, Magdalena Briones, and Irma Márquez. Subacute and chronic electrical stimulation of the hippocampus on intractable temporal lobe seizures: Preliminary report. *Archives of Medical Research*, 31(3):316 – 328, 2000. URL: <http://www.sciencedirect.com/science/article/pii/S0188440900000643>, doi:[https://doi.org/10.1016/S0188-4409\(00\)00064-3](https://doi.org/10.1016/S0188-4409(00)00064-3).
- [38] Ana Luisa Velasco, Francisco Velasco, Marcos Velasco, David Trejo, Guillermo Castro, and José Damián Carrillo-Ruiz. Electrical stimulation of the hippocampal epileptic foci for seizure control: A double-blind, long-term follow-up study. *Epilepsia*, 48(10):1895–1903, 2007. URL: <https://onlinelibrary.wiley.com/doi/abs/10.1111/j.1528-1167.2007.01181.x>, arXiv:<https://onlinelibrary.wiley.com/doi/pdf/10.1111/j.1528-1167.2007.01181.x>, doi:<https://doi.org/10.1111/j.1528-1167.2007.01181.x>.
- [39] Paul Boon, Kristl Vonck, Veerle De Herdt, Annelies Van Dycke, Maarten Goethals, Lut Goossens, Michel Van Zandijcke, Tim De Smedt, Isabelle Dewaele, Rik Achten, Wytse Wadman, Frank Dewaele, Jacques Caemaert, and Dirk Van Roost. Deep brain stimulation in patients with refractory temporal lobe epilepsy. *Epilepsia*, 48(8):1551–1560, 2007. URL: <https://onlinelibrary.wiley.com/doi/abs/10.1111/j.1528-1167.2007.01005.x>, arXiv:<https://onlinelibrary.wiley.com/doi/pdf/10.1111/j.1528-1167.2007.01005.x>, doi:<https://doi.org/10.1111/j.1528-1167.2007.01005.x>.
- [40] S A Chkhenkeli and I S Chkhenkeli. Effects of Therapeutic Stimulation of Nucleus caudatus on Epileptic Electrical Activity of Brain in Patients with Intractable Epilepsy. *Stereotactic and Functional Neurosurgery*, 69(1-4):221–224, 1997. URL: <https://www.karger.com/DOI/10.1159/000099878>, doi:10.1159/000099878.
- [41] Casey H. Halpern, Uzma Samadani, Brian Litt, Jurg L. Jaggi, and Gordon H. Baltuch. Deep Brain Stimulation for Epilepsy. *Neurotherapeutics*, 5(1):59–67, 2008. doi:10.1016/j.nurt.2007.10.065.
- [42] M Šramka and S A Chkhenkeli. Clinical Experience in Intraoperative Determination of Brain Inhibitory Structures and Application of Implanted Neurostimulators in Epilepsy. *Stereotactic and Functional Neurosurgery*, 54-55(1-8):56–59, 1990. URL: <https://www.karger.com/DOI/10.1159/000100190>, doi:10.1159/000100190.
- [43] Sozari A Chkhenkeli, Miron Šramka, George S Lortkipanidze, Tamaz N Rakviashvili, Eteri Sh Bregvadze, George E Magalashvili, Tamar Sh Gagoshidze, and Irina S Chkhenkeli. Electrophysiological effects and clinical results of direct brain stimulation for intractable epilepsy. *Clinical Neurology and Neurosurgery*, 106(4):318 – 329, 2004. URL: <http://www.sciencedirect.com/science/article/pii/S0303846704000289>, doi:<https://doi.org/10.1016/j.clineuro.2004.01.009>.
- [44] K Gale. Role of the substantia nigra in GABA-mediated anticonvulsant actions. *Advances in neurology*, 44:343–364, 1986.

- [45] Alim Louis Benabid, Adnan Koudsié, Abdelhamid Benazzouz, Laurent Vercueil, Valérie Fraix, Stéphan Chabardes, Jean François LeBas, and Pierre Pollak. Deep brain stimulation of the corpus luyisi (subthalamic nucleus) and other targets in Parkinson's disease. Extension to new indications such as dystonia and epilepsy. *Journal of Neurology*, 248(3):37–47, 2001. URL: <https://doi.org/10.1007/PL00007825>, doi:10.1007/PL00007825.
- [46] Alim Louis Benabid, Lorella Minotti, Adnan Koudsié, Anne de Saint Martin, and Edouard Hirsch. Antiepileptic Effect of High-frequency Stimulation of the Subthalamic Nucleus (Corpus Luysi) in a Case of Medically Intractable Epilepsy Caused by Focal Dysplasia: A 30-month Follow-up: Technical Case Report. *Neurosurgery*, 50(6):1385–1392, 2002. URL: <https://doi.org/10.1097/00006123-200206000-00037>, doi:10.1097/00006123-200206000-00037.
- [47] Irving S Cooper, Ismail Amin, Manuel Riklan, Joseph M Waltz, and Tung Pui Poon. Chronic Cerebellar Stimulation in Epilepsy: Clinical and Anatomical Studies. *Archives of Neurology*, 33(8):559–570, aug 1976. URL: <https://doi.org/10.1001/archneur.1976.00500080037006>, doi:10.1001/archneur.1976.00500080037006.
- [48] G. F. Molnar, A. Sailer, C. A. Gunraj, A. E. Lang, A. M. Lozano, and R. Chen. Thalamic deep brain stimulation activates the cerebellothalamocortical pathway. *Neurology*, 63(5):907–909, 2004. URL: <https://n.neurology.org/content/63/5/907>, arXiv:<https://n.neurology.org/content/63/5/907.full.pdf>, doi:10.1212/01.WNL.0000137419.85535.C7.
- [49] Francisco Velasco, José D. Carrillo-Ruiz, Francisco Brito, Marcos Velasco, Ana Luisa Velasco, Irma Marquez, and Ross Davis. Double-blind, randomized controlled pilot study of bilateral cerebellar stimulation for treatment of intractable motor seizures. *Epilepsia*, 46(7):1071–1081, 2005. URL: <https://onlinelibrary.wiley.com/doi/abs/10.1111/j.1528-1167.2005.70504.x>, arXiv:<https://onlinelibrary.wiley.com/doi/pdf/10.1111/j.1528-1167.2005.70504.x>, doi:<https://doi.org/10.1111/j.1528-1167.2005.70504.x>.
- [50] Kenou Van Rijckevorsel, Basel Abu Serieh, Marianne De Tourchaninoff, and Christian Raftopoulos. Deep eeg recordings of the mammillary body in epilepsy patients. *Epilepsia*, 46(5):781–785, 2005. URL: <https://onlinelibrary.wiley.com/doi/abs/10.1111/j.1528-1167.2005.45704.x>, arXiv:<https://onlinelibrary.wiley.com/doi/pdf/10.1111/j.1528-1167.2005.45704.x>, doi:<https://doi.org/10.1111/j.1528-1167.2005.45704.x>.
- [51] Sadaquate Khan, Ingram Wright, Shazia Javed, Peta Sharples, Philip Jardine, Michael Carter, and Steven S. Gill. High frequency stimulation of the mamillothalamic tract for the treatment of resistant seizures associated with hypothalamic hamartoma. *Epilepsia*, 50(6):1608–1611, 2009. URL: <https://onlinelibrary.wiley.com/doi/abs/10.1111/j.1528-1167.2008.01995.x>, arXiv:<https://onlinelibrary.wiley.com/doi/pdf/10.1111/j.1528-1167.2008.01995.x>, doi:<https://doi.org/10.1111/j.1528-1167.2008.01995.x>.
- [52] A Franzini, G Messina, C Marras, F Villani, R Cordella, and G Broggi. Deep Brain Stimulation of Two Unconventional Targets in Refractory Non-Resectable Epilepsy. *Stereotactic and Functional Neurosurgery*, 86(6):373–381, 2008. URL: <https://www.karger.com/DOI/10.1159/000175800>, doi:10.1159/000175800.
- [53] Juan C. Benedetti-Isaac, Martin Torres-Zambrano, Andres Vargas-Toscano, Esther Perea-Castro, Gabriel Alcalá-Cerra, Luciano L. Furlanetti, Thomas Reithmeier, Travis S. Tierney, Constantin Anastasopoulos, Erich T. Fonoff, and William Omar Contreras Lopez. Seizure frequency reduction after posteromedial hypothalamus deep brain stimulation in drug-resistant epilepsy associated with intractable aggressive behavior. *Epilepsia*, 56(7):1152–1161, 2015. URL: <https://onlinelibrary.wiley.com/doi/abs/10.1111/epi.13025>, arXiv:<https://onlinelibrary.wiley.com/doi/pdf/10.1111/epi.13025>, doi:<https://doi.org/10.1111/epi.13025>.
- [54] Vitaliya Blik. Electric stimulation of the tuberomammillary nucleus affects epileptic activity and sleep-wake cycle in a genetic absence epilepsy model. *Epilepsy Research*,

- 109:119 – 125, 2015. URL: <http://www.sciencedirect.com/science/article/pii/S0920121114002988>, doi:<https://doi.org/10.1016/j.eplepsyres.2014.10.019>.
- [55] Nicole C Swann, Coralie de Hemptinne, Margaret C Thompson, Svjetlana Miocinovic, Andrew M Miller, Ro'ee Gilron, Jill L Ostrem, Howard J Chizeck, and Philip A Starr. Adaptive deep brain stimulation for Parkinson's disease using motor cortex sensing. *Journal of neural engineering*, 15(4):46006, aug 2018. URL: <https://pubmed.ncbi.nlm.nih.gov/29741160><https://www.ncbi.nlm.nih.gov/pmc/articles/PMC6021210/>, doi:[10.1088/1741-2552/aabc9b](https://doi.org/10.1088/1741-2552/aabc9b).
- [56] Christopher Elder, Daniel Friedman, Orrin Devinsky, Werner Doyle, and Patricia Dugan. Responsive neurostimulation targeting the anterior nucleus of the thalamus in 3 patients with treatment-resistant multifocal epilepsy. *Epilepsia open*, 4(1):187–192, jan 2019. URL: <https://pubmed.ncbi.nlm.nih.gov/30868130><https://www.ncbi.nlm.nih.gov/pmc/articles/PMC6398101/>, doi:[10.1002/epi4.12300](https://doi.org/10.1002/epi4.12300).
- [57] Peter Coates and Jason Jones. System User Manual. 2019.
- [58] Dileep R. Nair, Kenneth D. Laxer, Peter B. Weber, Anthony M. Murro, Yong D. Park, Gregory L. Barkley, Brien J. Smith, Ryder P. Gwinn, Michael J. Doherty, Katherine H. Noe, Richard S. Zimmerman, Gregory K. Bergey, William S. Anderson, Christianne Heck, Charles Y. Liu, Ricky W. Lee, Toni Sadler, Robert B. Duckrow, Lawrence J. Hirsch, Robert E. Wharen, William Tatum, Shraddha Srinivasan, Guy M. McKhann, Mark A. Agostini, Andreas V. Alexopoulos, Barbara C. Jobst, David W. Roberts, Vicenta Salanova, Thomas C. Witt, Sydney S. Cash, Andrew J. Cole, Gregory A. Worrell, Brian N. Lundstrom, Jonathan C. Edwards, Jonathan J. Halford, David C. Spencer, Lia Ernst, Christopher T. Skidmore, Michael R. Sperling, Ian Miller, Eric B. Geller, Michel J. Berg, A. James Fessler, Paul Rutecki, Alica M. Goldman, Eli M. Mizrahi, Robert E. Gross, Donald C. Shields, Theodore H. Schwartz, Douglas R. Labar, Nathan B. Fountain, W. Jeff Elias, Piotr W. Olejniczak, Nicole R. Villemarette-Pittman, Stephan Eisenschenk, Steven N. Roper, Jane G. Boggs, Tracy A. Courtney, Felice T. Sun, Cairn G. Seale, Kathy L. Miller, Tara L. Skarpaas, and Martha J. Morrell. Nine-year prospective efficacy and safety of brain-responsive neurostimulation for focal epilepsy. *Neurology*, 95(9):e1244–e1256, 2020. doi:[10.1212/WNL.0000000000010154](https://doi.org/10.1212/WNL.0000000000010154).
- [59] Barbara C. Jobst, Ritu Kapur, Gregory L. Barkley, Carl W. Bazil, Michel J. Berg, Gregory K. Bergey, Jane G. Boggs, Sydney S. Cash, Andrew J. Cole, Michael S. Duchowny, Robert B. Duckrow, Jonathan C. Edwards, Stephan Eisenschenk, A. James Fessler, Nathan B. Fountain, Eric B. Geller, Alica M. Goldman, Robert R. Goodman, Robert E. Gross, Ryder P. Gwinn, Christianne Heck, Aamr A. Herekar, Lawrence J. Hirsch, David King-Stephens, Douglas R. Labar, W. R. Marsh, Kimford J. Meador, Ian Miller, Eli M. Mizrahi, Anthony M. Murro, Dileep R. Nair, Katherine H. Noe, Piotr W. Olejniczak, Yong D. Park, Paul Rutecki, Vicenta Salanova, Raj D. Sheth, Christopher Skidmore, Michael C. Smith, David C. Spencer, Shraddha Srinivasan, William Tatum, Paul Van Ness, David G. Vossler, Robert E. Wharen, Gregory A. Worrell, Daniel Yoshor, Richard S. Zimmerman, Tara L. Skarpaas, and Martha J. Morrell. Brain-responsive neurostimulation in patients with medically intractable seizures arising from eloquent and other neocortical areas. *Epilepsia*, 58(6):1005–1014, 2017. doi:[10.1111/epi.13739](https://doi.org/10.1111/epi.13739).
- [60] Eric B. Geller, Tara L. Skarpaas, Robert E. Gross, Robert R. Goodman, Gregory L. Barkley, Carl W. Bazil, Michael J. Berg, Gregory K. Bergey, Sydney S. Cash, Andrew J. Cole, Robert B. Duckrow, Jonathan C. Edwards, Stephan Eisenschenk, James Fessler, Nathan B. Fountain, Alicia M. Goldman, Ryder P. Gwinn, Christianne Heck, Aamar Herekar, Lawrence J. Hirsch, Barbara C. Jobst, David King-Stephens, Douglas R. Labar, James W. Leiphart, W. Richard Marsh, Kimford J. Meador, Eli M. Mizrahi, Anthony M. Murro, Dileep R. Nair, Katherine H. Noe, Yong D. Park, Paul A. Rutecki, Vicenta Salanova, Raj D. Sheth, Donald C. Shields, Christopher Skidmore, Michael C. Smith, David C. Spencer, Shraddha Srinivasan, William Tatum, Paul C. Van Ness, David G. Vossler, Robert E. Wharen, Gregory A. Worrell, Daniel Yoshor, Richard S. Zimmerman, Kathy Cicora, Felice T. Sun, and Martha J. Morrell. Brain-responsive neurostimulation in patients with medically intractable mesial temporal lobe epilepsy. *Epilepsia*, 58(6):994–1004, 2017. doi:[10.1111/epi.13740](https://doi.org/10.1111/epi.13740).

- [61] Elodie M Lopes, Maria Carmo Vilas-boas, Ricardo Rego, Ângela Santos, and João P S Cunha. Video-EEG and Percept TM PC Deep Brain Neurostimulator Fine- Grained Synchronization for Multimodal Neurodata Analysis. 2020.
- [62] Vicenta Salanova, Thomas Witt, Robert Worth, Thomas R. Henry, Robert E. Gross, Jules M. Nazzaro, Douglas Labar, Michael R. Sperling, Ashwini Sharan, Evan Sandok, Adrian Handforth, John M. Stern, Steve Chung, Jaimie M. Henderson, Jacqueline French, Gordon Baltuch, William E. Rosenfeld, Paul Garcia, Nicholas M. Barbaro, Nathan B. Fountain, W. Jeffrey Elias, Robert R. Goodman, John R. Pollard, Alexander I. Tröster, Christopher P. Irwin, Kristin Lambrecht, Nina Graves, and Robert Fisher. Long-term efficacy and safety of thalamic stimulation for drug-resistant partial epilepsy. *Neurology*, 84(10):1017–1025, 2015. doi:10.1212/WNL.0000000000001334.
- [63] John F Kerrigan, Brian Litt, Robert S Fisher, Stephen Cranstoun, Jacqueline A French, David E Blum, Marc Dichter, Andrew Shetter, Gordon Baltuch, Jurg Jaggi, Selma Krone, MaryAnn Brodie, Mark Rise, and Nina Graves. Electrical Stimulation of the Anterior Nucleus of the Thalamus for the Treatment of Intractable Epilepsy. *Epilepsia*, 45(4):346–354, apr 2004. URL: <https://doi.org/10.1111/j.0013-9580.2004.01304.x>, doi:<https://doi.org/10.1111/j.0013-9580.2004.01304.x>.
- [64] K J Lee, Y M Shon, and C B Cho. Long-Term Outcome of Anterior Thalamic Nucleus Stimulation for Intractable Epilepsy. *Stereotactic and Functional Neurosurgery*, 90(6):379–385, 2012. URL: <https://www.karger.com/DOI/10.1159/000339991>, doi:10.1159/000339991.
- [65] Soila Järvenpää, Eija Rosti-Otajärvi, Sirpa Rainesalo, Linda Laukkanen, Kai Lehtimäki, and Jukka Pelto. Executive Functions May Predict Outcome in Deep Brain Stimulation of Anterior Nucleus of Thalamus for Treatment of Refractory Epilepsy , 2018. URL: <https://www.frontiersin.org/article/10.3389/fneur.2018.00324>.
- [66] E. V. Evarts. Brain mechanisms in movement. *Scientific American*, 229(1):96–103, 1973. doi:10.1038/scientificamerican0773-96.
- [67] Hong Gi Yeom, June Sic Kim, and Chun Kee Chung. Brain mechanisms in motor control during reaching movements: Transition of functional connectivity according to movement states. *Scientific Reports*, 10(1):1–11, 2020. URL: <http://dx.doi.org/10.1038/s41598-020-57489-7>, doi:10.1038/s41598-020-57489-7.
- [68] Mark Hallett. *The Bereitschaftspotential Movement-Related*.
- [69] Fernando Lopes da Silva Donald L. Schomer. *Niedermeyer’s Electroencephalography: Basic Principles, Clinical Applications, and Related Fields 6th Edition*. Lippincott Williams Wilkins, 2010. URL: <http://gen.lib.rus.ec/book/index.php?md5=623847955d0c15ec9f0714b4bed71b9b>.
- [70] F. H. Lopes da Silva, A. van Rotterdam, P. Barts, E. van Heusden, and W. Burr. Models of Neuronal Populations: The Basic Mechanisms of Rhythmicity. *Progress in Brain Research*, 45(C):281–308, 1976. doi:10.1016/S0079-6123(08)60995-4.
- [71] G. Pfurtscheller. Functional brain imaging based on ERD/ERS. *Vision Research*, 41(10-11):1257–1260, 2001. doi:10.1016/S0042-6989(00)00235-2.
- [72] G. Pfurtscheller and F. H. Lopes Da Silva. Event-related EEG/MEG synchronization and desynchronization: Basic principles. *Clinical Neurophysiology*, 110(11):1842–1857, 1999. doi:10.1016/S1388-2457(99)00141-8.
- [73] P Derambure, J L Bourriez, L Defebvre, F Cassim, E Josien, A Duhamel, A Destée, and J D Guieu. Abnormal Cortical Activation During Planning of Voluntary Movement in Patients with Epilepsy with Focal Motor Seizures: Event-Related Desynchronization Study of Electroencephalographic mu Rhythm. *Epilepsia*, 38(6):655–662, 1997. URL: <https://onlinelibrary.wiley.com/doi/abs/10.1111/j.1528-1157.1997.tb01234.x>, doi:<https://doi.org/10.1111/j.1528-1157.1997.tb01234.x>.

- [74] Gert Pfurtscheller, Karin Zalaudek, and Christa Neuper. Event-related beta synchronization after wrist, finger and thumb movement. *Electroencephalography and Clinical Neurophysiology - Electromyography and Motor Control*, 109(2):154–160, 1998. doi:10.1016/S0924-980X(97)00070-2.
- [75] Zhichuan Tang, Shouqian Sun, Sanyuan Zhang, Yumiao Chen, Chao Li, and Shi Chen. A brain-machine interface based on ERD/ERS for an upper-limb exoskeleton control. *Sensors (Switzerland)*, 16(12), 2016. doi:10.3390/s16122050.
- [76] J. Satheesh Kumar and P. Bhuvaneshwari. Analysis of electroencephalography (EEG) signals and its categorization - A study. *Procedia Engineering*, 38:2525–2536, 2012. doi:10.1016/j.proeng.2012.06.298.
- [77] Gonzalo Rojas, Carolina Alvarez, Carlos Montoya Moya, Maria de la Iglesia Vaya, Jaime Cisternas, and Marcelo Gálvez. Study of resting-state functional connectivity networks using eeg electrodes position as seed. *Frontiers in Neuroscience*, 12, 03 2018. doi:10.3389/fnins.2018.00235.
- [78] Shelagh J.M. Smith. EEG in the diagnosis, classification, and management of patients with epilepsy. *Neurology in Practice*, 76(2), 2005. doi:10.1136/jnnp.2005.069245.
- [79] Ander Ramos-Murguialday and Niels Birbaumer. Brain oscillatory signatures of motor tasks. *Journal of neurophysiology*, 113(10):3663–3682, jun 2015. URL: <https://pubmed.ncbi.nlm.nih.gov/25810484https://www.ncbi.nlm.nih.gov/pmc/articles/PMC4468978/>, doi:10.1152/jn.00467.2013.
- [80] Oscar Herreras. Local field potentials: Myths and misunderstandings. *Frontiers in Neural Circuits*, 10(DEC):1–16, 2016. doi:10.3389/fncir.2016.00101.
- [81] Manuela Rosa, Sara Marceglia, Sergio Barbieri, and Alberto Priori. Encyclopedia of Computational Neuroscience. *Encyclopedia of Computational Neuroscience*, pages 1–20, 2020. doi:10.1007/978-1-4614-7320-6.
- [82] Amber L.Harris Bozer, Megan L. Uhelski, and Ai Ling Li. Extrapolating meaning from local field potential recordings. *Journal of Integrative Neuroscience*, 16(1):107–126, 2017. doi:10.3233/JIN-170011.
- [83] Eileen Lew, Ricardo Chavarriaga, Huaijian Zhang, Margitta Seeck, and Jose Del R. Millan. Self-paced movement intention detection from human brain signals: Invasive and non-invasive EEG. *Proceedings of the Annual International Conference of the IEEE Engineering in Medicine and Biology Society, EMBS*, pages 3280–3283, 2012. doi:10.1109/EMBC.2012.6346665.
- [84] Zhichuan Tang, Hongnian Yu, Chunfu Lu, Pengcheng Liu, and Xuexue Jin. Single-trial classification of different movements on one arm based on erd/ers and corticomuscular coherence. *IEEE Access*, 7:128185–128197, 2019. doi:10.1109/ACCESS.2019.2940034.
- [85] Giorgio Macchi and Edward G. Jones. Toward an agreement on terminology of nuclear and subnuclear divisions of the motor thalamus. *Journal of Neurosurgery*, 86(4):670–685, 1997. doi:10.3171/jns.1997.86.4.0670.
- [86] Marc A. Sommer. The role of the thalamus in motor control. *Current Opinion in Neurobiology*, 13(6):663–670, 2003. doi:10.1016/j.conb.2003.10.014.
- [87] Martina Bočková, Jan Chládek, Pavel Jurák, Josef Halánek, Klára Štillová, Marek Baláž, Jan Chrastina, and Ivan Rektor. Complex Motor–Cognitive Factors Processed in the Anterior Nucleus of the Thalamus: An Intracerebral Recording Study. *Brain Topography*, 28(2):269–278, 2015. doi:10.1007/s10548-014-0373-7.
- [88] Wenchang Zhang, Chuanqi Tan, Fuchun Sun, Hang Wu, and Bo Zhang. A Review of EEG-Based Brain-Computer Interface Systems Design. *Brain Science Advances*, 4(2):156–167, 2018. doi:10.26599/bsa.2018.9050010.

- [89] D. Sochurkova and I. Rektor. Event-related desynchronization/synchronization in the putamen. An SEEG case study. *Experimental Brain Research*, 149(3):401–404, 2003. doi:10.1007/s00221-003-1371-2.
- [90] Andrea A. Kühn, David Williams, Andreas Kupsch, Patricia Limousin, Marwan Hariz, Gerd Helge Schneider, Kielan Yarrow, and Peter Brown. Event-related beta desynchronization in human subthalamic nucleus correlates with motor performance. *Brain*, 127(4):735–746, 2004. doi:10.1093/brain/awh106.
- [91] Jose Antonio Urigüen and Begoña Garcia-Zapirain. {EEG} artifact removal{\textemdash}state-of-the-art and guidelines. *Journal of Neural Engineering*, 12(3):31001, 2015. URL: <https://doi.org/10.1088/1741-2560/12/3/031001>, doi:10.1088/1741-2560/12/3/031001.
- [92] Aapo Hyvärinen. Independent component analysis: recent advances. *Philosophical Transactions of the Royal Society A: Mathematical, Physical and Engineering Sciences*, 371(1984):20110534, feb 2013. URL: <https://doi.org/10.1098/rsta.2011.0534>, doi:10.1098/rsta.2011.0534.
- [93] A Hyvärinen and E Oja. Independent component analysis: algorithms and applications. *Neural Networks*, 13(4):411–430, 2000. URL: <https://www.sciencedirect.com/science/article/pii/S0893608000000265>, doi:[https://doi.org/10.1016/S0893-6080\(00\)00026-5](https://doi.org/10.1016/S0893-6080(00)00026-5).
- [94] M Doppelmayr, W Klimesch, T Pachinger, and B Ripper. Individual differences in brain dynamics: important implications for the calculation of event-related band power. *Biological Cybernetics*, 79(1):49–57, 1998. URL: <https://doi.org/10.1007/s004220050457>, doi:10.1007/s004220050457.
- [95] Taeho Kim, Phuc Nguyen, Nhat Pham, Nam Bui, Hoang Truong, Sangtae Ha, and Tam Vu. Epileptic Seizure Detection and Experimental Treatment: A Review. *Frontiers in Neurology*, 11(July), 2020. doi:10.3389/fneur.2020.00701.
- [96] Arnaud Delorme and Scott Makeig. EEGLAB: An open source toolbox for analysis of single-trial EEG dynamics including independent component analysis. *Journal of Neuroscience Methods*, 134(1):9–21, 2004. doi:10.1016/j.jneumeth.2003.10.009.
- [97] D J Thomson. Spectrum estimation and harmonic analysis. *Proceedings of the IEEE*, 70(9):1055–1096, 1982. doi:10.1109/PROC.1982.12433.
- [98] Soheyl Noachtar and Astrid S. Peters. Semiology of epileptic seizures: A critical review. *Epilepsy and Behavior*, 15(1):2–9, 2009. URL: <http://dx.doi.org/10.1016/j.yebeh.2009.02.029>, doi:10.1016/j.yebeh.2009.02.029.
- [99] Nancy Foldvary-Schaefer and Kanjana Unnwongse. Localizing and lateralizing features of auras and seizures. *Epilepsy and Behavior*, 20(2):160–166, 2011. URL: <http://dx.doi.org/10.1016/j.yebeh.2010.08.034>, doi:10.1016/j.yebeh.2010.08.034.
- [100] Jose F. Téllez-Zenteno and Lizbeth Hernández-Ronquillo. A Review of the Epidemiology of Temporal Lobe Epilepsy. *Epilepsy Research and Treatment*, 2012:1–5, 2012. doi:10.1155/2012/630853.
- [101] Norashikin Yahya, Huwaida Musa, Zhong Yi Ong, and Irraivan Elamvazuthi. Classification of motor functions from electroencephalogram (EEG) signals based on an integrated method comprised of common spatial pattern and wavelet transform framework. *Sensors (Switzerland)*, 19(22):1–20, 2019. doi:10.3390/s19224878.
- [102] Joohee Jimenez-Shahed. Device profile of the percept PC deep brain stimulation system for the treatment of Parkinson’s disease and related disorders. *Expert Review of Medical Devices*, 18(4):319–332, 2021. URL: <https://doi.org/10.1080/17434440.2021.1909471>, doi:10.1080/17434440.2021.1909471.

- [103] Mohammad S. Islam, Khondaker A. Mamun, and Hai Deng. Decoding of Human Movements Based on Deep Brain Local Field Potentials Using Ensemble Neural Networks. *Computational Intelligence and Neuroscience*, 2017, 2017. doi:[10.1155/2017/5151895](https://doi.org/10.1155/2017/5151895).
- [104] Matthew S D Kerr, Pierre Sacré, Kevin Kahn, Hyun-Joo Park, Mathew Johnson, James Lee, Susan Thompson, Juan Bulacio, Jaes Jones, Jorge González-Martínez, Catherine Liégeois-Chauvel, Sridevi V Sarma, and John T Gale. The Role of Associative Cortices and Hippocampus during Movement Perturbations. *Frontiers in neural circuits*, 11:26, apr 2017. URL: <https://pubmed.ncbi.nlm.nih.gov/28469563><https://www.ncbi.nlm.nih.gov/pmc/articles/PMC5395558/>, doi:[10.3389/fncir.2017.00026](https://doi.org/10.3389/fncir.2017.00026).
- [105] A.R.M. UPTON, I. AMIN, S. GARNETT, M. SPRINGMAN, C. NAHMIAS, and I.S. COOPER. Evoked metabolic responses in the limbicstriate system produced by stimulation of anterior thalamic nucleus in man. *Pacing and Clinical Electrophysiology*, 10(1):217–225, 1987. URL: <https://onlinelibrary.wiley.com/doi/abs/10.1111/j.1540-8159.1987.tb05952.x>, arXiv:<https://onlinelibrary.wiley.com/doi/pdf/10.1111/j.1540-8159.1987.tb05952.x>, doi:<https://doi.org/10.1111/j.1540-8159.1987.tb05952.x>.
- [106] Mojgan Hodaie, Richard A. Wennberg, Jonathan O. Dostrovsky, and Andres M. Lozano. Chronic anterior thalamus stimulation for intractable epilepsy. *Epilepsia*, 43(6):603–608, 2002. URL: <https://onlinelibrary.wiley.com/doi/abs/10.1046/j.1528-1157.2002.26001.x>, arXiv:<https://onlinelibrary.wiley.com/doi/pdf/10.1046/j.1528-1157.2002.26001.x>, doi:<https://doi.org/10.1046/j.1528-1157.2002.26001.x>.
- [107] John F. Kerrigan, Brian Litt, Robert S. Fisher, Stephen Cranstoun, Jacqueline A. French, David E. Blum, Marc Dichter, Andrew Shetter, Gordon Baltuch, Jurg Jaggi, Selma Krone, MaryAnn Brodie, Mark Rise, and Nina Graves. Electrical stimulation of the anterior nucleus of the thalamus for the treatment of intractable epilepsy. *Epilepsia*, 45(4):346–354, 2004. URL: <https://onlinelibrary.wiley.com/doi/abs/10.1111/j.0013-9580.2004.01304.x>, arXiv:<https://onlinelibrary.wiley.com/doi/pdf/10.1111/j.0013-9580.2004.01304.x>, doi:<https://doi.org/10.1111/j.0013-9580.2004.01304.x>.
- [108] K. J. Lee, K. S. Jang, and Y. M. Shon. *Chronic deep brain stimulation of subthalamic and anterior thalamic nuclei for controlling refractory partial epilepsy*, pages 87–91. Springer Vienna, Vienna, 2006. URL: https://doi.org/10.1007/978-3-211-35205-2_17, doi:[10.1007/978-3-211-35205-2_17](https://doi.org/10.1007/978-3-211-35205-2_17).
- [109] Siew-Na Lim, Shih-Tseng Lee, Yu-Tai Tsai, I-An Chen, Po-Hsun Tu, Jean-Lon Chen, Hsiu-Wen Chang, Yu-Chin Su, and Tony Wu. Electrical stimulation of the anterior nucleus of the thalamus for intractable epilepsy: A long-term follow-up study. *Epilepsia*, 48(2):342–347, 2007. URL: <https://onlinelibrary.wiley.com/doi/abs/10.1111/j.1528-1167.2006.00898.x>, arXiv:<https://onlinelibrary.wiley.com/doi/pdf/10.1111/j.1528-1167.2006.00898.x>, doi:<https://doi.org/10.1111/j.1528-1167.2006.00898.x>.
- [110] Ivan Osorio, John Overman, Jonathon Giftakis, and Steven B. Wilkinson. High frequency thalamic stimulation for inoperable mesial temporal epilepsy. *Epilepsia*, 48(8):1561–1571, 2007. URL: <https://onlinelibrary.wiley.com/doi/abs/10.1111/j.1528-1167.2007.01044.x>, arXiv:<https://onlinelibrary.wiley.com/doi/pdf/10.1111/j.1528-1167.2007.01044.x>, doi:<https://doi.org/10.1111/j.1528-1167.2007.01044.x>.
- [111] Yoon-Sang Oh, Hye Jin Kim, Kyung Jin Lee, Yeong In Kim, Sung-Chul Lim, and Young-Min Shon. Cognitive improvement after long-term electrical stimulation of bilateral anterior thalamic nucleus in refractory epilepsy patients. *Seizure - European Journal of Epilepsy*, 21(3):183–187, apr 2012. URL: <https://doi.org/10.1016/j.seizure.2011.12.003>, doi:[10.1016/j.seizure.2011.12.003](https://doi.org/10.1016/j.seizure.2011.12.003).

- [112] Jamie J. Van Gompel, Bryan T. Klassen, Gregory A. Worrell, Kendall H. Lee, Cheolsu Shin, Cong Zhi Zhao, Desmond A. Brown, Steven J. Goerss, Bruce A. Kall, and Matt Stead. Anterior nuclear deep brain stimulation guided by concordant hippocampal recording. *Neurosurgical Focus FOC*, 38(6):E9, 01 Jun. 2015. URL: <https://thejns.org/focus/view/journals/neurosurg-focus/38/6/article-pE9.xml>, doi:10.3171/2015.3.FOCUS1541.
- [113] Massimo Piacentino, Christine Durisotti, Pier Gaetano Garofalo, Paolo Bonanni, Anna Volzone, Federica Ranzato, and Giacomo Beggio. Anterior thalamic nucleus deep brain Stimulation (DBS) for drug-resistant complex partial seizures (CPS) with or without generalization: long-term evaluation and predictive outcome. *Acta Neurochirurgica*, 157(9):1525–1532, 2015. URL: <https://doi.org/10.1007/s00701-015-2498-1>, doi:10.1007/s00701-015-2498-1.
- [114] Berthold R. Voges, Friedhelm C. Schmitt, Wolfgang Hamel, Patrick M. House, Christian Kluge, Christian K. E. Moll, and Stefan R. Stodieck. Deep brain stimulation of anterior nucleus thalami disrupts sleep in epilepsy patients. *Epilepsia*, 56(8):e99–e103, 2015. URL: <https://onlinelibrary.wiley.com/doi/abs/10.1111/epi.13045>, arXiv:<https://onlinelibrary.wiley.com/doi/pdf/10.1111/epi.13045>, doi:<https://doi.org/10.1111/epi.13045>.
- [115] K Lehtimäki, T Möttönen, K Järventausta, J Katisko, T Tähtinen, J Haapasalo, T Niskakangas, T Kiekara, J Öhman, and J Peltola. Outcome based definition of the anterior thalamic deep brain stimulation target in refractory epilepsy. *Brain Stimulation: Basic, Translational, and Clinical Research in Neuromodulation*, 9(2):268–275, mar 2016. URL: <https://doi.org/10.1016/j.brs.2015.09.014>, doi:10.1016/j.brs.2015.09.014.
- [116] E Tessa, P P Muhammed Shanir, and Shaleena Manafuddin. Time domain analysis of epileptic EEG for seizure detection. *2016 International Conference on Next Generation Intelligent Systems (ICNGIS)*, pages 1–4, 2016.
- [117] Vicenta Salanova, Thomas Witt, Robert Worth, Thomas R. Henry, Robert E. Gross, Jules M. Nazaro, Douglas Labar, Michael R. Sperling, Ashwini Sharan, Evan Sandok, Adrian Handforth, John M. Stern, Steve Chung, Jaimie M. Henderson, Jacqueline French, Gordon Baltuch, William E. Rosenfeld, Paul Garcia, Nicholas M. Barbaro, Nathan B. Fountain, W. Jeffrey Elias, Robert R. Goodman, John R. Pollard, Alexander I. Tröster, Christopher P. Irwin, Kristin Lambrecht, Nina Graves, Robert Fisher, and . Long-term efficacy and safety of thalamic stimulation for drug-resistant partial epilepsy. *Neurology*, 84(10):1017–1025, 2015. URL: <https://n.neurology.org/content/84/10/1017>, arXiv:<https://n.neurology.org/content/84/10/1017.full.pdf>, doi:10.1212/WNL.0000000000001334.
- [118] Vibhor Krishna, Nicolas Kon Kam King, Francesco Sammartino, Ido Strauss, Danielle M Andrade, Richard A Wennberg, and Andres M Lozano. Anterior Nucleus Deep Brain Stimulation for Refractory Epilepsy: Insights Into Patterns of Seizure Control and Efficacious Target. *Neurosurgery*, 78(6):802–811, jun 2016. URL: <https://doi.org/10.1227/NEU.0000000000001197>, doi:10.1227/NEU.0000000000001197.
- [119] Ana Franco, José Pimentel, Alexandre Rainha Campos, Carlos Morgado, Sara Pinelo, António Gonçalves Ferreira, and Carla Bentes. Stimulation of the bilateral anterior nuclei of the thalamus in the treatment of refractory epilepsy: two cases of subcortical band heterotopia. *Epileptic Disorders*, 18(4):426–430, dec 2016. doi:10.1684/epd.2016.0878.
- [120] Antonio Valentín, Richard P Selway, Meriem Amarouche, Nilesh Mundil, Ismail Ughratar, Leila Ayoubian, David Martín-López, Farhana Kazi, Talib Dar, Diego Jiménez-Jiménez, Elaine Hughes, and Gonzalo Alarcón. Intracranial stimulation for children with epilepsy. *European Journal of Paediatric Neurology*, 21(1):223–231, jan 2017. URL: <https://doi.org/10.1016/j.ejpn.2016.10.011>, doi:10.1016/j.ejpn.2016.10.011.
- [121] Tommi Nora, Hanna Heinonen, Mirja Tenhunen, Sirpa Rainesalo, Soila Järvenpää, Kai Lehtimäki, and Jukka Peltola. Stimulation induced electrographic seizures in deep brain stimulation of the anterior

- nucleus of the thalamus do not preclude a subsequent favorable treatment response. *Frontiers in Neurology*, 9:66, 2018. URL: <https://www.frontiersin.org/article/10.3389/fneur.2018.00066>, doi:10.3389/fneur.2018.00066.
- [122] Massimo Piacentino, Giacomo Beggio, Lara Zordan, and Paolo Bonanni. Hippocampal deep brain stimulation: persistent seizure control after bilateral extra-cranial electrode fracture. *Neurological Sciences*, 39(8):1431–1435, 2018. URL: <https://doi.org/10.1007/s10072-018-3444-9>, doi:10.1007/s10072-018-3444-9.
- [123] Soila Järvenpää, Eija Rosti-Otajärvi, Sirpa Rainesalo, Linda Laukkanen, Kai Lehtimäki, and Jukka Peltola. Executive functions may predict outcome in deep brain stimulation of anterior nucleus of thalamus for treatment of refractory epilepsy. *Frontiers in Neurology*, 9:324, 2018. URL: <https://www.frontiersin.org/article/10.3389/fneur.2018.00324>, doi:10.3389/fneur.2018.00324.